



Human Face Mapping

Based on TEWL, Hydration and Ultrasound

Elena Chirikhina

School of Engineering

London South Bank University

Supervisor: Dr Perry Xiao

Submitted: April 2021

Table of Contents

Chapter 1. Introduction	12
1.1 Motivation for Research	15
1.2 Aims and Objectives.....	16
1.3 The Physiology of Skin.....	17
1.3.1 Layers of Skin	17
1.3.2 Aquaporins Facilitating Hydration	18
1.4 Association of Skin Anatomy with Hydration and Dermatology.....	22
1.4.1 Face Mapping.....	23
1.4.2 Acne Face Mapping.....	30
1.5 Hydration vs. Moisturizing in Dermatology	32
1.6 Measurement of Skin Hydration.....	34
1.7 Ethical Approval	37
1.8 Organisation of the Thesis	37
1.8.1 Synopsis of Thesis	38
1.8.2 Prospective Exertion	42
1.9 Chapter Summary	43
Chapter 2. Literature Review	44
2.1 Introduction	44
2.2 Skin Analysis.....	45
2.2.1 Facial Skin Analysis.....	46
2.2.2 Facial Skin Thickness and Echogenicity in Different Anatomical Locations	46
2.3 Facial Skin Mapping	49
2.3.1Capacitance and Trans Epidermal Loss Mapping.....	51
2.3.2Study of Moisturising Using Skin Mapping	52
2.4 Stratum Corneum (SC)	54
2.4.1 Functional Characterisation of SC.....	55
2.5. 1 Facial Skin Hydration and pH	57

2.5.3 Facial Skin Hydration and Temperature.....	58
2.5.5 Skin Hydration and Natural Moisturising Factor (NMF)	59
2.6 In-Vivo Measurement of Skin Hydration	60
2.6.1 Electrical-Based Methods	60
2.6.2 Differential Scanning Calorimeter.....	60
2.6.8 Raman Spectroscopy.....	63
2.6.9 Photothermal Radiometry	64
2.7 Analysis of Instruments to Measure Skin Hydration.....	65
2.8 Epsilon.....	65
2.9 AquaFlux.....	70
2.10 Skin Ultrasound and Episcan.....	74
2.10.1 Skin Ultrasound	74
2.10.2 Episcan	75
2.11 Mathematical Analysis.....	78
2.12 Chapter Summary	79
Chapter 3. Skin TEWL Measurements	81
3.1 Experimental Results of Transepidermal Water Loss (TEWL).....	81
3.2 Causes of High TEWL on the Lip and Upper Lip	82
3.3 Eye Corners and Under-Eye TEWL Difference	84
3.4 Nose and TEWL	85
3.5 Neck and TEWL	85
3.6 Forehead and TEWL	85
3.7 Chin and TEWL	86
3.8 Cheek and TEWL	86
3.9 Variance of TEWL with Age for Different Anatomical Sites	87
3.10 Welch t-TEST	87
3.11 Age Based Variance in TEWL.....	89
3.11.1 Neck	89
3.11.2 Lips	90
3.11.3 Nose	91
3.11.4 Under-Eye	93
3.11.5 Eye Corner.....	94

3.11.6 Forehead	95
3.11.7 Cheeks	96
3.11.8 Chin	97
3.12 Chapter Summary	98
Chapter 4. Skin Hydration Measurements	100
4.1 Experimental Results of Epsilon	100
4.2 Causes of High Epsilon Values on the Under-eye and Eye Corner.....	102
4.3 Cheek in Epsilon Values	103
4.4 Neck in Epsilon Values	104
4.5 Chin in Epsilon Values	105
4.6 Forehead in Epsilon Values	105
4.7 Nose in Epsilon Values	106
4.8 Lip in Epsilon Values.....	106
4.9 Variance of Epsilon Values with Exercise for Different Anatomical Sites.....	107
4.10 Forehead	111
4.11Undereye Right and Undereye Left	112
4.12 Nose	114
4.13 Cheek Right and Cheek Left	115
4.15 Chin	116
4.16 Lips	118
4.17 Hydration-based Face Mapping.....	120
4.18 Chapter Summary	121
Chapter 5. Skin Ultrasound Measurements.....	122
5.1 Variance of Episcan in Skin Layer Assessment for Different Anatomical Sites	124
5.2 Variation in Skin Assessment Through Welch-T-Test	133
5.3 Skin SiteClassification by Machine Learning	142
5.4 Chapter Summary	147
Chapter 6. Conclusions& Future Work	149
6.1 Conclusions	149
6.2 Future Work.....	151
Original Contribution to Knowledge	153
List of Publications	154

References155

Appendix: Ethical Approval..... 170

List of Figures

FIGURE 1.1. AQUAPORINS FACILITATING HYDRATION (LABIOTECH, 2019).....	20
FIGURE 1.2. FACIAL SKIN THICKNESS (MM) IN DIFFERENT ANATOMICAL LOCTIONS	46
FIGURE 2.2. IMAGE ANALYSIS OF PORES IN THE NASAL REGION.....	48
FIGURE 2.3. PICTORIAL REPRESENTATION OF FACE MAPPING ZONES.....	49
FIGURE 2.4. THIRTY PREDEFINED SITES FOR SKIN MAPPING.....	50
FIGURE 2.5. INTERETHNIC SKIN AND CAPACITANCE MAPPING.....	51
FIGURE 2.6. MOISTURISATION SKIN MAPPING.....	52
FIGURE 2.7. STRUCTURE OF STRATUM CORNEUM.....	54
FIGURE 2.8. THE SC OF INFANT SKIN (A) AND ADULT SKIN (B) IS HYDRATED (SMALL BLUE SPHERES) UNDER NORMAL CONDITIONS.....	55
FIGURE 2.9. RAMAN SPECTRUM OF FOREARM SKIN.....	61
FIGURE 2.10. SCHEMATIC DIAGRAM OF THE PHOTOTHERMAL RADIOMETRY SETUP.....	63
FIGURE 2.11. EPSILON HAND-HELD PROBE AND PARKING STAND.....	65
FIGURE 2.12. WATER CONTENT AT FIVE BODY SITES MEASURED WITH THE EPSILON.....	67
FIGURE 2.13. ULTRASOUND IMAGE.....	68
FIGURE 2.14. AQUAFLUX INSTRUMENT.....	70
FIGURE 2.15. CUT-OUT VIEW OF THE AQUAFLUX CONDENSER CHAMBER.....	71
FIGURE 2.16. EPISCAN.....	74
FIGURE 2.17. 35 MHZ IMAGE OF SUPERFICIAL SOFT TISSUE THROUGH EPISCAN.....	75
FIGURE 2.18. TWO A-SCANS SHOWING THE DIFFERENCE BETWEEN NORMAL TISSUE AND SKIN LESION	76
FIGURE 3.1. GRAPHICAL ILLUSTRATION OF TEWL WITH MEAN AND SD	82
FIGURE 3.2. SC THICKNESS COMPARISON BETWEEN LIP & FACIAL SKIN.....	82
FIGURE 3.3. WELCH T-TEST UNDER AGE 35.....	87
FIGURE 3.4. WELTCH T-TEST ABOVE AGE 35.....	87

FIGURE 3.5 TEWL MEASUREMENTS PERFORMED ON THE NECK	89
FIGURE 3.6. TEWL MEASUREMENTS PERFORMED ON LIPS.....	90
FIGURE 3.7. TEWL MEASUREMENTS PERFORMED ON THE NOSE	91
FIGURE 3.8. TEWL MEASUREMENTS PERFORMED ON THE UNDER EYE.....	92
FIGURE 3.9. TEWL MEASUREMENTS PERFORMED ON THE EYE CORNER.....	93
FIGURE 3.10. TEWL MEASUREMENTS PERFORMED ON THE FOREHEAD.....	94
FIGURE 3.11. CHEEK.....	95
FIGURE 3.12. TEWL MEASUREMENTS PERFORMED ON THE CHEEK BELOW 35.....	96
FIGURE 3.13. TEWL MEASUREMENTS PERFORMED ON THE CHIN BELOW 35.....	97
FIGURE 4.1. GRAPHICAL ILLUSTRATION OF EPSILON VALUES WITH MEAN AND SD.....	100
FIGURE 4.2. CROSS-SECTION OF CHEEK SKIN.....	102
FIGURE 4.3. GRAPHICAL ILLUSTRATION OF EPSILON VALUES OF FEMALES.....	108
FIGURE 4.4. GRAPHICAL ILLUSTRATION OF EPSILON VALUES OF MALES.....	109
FIGURE 4.5. ILLUSTRATION OF EPSILON VALUES OF MALE AND FEMALE.....	110
FIGURE 4.6. ILLUSTRATION OF UNDER-EYE R AND UNDER-EYE L VALUES OF MALE AND FEMALE.....	112
FIGURE 4.7. ILLUSTRATION OF NOSE VALUES OF MALE AND FEMALE.....	113
FIGURE 4.8. ILLUSTRATION OF CHEEK R AND CHEEK L VALUES OF MALE AND FEMALE.....	115
FIGURE 4.9. CHIN VALUES OF MALES AND FEMALES BEFORE AND AFTER EXERCISE.....	116
FIGURE 4.10. LIPS VALUES OF MALES AND FEMALES BEFORE AND AFTER EXERCISE.....	118
FIGURE 4.11. HYDRATION VISUALS OF DIFFERENT CAUCASIAN FEMALES.....	119
FIGURE 5.1. CROSS-SECTIONAL ILLUSTRATION OF SKIN (LONGPORT, 2018).....	123
FIGURE 5.2. SIGMA VALUES OF DERMIS SKIN LAYERS.....	126
FIGURE 5.3. THE CROSS-SECTIONAL HIGH-RESOLUTION ULTRASOUND IMAGES FOR CHEEKS, CHIN, FOREHEAD, ARM, LIPS, AND NOSE.....	129
FIGURE 5.4. SIGMA VALUES OF SC SKIN LAYERS.....	134
FIGURE 5.5. SIGMA VALUES OF EPIDERMAL SKIN LAYERS.....	135
FIGURE 5.6. SIGMA VALUES OF DERMIS SKIN LAYERS.....	135

FIGURE 5.7 SAMPLE RAW EPISCAN IMAGES TO BE USED IN THE ML-BASED CLASSIFICATION.....143

FIGURE 5.8 IMAGE TRANSFORMATION FOR ML-BASED CLASSIFICATION.....145

List of Tables

TABLE 3.1. TEWL VALUES MEASURED AT 9 (501 INSTANCES) ANATOMICAL SITES AS GRAMS OF WATER PER SQUARE METER PER HOUR ($G \cdot M^{-2} \cdot H^{-1}$)	81
TABLE 3.2. TEWL VALUES MEASURED UNDER THE AGE 35 AND ABOVE OF 125 INSTANCES AS GRAMS OF WATER PER SQUARE METER PER HOUR ($G \cdot M^{-2} \cdot H^{-1}$)	88
TABLE 3.3. VARIANCE IN TEWL OF NECK LESS THAN 35 AND ABOVE, AS GRAMS OF WATER PER SQUARE METER PER HOUR ($G \cdot M^{-2} \cdot H^{-1}$).	89
TABLE 3.4. VARIANCE IN TEWL OF LIPS, AS GRAMS OF WATER PER SQUARE METER PER HOUR ($G \cdot M^{-2} \cdot H^{-1}$)	91
TABLE 3.5. VARIANCE IN TEWL OF NOSE, AS GRAMS OF WATER PER SQUARE METER PER HOUR ($G \cdot M^{-2} \cdot H^{-1}$)	92
TABLE 3.6. VARIANCE IN TEWL OF EYES, AS GRAMS OF WATER PER SQUARE METER PER HOUR ($G \cdot M^{-2} \cdot H^{-1}$)	93
TABLE 3.7. VARIANCE IN TEWL OF EYE CORNER, AS GRAMS OF WATER PER SQUARE METER PER HOUR ($G \cdot M^{-2} \cdot H^{-1}$)	94
TABLE 3.8. VARIANCE IN TEWL OF FOREHEAD, AS GRAMS OF WATER PER SQUARE METER PER HOUR ($G \cdot M^{-2} \cdot H^{-1}$)	95
TABLE 3.9. VARIANCE IN TEWL OF CHIN, AS GRAMS OF WATER PER SQUARE METER PER HOUR ($G \cdot M^{-2} \cdot H^{-1}$)	97
TABLE 4.1. ILLUSTRATION OF EPSILON VALUES (DIELECTRIC CONSTANTS) WITH MEAN AND SD.	100
TABLE 4.2. ILLUSTRATION OF EPSILON VALUES OF MALE AND FEMALE BEFORE AND AFTER EXERCISE	112
TABLE 5.1. WELCH T-TEST ON THE SC OF ANATOMICAL SITES	134
TABLE 5.2. WELCH T-TEST OF THE EPIDERMIS OF ANATOMICAL SITES	136
TABLE 5.3. WELCH T-TEST OF THE DERMIS LAYER OF ANATOMICAL SITES	137
TABLE 5.4. WELCH T-TEST OF ALL SKIN LAYER FOR DIFFERENT ANATOMICAL SITES	140
TABLE 5.5. MEAN, SD, AND Z-SCORE OF SKIN LAYERS OF DIFFERENT ANATOMICAL SITES	141
TABLE 5.6 FACIAL SITES USED FOR ML-BASED CLASSIFICATION	144
TABLE 5.7 ML CLASSIFIER PARAMETERS	146
TABLE 5.8 ML TRAINING OUTPUT	146

Acknowledgements

I would like to give sincere thanks to my supervisor Dr. Perry Xiao for his professionalism, patience, understanding, support and guidance. I would also like to thank Dr. Andrey Chirikhin for inspiration and his help, and encouragement and Dr. Francesco Bianconi for his time, advice and support.

I am also grateful to Sinlen beauty clinic and its friendly team and to all volunteers who made this research unique and special. I thank them for the valuable time they spent with me over the several years during which I collected data for this research.

Finally, I am grateful to my beloved family and friends: to my amazing sons with their constant questions about my PhD progress, to my parents for their love and care, and all my amazing friends who supported me during this long, delayed research journey.

Abstract

Biophysical properties of the skin vary depending on the skin location. Such properties include skin structure, density of skin layers, pH, temperature, hydration and Trans epidermal Water Loss (TEWL). Modern technologies and quantitative methods allow reading and analysing the skin properties using in-vivo based analysis. One goal of such analysis is partitioning the skin in areas with similar properties, which is referred as *mapping*. The purpose of our study, also the novelty of the project, is mapping of the facial skin in terms of TEWL, hydration and skin layer thickness, as well as measuring the effect of physical exercise on facial skin; where possible, effect of sex and age were also considered. TEWL was measured with AquaFlux, skin layer thickness was measured with Episcan high resolution ultrasound imaging, and skin hydration was measured with Epsilon.

Our study reveals material difference of TEWL between the facial sites being analysed; the largest differences were noted between the lips and the neck. It was found that skin hydration levels decrease with the advancement of age. Skin hydration readings reveal larger general effect of exercise for females, and strongest effect for males observed on the nose. Skin ultrasound images were used in two ways. First, face was mapped in terms of the thickness of the individual skin layers and such mapping was found to be different for each layer. Secondly, the differences between the sites in terms of thickness were quantified using Welch test, where age was also found to be a factor. Several Machine Learning-based classifiers of the skin location were also trained, which are based on the cross-sectional image with moderate positive outcome.

The study showed that the combination of TEWL, Epsilon and Episcan provides useful information about skin health. The study also showed variations in the values for different facial skin sites of several skin samples, which was likely due to the degree of corneocyte formation, the lipid contents of the Stratum Corneum (SC), skin temperature, damaged barrier function, bodily health and skin blood flow.

Chapter 1. Introduction

The demand and desire for attractive facial features is increasing among individuals worldwide. Both males and females wish to look attractive and youthful and turn to the cosmetic industry to achieve this. Indeed, it is one of the most significant reasons for the growth of cosmetics market. Every year, the business of these industries is expanding more and more. A recent study revealed that the beauty business industry has grown to around \$500 billion in 2019 (Huemer & Ferran, 2019). The demand for attractive features—particularly the hair, neck, chin, eyes, cheeks and lips—is widespread, and facial features are considered the most essential and prominent indicators of expression for both women and men.

The skin is the human body's largest organ, covering around 1.86 square meters. The skin's protective layer prevents microbes from interacting with human beings. Skin facilitates bodily sensations with respect to cold, heat, and touch. The skin's sensitivity varies according to the anatomical location and layer. The facial skin must appear fresh and relaxed for an individual to appear youthful. Sagging of the facial skin indicates old age, and wrinkles may also appear at multiple anatomical facial skin sites.

The face is the first feature that people see on first encountering one another. It is responsible for revealing individuals' age. The facial skin is also instrumental in revealing individuals' emotions, habits, gender, ethnicity, and age. People who engage in unhealthy habits, such as smoking, drinking or drug abuse, are more likely to have facial skin that appears older, as it loses its freshness and can develop darkened patches in various locations. Issues of restlessness and insomnia cause similar problems, for

instance people who have difficulty in sleeping or who suffer from irregular sleep patterns are more likely to have poor-quality facial skin (Alarifi, et al., 2017).

People with fresh and young facial skins enjoy higher confidence than others and frequently excel in their performance at work owing to their heightened morale and confidence. Likewise, men and women with healthy facial skin enjoy better mental health and social lives and are more willing to actively participate in social activities and gatherings.

The demand for plastic surgery and advanced cosmetic science increased after World War II, during which the use of explosive weapons caused soldiers to suffer deadly injuries and wounds. Many lost their lives during this struggle, while others sustained severe injuries, including severe facial damage that, in some instances, left their faces unrecognisable. Against this background, the need for treatment that would allow soldiers to regain their confidence and reintegrate into society arose (Reid, 2017). The most common damage was to the chin, nose, cheekbones and jawbone, which harmed the facial structure and skin. This created a massive need for full-face recognition, owing to the loss of bones and volume (Stone, et al., 2016). Healthcare staffs, such as nurses, pharmacists, doctors and military surgeons, were required to contribute their best effort to improve the appearances of the affected individuals, who were left vulnerable, afraid even to confront their families (Marno, 2020). Mental and social wellbeing declined drastically, and confidence levels deteriorated. Some of the victims were left unrecognisable by their deep wound and injuries. They were subjected to post-facial surgery treatments to regain the actual appearance of human skin with improved skin structure and texture (Mitchener, et al., 2017). These treatments remedied skin nutrient

deficiencies and increased facial blood circulation with the help of dermatological services to nourish the skin and recover skin tissue.

The alteration of facial appearance due to accidents, radiation, chemical burns and fire burns is increasingly easy to remedy with advances in science research for beautification. It has contributed in-depth and a significant knowledge that has helped reduce vulnerability to the individuals' suffering, and supports future science and research. Various crucial standard skin structure parameters exist that define the skin's layers: the hypodermis, dermis and epidermis. The epidermis is the topmost layer and acts as a barrier against harm, hypodermis is the bottom layer and dermis is middle layer. Skin type varies from individual to individual and can be normal, sensitive, dry or oily. Skin dryness can be painful, and the intensity of this pain varies according to the extent of dryness. Thinning of the skin can occur primarily due to neglect and dehydration.

The facial skin contains pores at different sites, contributing to oil and moisture efflux (Lee, n.d.). This also leads to an influx of dust, dirt and pollution upon exposure to the external environment. The size and number of skin pores at different sites vary; hence, the rate of influx and efflux varies. Enlarged pore size or frequent exposure to the environment can lead to blackheads. Moreover, facial skin includes hair follicles that function as a barrier for the skin (Nkengne, et al., 2020). The skin's barriers protect against direct exposure to the external environment, including sunlight, resisting the penetration of harmful UV rays entering the skin and preventing the maximum impact of hazardous effects.

Thin skin cannot provide perfect protection and it can be easily affected by hazardous substances (Wang, et al., 2019). Besides this, the most prominent parameter that influences skin colour is sunlight exposure (Gupta & Sharma, 2019). People from different geographical regions and ethnicities have variable skin colours. Six different types of facial skin can be easily determined on the Fitzpatrick scale, which is used to determine how skin reacts to ultra violet light or sun exposure.

1.1 Motivation for Research

Environmental and genetic factors commonly influence the skin's characteristics. Dermatological science contributes significantly to enhancing and improving skin quality. These benefits also aid considerably in rejuvenating the skin. Drastic skin damage can be treated with advanced dermatological science, including laser technology, micro-needling and platelet-rich plasma (PRB), etc. The aim of Dermatology is to provide medication and analysis to beautify and maintain deep skin integrity.

The functionality of every dermatological treatment varies and is selected based on skin damage. This damage maybe due to burns, exposure to acid, wrinkles, acne, open pores or deep cuts, etc. Hydration plays a vital role in maintaining the skin's integrity and nourishing its cells. Indeed, it ensures the success of dermatological procedures and is indicative of speedy recovery. How hydration affects different anatomical sites of facial skin for its beauty, glow, freshness, rejuvenation and healing has been a key motivating factor in this study (Hubbard, 2019). Skin structure which is composed of different

layers and their parameters has significant impact on its physical appearance. There are three layers of skin in general; Epidermis, Dermis and Hypodermis. Each of these layers have their own properties responsible of maintaining the physical as well as internal state of skin, for instance, colour, thickness, temperature, and hydration level. Epidermis is the outer most layer that protects human body from outside. The skin thickness can vary from the range 0.8 – 1.5 mm, or 0.07 – 0.15 mm that correspond to average thick and thin skins. Maximum thickness can be more than 5 mm, for instance, palms and ankles (Arda et al., 2014). Age and geographical location counts variations in skin measurements, for more details about facial skin measurements reader is advised to see (Ha et al., 2005). The healthy skin contains more hydration than thin skin which helps skin glow and remains less prone to dust and heat. In the next section every layer of skin has been discussed in much detail along with the facts how each layer functions for skin health and beauty.

Moreover, understanding the state of internal body organs reflected by different regions of face is another interesting part of this study. How the skin which is virtually composed of different regions is affected by changes in hydration levels when the physical exercise stimulates internal body organs. This relates how the health of internal body organs can be reflected by different regions of facial skin. For this purpose a brief introduction is given in this chapter on Traditional Chinese Medicine (TCM).

1.2 Aims and Objectives

The aims and objectives of the present study on face mapping are as follows:

- To assess the TEWL, the skin hydration levels and the skin layer thicknesses at different anatomical sites of facial skin.
- To determine the effect of exercise on the hydration levels of different anatomical sites of facial skin.
- To evaluate variations in hydration with respect to age and gender.

1.3 The Physiology of Skin

1.3.1 Layers of Skin

The outermost layer of skin contributes to the skin tone of the human body which is known as epidermis that reflects the individuals' skin tone. Some specialised cells contribute to skin pigments which are known as melanocytes and are responsible for producing melanin in the body; the dark colour of skin is directly proportional to the amount of these pigments. Beneath this waterproof layer lies the dermis, composed of sweat glands, hair follicles and tough connective tissues (Bozorgtabar, et al., 2017).

The skin's outer layer (epidermis) forms a barrier between the environment and body. It contains five layers: the stratum corneum (SC), stratum lucidum, stratum granulosum, stratum spinosum and stratum basale. The epidermis contains keratin and specialised skin cells that exhibit resilient behaviour. The epidermis skin layer that is light in appearance and thin, which covers the soles and palms, is the stratum lucidum. The epidermis layer that contains granular components is the stratum granulosum, while the layer that has a microscopic spiny appearance is the stratum spinosum (Abdo, et al., 2020). It contains desmosomes that are connected throughout the skin layer. The columnar and cuboidal cells form the epidermis's deepest layer, known as the stratum basale (Iuchi, et al., 2019). The SC is the layer that sheds continuously over time. It is

also known as the horny layer, which is tougher in its features and resembles an animal's horn. The continuous shedding of specialised skin cells leads to a horny skin structure. This layer functions to offer protection to the skin's inner layer. It is also commonly known as the brick wall, which constitutes the cell envelope through corneocytes.

The presence of lipids mortared with the corneocytes is responsible for creating the skin's water barrier capability (Westermann, et al., 2020). On average, it takes a thickness of about 20 layers of cells. It is thick at some locations, while at other anatomical locations, the skin layer is comparatively thinner. For instance, it is particularly thick at the heels, while on the eyelids, it is thinner in structure. The SC offers protection against bacteria, toxins, and dehydration. It locks in the skin's water content by offering resistance to water absorption or water loss. Moreover, it ensures that the skin's structure is protected against disorders and helps maintain a healthy body temperature (Mojumdar, et al., 2017).

1.3.2 Aquaporins Facilitating Hydration

Aquaporins (AQPs) facilitate water transportation across the cell membrane, see Figure 1.1. Skin hydration is largely dependent on the functionality of these proteins. They include aquaglycerolporins for glycerol and water transportation and aim to improve skin hydration levels by facilitating adequate transportation (Thiagarajah, et al., 2018). The credit for the influx and efflux of small molecules and water goes to these aquaporins. Previously, it was assumed that water and other small molecules move freely through the biological membranes. However, recent studies have revealed that the

biophysical properties of membrane lead to transportation. These are meant to control water movement across biological membranes and enhance or reduce hydration levels depending upon the need and circumstances. Different biological membranes exhibit different permeability levels with respect to molecules owing to their nature and the pores' size. The structure of these molecules is selectively permeable and controls the movement of water, small molecules and ions (Deuticke, 2018). The water movement depends on diffusional permeability, osmotic permeability or temperature-dependent water transport through pore channels (Bollag, et al., 2020).

Peter Agre confirmed in 1992 that AQPs conserve water inside the tissues for longer. Water preservation characteristics in the skin lead to freshness, glow and improved skin health. This function has been observed in mammals, amphibians, insects and plants. AQPs play an efficient role in the homeostasis of cellular water. The small uncharged molecules enjoy osmotically driven bidirectional movement through the porous cell membranes (Tamma, et al., 2018). These uncharged molecules most commonly include urea, glycerol and water.

Mammals typically have around 13 different types of AQP, which differ with respect to function, tissue allocations and transportation capabilities. Some AQPs are concerned with the transportation of all uncharged molecules, including urea, glycerol and water, while others contribute solely to water transportation. However, the most abundant AQP present in human beings is aquaporin 3 (AQP3) (Fenton, et al., 2020). It is located in the epidermal keratinocytes of the plasma membrane and is the key transporter of both glycerol and water—hence, it is known as aquaglyceroporin. Individuals lacking AQP3

exhibit low SC hydration, so they cannot keep their skin protected in a drastic environment (Rodriguez, et al., 2019).

Studies conducted on mice revealed that the absence of AQP3 causes the lowest SC hydration levels, which cannot be corrected by a high-humidity environment or skin occlusion (Abir-Awan, et al., 2019). The mice were revealed to have low levels of glycerol in their epidermis and SC. However, their glycerol content in the serum and dermis was appropriate. The results revealed that AQP3 contributes to skin hydration at various sites of the epidermis. The main reason that glycerol assists skin hydration is its nature. It is an endogenous humectant and easily diffuses into the epidermis and SC through the osmotic process.

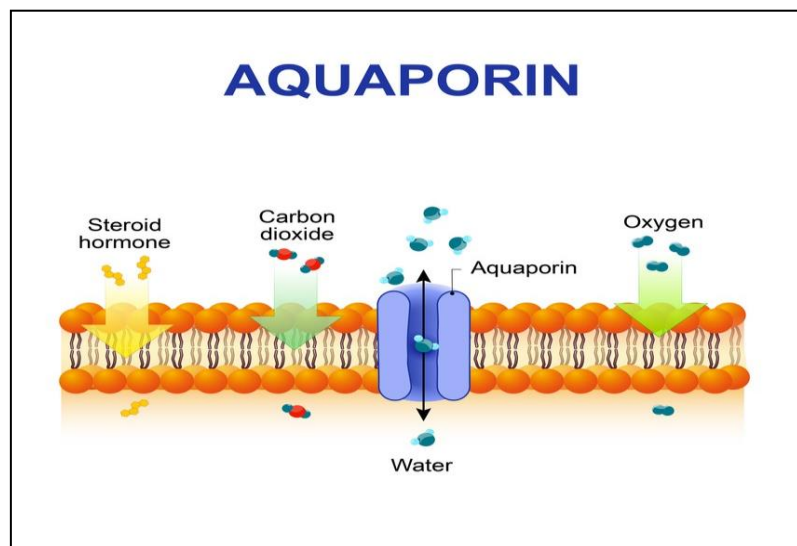


Figure 1.1. Aquaporins Facilitating Hydration (Labiotech, 2019)

The stratum basale of the epidermis is the layer in which AQP3 expresses itself. However, it declines as it approaches the stratum granulosum. The movement from the

dermis to the SC reflects the decline in AQP3 expression. A direct relationship exists between glycerol and SC hydration. It can be analysed using the tape-stripping technique and the glycerol analysis test.

Another key technique for the determination of skin hydration is the use of a corneometer (Nakazawa, et al., 2019). A corneometer can measure the level of water content or hydration of SC at different anatomical sites with accuracy and reliability. The distribution of AQP3 differs at different skin sites, reflecting the water gradient and epidermal water allocation throughout the skin. AQP3 expression throughout the skin is easily determined using immune-histochemical analysis, which reflects the permeability of the membranes and confirms the functionality level of AQP3 (Cerdà, et al., 2017). A healthy epidermis contains AQPs in the stratum basale.

Dermatologists treat most dry skin conditions by altering APQ3 expression, leading to the potentiated mechanism of APQ3. They are currently striving to develop important compounds that might stimulate the AQP3 channels through a pharmacological approach (Proksch, 2018). This may facilitate enhanced skin hydration through the use of endogenous means. Glycerol does not merely contribute to skin hydration but also contributes to optimal hydration maintenance over longer periods of time. Prolonged hydration of the skin is due to the functionality of glycerol at the AQP channels. APQ3 modulators can help to develop and improve the channels for improved functionality (Evans, et al., 2017).

1.4 Association of Skin Anatomy with Hydration and Dermatology

The cosmetic and aesthetic industries are continually improving their knowledge about how facial skin might be improved, and have developed numerous efficient and high-quality skincare and beauty products, including masks, cleansers, serums, lotions, and creams. These address skin issues and provide synergistic skin protection (Kelchen, et al., 2018) for routine care. Medical aesthetic treatment protocols design more effective approaches aimed at restoring the features and improving skin health in most prominent areas, including the eyes, nose, chin, lips, forehead and cheeks (Zhang, 2020). Healthy skin contains collagen and exhibits excellent elasticity. These properties are affected by the passage of time and by damage resulting from accidental injuries or harm. Skin hydration and firmness are dependent on these elements. One of the most beneficial acids found in human skin is hyaluronic acid (HA), which helps maintain a low skin pH. Like collagen, elasticity and other parameters, the skin begins to lose hyaluronic acid with age. Consequently, the cosmetic industry adds this acid and several vitamins to beauty products and cosmetics. The application of these products to the skin leads to remarkable growth and nourishment. Niacin, also known as vitamin B3, is present in cosmetic creams and lotions. Dermatologists design and recommend cosmetic products based on the individual characteristics of the skin (Dattola, et al., 2020). Kojic acid improves skin tone gradually over time (Saeedi, et al., 2019).

The SC of human skin varies in pH range from acidic to neutral. Maintenance of a pH between these extremes offers protection against various unfavourable factors. One of the major factors contributing to the pH of human skin is circadian rhythm. Variations in

the enzyme function of the SC's circadian rhythm lead to pH changes (Proksch, et al., 2020). A high TEWL value is indicative of a high pH. With the increased pH of the SC, the rate of enzymatic reaction increases, leading to lipid metabolism. Syndets are highly preferable in view of their bacteria-regulating properties. They also function well in enhancing the tolerability profile of human skin. People with healthy skin can obtain optimum benefits using acidic syndets. Indeed, syndets are also usefully applied to cleanse patients' skin in treating seborrheic-type diseases (Jansen van Rensburg, et al., 2019).

The electronic instrument responsible for the determination of alkalinity or acidity of substances is known as the pH meter. It also offers the opportunity to measure skin properties. The pH meter's electrode is associated with the electronic display (Wallace, et al., 2019). The electrode comes into contact with the skin and the skin's pH values are displayed on the digital screen. The pH electrode must be standardised before being used to measure skin pH. The standardised solution in which it must be immersed should be between pH 4.0 and 7.0 (Ye, et al., 2020).

1.4.1 Face Mapping

Face mapping is a revolutionary approach to **skin analysis**, stemming from the Chinese belief that an individual's inner health is reflected in their skin. Some facts are also discussed about Traditional Chinese Medicine (TCM) that uses face mapping to treat internal diseases entirely different than modern face mapping. Traditional Chinese Medicine (TCM) has evolved based on thousands years of experiments and observations in Chinese culture. TCM is deeply rooted into Chinese cultural belief system rather than

the scientific evidence. It is hard to find the numerical measurement data in terms of physical state of facial area and its links with the state of internal body organs (Johnson, 2002). The main reason that physicians have adopted using TCM because it is side effect free and easy to use.

Chinese medical belief system which is spiritually governed assumes the existence of invisible forces that flow throughout human body organs connecting each with symptoms which are observable on facial skin. TCM includes four basic types of treatments in Chinese culture: Acupuncture, Herbs and Diet, Massage Therapy and Medical Qigong. The literature of these medications is more qualitative rather than quantitative that cannot be considered as scientific evidence. Methods used for any type of TCM medications are derived from the combinatorial facts which are rather symbolic than the numerical facts. For example, a symptom can be thought of as a result of a combination of the state of several body parts and the effects of outer atmosphere. Therefore the symbolic qualifiers are used to evaluate a symptom, for instance, “tongue colour fades and the taste is sour” that could be considered as a symptom of some internal disease.

These effects cannot be measured in numbers, or the concerned chemical reaction in body cannot be assessed on molecular level. However, some computational approaches are used for example, data analytics techniques which are applied on databases of each type of diseases and herbs or formulations used in TCM medication. Some of the mining tools for TCM herbs and formulation are: MeDisco/3T, Ontology Learning System, Compound Innovation Method, and TCMiner. The databases of each disease have been acquired from the years of experiences by TCM practitioners (Lukman et al.,

2007). Other than this, TCM expert systems have been developed such as: Electronic-Brain Medical Erudite (EBME)/Medical Expert System (MES), Chinese Medical Diagnostic System (CMDS), A self-learning expert system, Traditional Chinese Medicine Sizheng Integrated Recorder and aided syndrome Differentiator (TCM-SIRD). These expert systems use some of the computational methods, such as, weighted summation (algebraic sum methods), ontology, hybrid Bayesian network learning algorithm, speech, facial and odor recognition algorithms. TCM diagnosis consists of four types of approaches; Inspection, Auscultation and Olfaction, Inquiring, and Palpation.

Face mapping is one of the computer based in-vivo technique that can be used with TCM to analyse the facial signs for skin beautification or diagnosis of internal body diseases. For instance, other than the facial skin care, face mapping has been used to detect diseases in kidneys, lungs, blood, digestions, etc. The literature suggests there is a number of TCM treatment methods available for each disease, such as, the external use of Chinese herbs and some methods: applicator, dipping, ironing, smoked, acupuncture, cut scores, knife kyu, washing Fengta. The TCM treatment methods are in fact different patterns of Chinese medication which have been practised in years by number independent physicians who have set their own standards for the treatment of each disease based on their own successful experiences (R Zhang et al., 2018). Since the aim is to discuss face mapping therefore TCM treatments and diseases are not discussed further. One of the major aims of this thesis gives reasoning about the internal body diseases by using In-Vivo methods instead of TCM. The TCM methods have insufficient scientific proof as compared to the specialised face mapping methods given

in this thesis. The face mapping methods defined in this thesis can be used to support TCM.

The International Dermal Institute contributed to the foundation of face mapping. The fourteen significant face mapping zones are distinct in features and contain their own needs and set of potential issues. Hence, rather than analysing it generally, it is analysed in distinct zones. The body comprises various vital organs that perform different functions (Wegrzyn, et al., 2017). The functionality of each organ varies from that of the others. The quality of the organs' performance contributes to the face's appearance, and face mapping is the practice of discerning the organs' health from the skin on different parts of the face in the complexion, manifesting as colour, dullness, lustre, or breakouts. According to Asian and European belief systems, aspects of facial appearance, such as complexion and shape, have the ability to reveal everything about the inner body. This ancient technique seeks to comprehend the reasons behind breakouts (Cowen & Keltner, 2020). Different types of facial breakouts help doctors to diagnose diseases and bodily health. Knowing how different facial zones work and what they reflect, they analyse the skin in these zones as a means of evaluating health status.

The roots of face mapping can be found in Chinese medicine and Ayurveda teachings. These teachings provided a road map indicating the underlying issues associated with bodily health and offering guidance regarding the use of **Chinese medicine** in treatment (Yang, 2019). Nowadays, treatment protocols have become more advanced and utilise the latest technology to improve facial features and to treat morbidity, and frequently facilitating diagnosis before the occurrence of symptoms (Kwon, 2019).

Today the TCM is practised with latest software and devices that help physicians recognize symptoms on skin surface by getting the deep skin images and measurements of different parameters i.e., temperature, hydration level, pH, skin thickness and Transepidermal Water Loss (TEWL). The devices used for this purpose consists computer programs, sophisticated cameras and light emitting sensors that first capture the skin surface and deep images and then software refines images to level that a human eye or even high resolution visual devices cannot identify the variations in each pixel. Some of these devices are given here:

Condenser-chamber system (AquaFlux, Biox systems Ltd, London, UK). It has a closed chamber equipped with a condenser cooler to below the freezing point of water (-7.65 C). The water vapour flux is determined by a humidity sensor, using Nilsson's diffusion gradient principle. No recovery time is necessary of the controlled microclimate.

Unventilated-chamber system. (SWL-2, Delfin Technologies Ltd, Kuopoi, Finland) is a portable and battery operated device containing a Honeywell humidity sensor HIH 3605-B in a closed chamber. The closed-chamber conditions are created upon skin contact with surface area of a 1 cm diameter. Measuring time is between 7 and 12 seconds. The instrument has to rest for at least 20 seconds between the measurements to allow the elevated RH (relative humidity) and temperature inside the closed chamber to return to ambient.

Open-chamber system. (Tewameter TM210, Courage+ Khazaka Electronic, Koln, Germany) This system is based on the principle of the diffusion gradient in an open chamber. The gradient of the water vapor pressure is measured indirectly by two pairs of

a combined thermistor and hygrosensor, which are mounted at two different heights inside a hollow cylinder (height 2 cm, diameter 1 cm). The probe head is placed horizontally on the skin and a constant pressure is applied. Once equilibration has been reached, measuring time is set to 45 seconds. During the whole experiment, determinations are performed according to published standardized protocols (Farahmand et al., 2009). OTTER, Fibre-optic OTTER (F-OTTER) and photoacoustic spectroscopy. The mechanical methods include the suction cup method (Dermaflex and Cutometer) and the torsional method (Torquemeter). In addition, magnetic resonance imaging has some specific features. Hundreds of similar devices are given in the literature accessible online from their company websites, or in the papers available on Google scholar.

Owing to these advancements, Chinese medicine is increasingly used for clinical tests, including scans and various types of blood test. Doctors complement it using modern techniques to examine the facial skin in detail for proper diagnosis (Qassem & Kyriacou, 2014).

Two main categories of skin exist: palmoplantar skin and glabrous skin. Palmoplantar skin covers the majority of the human body and is vital for ensuring hydration. The tissues retain moisture and prevent desiccation owing to this skin's hydration abilities. Its surface texture is soft and it is covered by a thick SC. It can withstand dry terrestrial environments owing to its potentiated surface barrier. Glabrous skin is the hairless skin that is present on the soles and palms. It is unable to maintain hydration levels owing to its inadequate surface barrier (Tognetti, et al., 2020).

Hydration plays a role in flushing out toxins and waste from the body, and skin hydration is responsible for the optimum functionality of vital organs. It nourishes the

skin and ensures an optimum glow that enhances one's attractiveness. As the body's largest organ, the skin must contend with unfavourable conditions to retain adequate moisture levels. Loss of moisture is particularly evident in extreme weather or as a result of sun exposure, morbidity, use of antibiotics, etc.(Arora et al., 2020). In such conditions, a higher water intake than normal is recommended. Dryness, brittleness of the skin, cracks and wrinkles are associated with chronic skin dehydration. The facial skin may be rejuvenated through hydration, which can combat signs of ageing and restore the skin's soft, smooth and glowing properties. As moisture in the skin's outermost layer is instrumental in flushing out toxins, when this skin layer is dehydrated, the toxins are retained and accumulate in the skin, which leads to drastic consequences. Carrying nutrients and flushing out toxins are the primary functions of the outermost skin layer leading to hydration (Yonezawa, et al., 2018).

The management of skin health relies on an optimum understanding of skin characteristics. These characteristics include biophysical, chemical and physiological parameters. The most significant biophysical features of facial skin include elasticity, the melanin index, and the erythema index. Moreover, it includes transepidermal water loss (TEWL), hydration and sebum content. All skin characteristics are affected by anatomical site, age, sex, morbidities, environmental exposure and physical activities.

Any change in skin appearance and structure may be indicative of a disorder. Rashes represent an early change to the skin that result mainly from irritation. Inflammation that manifests as redness and itchy rashes is known as eczema.

1.4.2 Acne Face Mapping

The American Academy of Dermatology conducted a study of acne prevalence and found that every year about 50 million Americans suffer from acne. Acne is the most common skin complaint and is particularly associated with major breakouts during the teenage years. Acne face mapping has shown that it may erupt in various zones as a result of lifestyle or medical issues. Acne on the head is thought to indicate an abnormal, inadequate or unbalanced diet and stress. The most significant remedy for forehead acne breakouts is increased fruit and vegetable intake. Additionally, higher water intake and adequate sleep are also beneficial in tackling forehead acne. Chinese medicine has also revealed that problems can occur at the hairline, which are most commonly the result of clogged pores due to makeup use, leading to skin problems at the hairline. Pomade acne occurs as a result of hair product use. According to Chinese medicine, the use of non-comedogenic cosmetics and double-cleansing can prevent the occurrence of pomade acne. The occurrence of acne between the brows is linked with dietary issues (Chen et al., 2020). It may be related to the excessive consumption of processed foods, fatty foods and alcohol. Cheek skin is affected by external influences, such as bacteria and air pollution, from cell phones and pillowcases, etc., which must be cleaned thoroughly to combat any potential skin issues.

Excessive sugar intake is linked to a high risk of acne. Acne on the jawline and chin indicates a hormonal imbalance. During pregnancy and menstruation, women typically experience hormonal imbalances leading to acne breakouts at the jawline and chin. In females, polycystic ovary syndrome also contributes to jawline acne, owing to the production of high levels of male hormones (Chen et al., 2016). Aestheticians use face

mapping to identify underlying issues, select the appropriate treatment and recommend lifestyle adjustments and dietary changes.

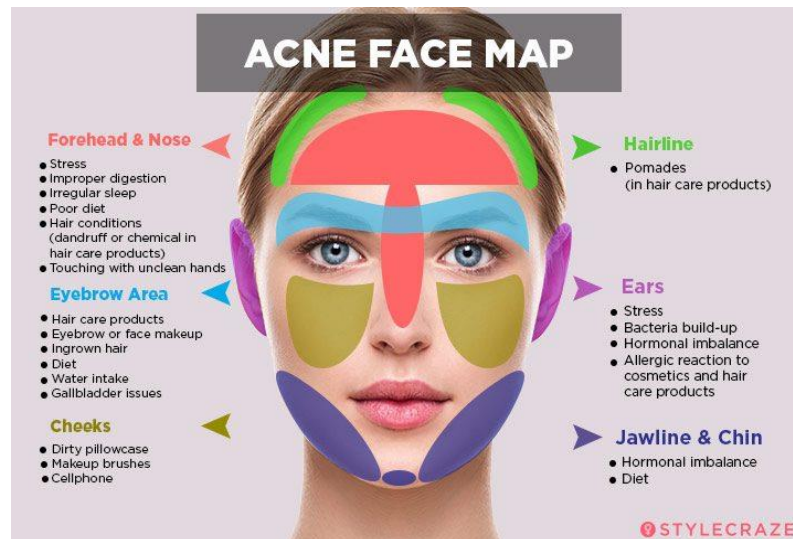


Figure 1.2. Acne Face Mapping (Healthline, 2019)

Skin pores and oil are the two most significant parameters leading to acne. Besides this, hormonal imbalance is the most common contributor to acne in teenagers. Oily skin may appear greasy and thus may impact individuals' confidence levels. Even blotting it with tissue paper may not be effective (Tsankov, et al., 2018). Poor skin hydration level can contribute to excessively oily skin. Individuals who suffer with acne may lose interest in their studies and experience social difficulties. Chinese face mapping deals with acne-related issues from the initial stages (Liaqat, et al., 2020).

1.5 Hydration vs. Moisturizing in Dermatology

The infusion of the human body's tissues and cells through the absorption of moisture is known as hydration. The body can absorb moisture from the environment, such as from the air, or can gain it from nutrients to improve the skin. However, moisturising actually refers to the process of locking or trapping moisture in the skin for longer, which works as a protective barrier. Both of these address the significance of water for the skin. These are valuable skin health parameters to help fight gigantic issues regarding environmental damage, premature signs of ageing, dehydration, and dryness. When the skin tissues or cells lose water content, the cells become thin, lose their elasticity and become dehydrated. Moisturising helps minimise the risk of water loss by sealing moisture inside the skin. The ability to form a protective barrier on the skin and grant smoothness to it is the key benefit of moisturizing.

The evaporation of moisture from the skin is natural. It normally occurs in conditions such as exposure to unfavourable conditions, stress, nervousness, health disorders, lack of skin barrier, etc. Minimal TEWL prevents excessive evaporation and seals moisture inside the cells. Skin that is flaking and peeling due to the cold in the winter or as a result of the impact of chemicals benefits from moisturizing (Samadi, et al., 2020). Another complication with skin is wrinkles and fine lines, which commonly occur with a lacklustre or dull complexion. It indicates that the skin is battling hard against dehydration.

Dehydration of the skin can be characterised by starved and parched cells. According to dermatologists, the easiest and most efficient way to deal with dehydration is to consume an adequate amount of water and supplement it with an effective topical

hydrator that draws and binds the water molecules to the skin tissues (Cadavona, et al., 2018). Dermatologists highly recommend products that contain HA (hyaluronic acid) for the improvement of skin health that potentiates the skin's ability to hydrate itself. Hence, it is important to look for ingredients in cosmetic and medicinal topical products for better health and skincare. These advantageous ingredients also include marine extracts, honey and aloe (Crowther, 2016).

Similarly, some highly effective synthetic humectants for gaining and retaining moisture are propylene glycol, urea and glycerin, and individuals should look for these ingredients when selecting their beauty products. While skin type varies from individual to individual, hydrating ingredients are suited to each skin type. These are easily soluble in water and do not lead to clogging of pores. These products must be devoid of alcohol, which can irritate and dry out the skin. There exist numerous options for ingredients and formulae in cosmetic products. Moisturisers are available in various types, such as heavier or lighter, for different skin types, or with different formulations. For the months of summer or spring, light lotions or gels are recommended (Spada, et al., 2018). By contrast, heavy formulation products with ceramides, dimethicone or butters and oils work better for cold and dry weather. These serve dual functions—skin nourishment and moisturisation. Additionally, they can counteract signs of ageing and prevent damage caused by free radicals. According to the renowned dermatologist, Guanche, oil-free moisturisers are best for acne-prone skin. These contain more water for skin hydration, and their oil content is negligible. Morning and night are the best times for the application of moisturisers and skin hydrators. Apply hydration after using moisturising creams or lotions so that the skin remains prevented from peeling (Has, 2018). The

multifaceted benefits of HA for human skin are commendable. It regulates various biological processes, including immunomodulation, anti-inflammatory processes, tissue regeneration, wound healing, and skin repair. HA's remarkable tissue regeneration properties and biomedical uses compel dermatologists to include it in nutricosmetic products. The clinical evidence for HA's high efficiency in cosmetic items leads to its use in cosmetic products, especially for skin rejuvenation (Abatangelo, et al., 2020). The most commonly used HA-based formulations are implants, serums, lotions, autologous fat gels, facial fillers, dermal fillers, intradermal filler injections, creams and gels (Aragona, et al., 2019). Besides its face-rejuvenating properties, it grants the benefits of space-filling, anti-ageing, anti-nasolabial fold and anti-wrinkle properties (Huynh & Priefer, 2020).

1.6 Measurement of Skin Hydration

Rigid probes are used to assess skin hydration. These devices come into contact with the skin and automatically calculate and display the hydration level of that particular region by computing the dielectric permittivity (dielectric constant ϵ) between water and other substances as a standard. In electronic engineering the devices that compute the physical quantities are called Transducers. The device senses the physical quantity by transforming the detected signals into electrical pulses generated by changes into electronic quantities such as capacitance, resistance, voltage or current of device's internal components. For instance, the device gets impairments in its capacitance when detecting the water quantity in skin. The capacitance variations are measured by different devices by different statistical formulae. The most commonly used measuring

devices for skin hydration are Nova DPM 9003, Corneometer CM820, and Skicon200. The moisture barrier of the skin is mainly responsible for locking water content inside the skin. It is known as the lipid barrier and ensures the health and hydration of the facial skin. A balanced diet that contains abundant organic food also helps boost the skin's water content. However, spicy food has the potential to lead to skin dryness.

One of the most popular corneometer devices is Epsilon. It utilises the calibrated dielectric permittivity scale to measure the hydration level of different anatomical sites of facial skin. The contact imaging of skin and dielectric permittivity of the near surface are measured with the help of the novel instrument. It contains signal processing algorithms and proprietary electronics that detect signals with the help of a sensor (Al Hashimi & Xiao, 2018). The measuring abilities of Epsilon's calibrated scale provide the hydration level of the SC and TEWL. Epsilon's main difference from various other systems lies in the features of dielectric permittivity's linear response and calibration. These work well in Epsilon because water contains much higher dielectric permeability compared to various other skin constituents. The relationship between permittivity and hydration is direct; therefore it gives a linear response. The visibility of the skin's anatomy is necessary for the determination of injuries, diseases and the condition of the skin. The more visible the skin's anatomy is, the more detailed and accurate is the information it can provide (Logger et al., 2019). Indeed, it is the main element that is required for the diagnosis and selection of treatment protocols. The efficient probe easily determines the best treatment, which significantly impacts the skin and the underlying soft tissues. One such device is known as the EPSICAN I-200.

This device works (emits) in the range of 20 MHz to 50Hz and hence enables the dermatologist and cosmetologist to visualise skin anatomy and detect injuries and diseases. Skin texture can be significantly improved through enhanced skin hydration (Xiao et al, 2020). The ultrasound images produced by different devices vary in terms of quality and the detail these provide which are numerically given in each chapter. Images produced with lower resolution yield ambiguous results and hence affect the outcomes. High-resolution images allow the application of the appropriate devices in aesthetic and beauty care (Wei, et al., 2018). Gauging the results obtained from different devices, as given in the next chapters, is ample to select rational devices for skin condition diagnosis. The images produced during facial skin analysis by Episcan are more accurate as discussed in chapter 4. Visible variances in the facial skin may be attributed to numerous factors, including medical conditions, geographical regions, gender, race and age (Jansen, Franken and Du, 2019).

All these parameters were excluded from the present study and considered hydration or water content at different anatomical sites of facial skin. Likewise, various research devices help in the analysis of skin conditions through in-depth imaging. These offer pictorial representations of facial skin from different aspects. The outcome for each instrument varied from those of the others due to the use of different techniques, the instrument's calibration and the instrument's functionality. Various instruments' modes of working also vary. The most useful devices for measuring and analysing facial skin are Episcan, Epsilon and AquaFlux. All of these are intended to provide different outcomes and conclusions for facial analysis (Al Hashimi and Xiao, 2018). Episcan provides details about the facial skin through the use of ultrasound imaging. AquaFlux

makes it easy and swift to determine TEWL for different facial skin sites. However, Epsilon is the best corneometer for determining skin hydration.

For the measurement of hydration levels with Epsilon, all participating individuals had healthy skin. None of these suffer from injuries, bruises, wounds or harm to their facial skin.

1.7 Ethical Approval

Approval for the study was obtained from the Ethical Committee of London's South Bank University, Application Number: UREC 1412, see Appendix for the approval letter. The professional aesthetic beauty clinic was approached to obtain the measurement results of healthy male and female participants (Wu, et al., 2019). Both male and female participants were enrolled in the study with their consent, and their confidentiality was appropriately maintained. For each participant, the Epsilon reading at multiple facial locations was determined and recorded carefully. The result was determined after compiling the whole data using the most suitable statistical analysis tool. Gathering the results and dealing with them was comparatively more manageable in the aesthetic clinic's comfortable environment (Ezerskaia, et al., 2016).

1.8 Organisation of the Thesis

The thesis is arranged in seven chapters, of which five chapters are descriptive portions of the thesis, including the Introduction, Literature Review, Skin TEWL Measurements, Skin Hydration Measurements and Skin Ultrasound Measurements. Chapter 6 gives the

concluding remarks and the future outlook. Chapter 7 summarizes the original contribution to knowledge, which is followed by the list of the author's publications and the bibliography.

1.8.1 Synopsis of Thesis

The demand and desire for attractive facial features has contributed the cosmetic market's tremendous success. For an individual to appear young, their facial skin of the face must be fresh and relaxed. Sagging of the facial skin reflects old age and may also involve wrinkles at multiple sites. Individuals with fresh and young-looking facial skin have higher confidence levels than others. War can cause damage to the human body, including deadly injuries and wounds, especially among soldiers. The most common damage was seen to affect the chin, nose, cheekbones and jawbones, harming the facial structure and skin. Some victims were left unrecognisable due to deep wounds, cuts and injuries. They were subjected to post-facial surgery treatments that attempted to recover their original appearance with improved skin structure and texture. This works by rectifying skin nutrient deficiencies and increasing facial blood circulation with the help of dermatological services aimed at nourishing the skin and recovering skin tissues. The skin layers discussed in this thesis are the hypodermis, dermis and epidermis. The epidermis is the skin's topmost layer and acts as a barrier for skin against harm. It contains pores at different anatomical sites, contributing to oil and moisture efflux. These can also lead to an influx of dust, dirt and pollution upon exposure to the external environment.

The size and number of pores at different sites vary; hence, the rate of influx and efflux varies. It resists the penetration of harmful UV rays entering the skin and avoids

hazardous effects to a maximum extent. Thinning of the skin primarily occurs due to neglect and dehydration. Thus, this thesis aims to determine the hydration levels at different anatomical sites of the facial skin. It also aims to determine the effect of exercise on the hydration levels of different skin sites, keeping in mind the variation of hydration with respect to age and gender. It will also measure facial skin quality at various sites using Epsilon.

Highlights of Chapter 1

In Chapter One, “Introduction”, the scenario wherein people are becoming more concerned about their skin’s health and seeking reliable skincare solutions is described. As more individuals are attracted to the wellbeing of their skin and health, the aesthetic industry has grown. Face mapping is the art of identifying the underlying issues in the body from the facial skin. They are convinced that the face reflects the body's inner condition and health. Hence, the technique can be used in the aesthetic industry to optimise elegance, appeal and younger looks. The chief objective of this study was to determine the hydration levels of facial skin at various anatomical sites.

Moreover, the study is directed at visualising the skin in depth for the purpose of analysing underlying issues. The method involves the use of the latest technology for skin assessment. The study was conducted without any gender discrimination. Dermatology and cosmetology increasingly use ultrasonic techniques more frequently for the determination of skin health and integrity. The main reason for using such techniques for skin analysis is that they are non-invasive. They visualise the skin optimally and provide information about scars, tissue inflammation, echogenic variations, and epidermal thickness. This section will also discuss face mapping, which

divides the human face into fourteen distinct zones, each zone being representative of a different body organ.

Highlights of Chapter 2

Chapter Two, “Literature Review,” focuses on the association between skin health and the diseases that can be estimated from the quality of the skin and the underlying integrity of skin tissues. Face mapping clearly indicates the organ that is suspected of causing problems in the body based on the results of skin assessment. Hence, the dermatologist assesses the skin of the individual understudy and recommends the most appropriate and rational treatment for their complaint. Giovanni and Stefania conducted a study to evaluate facial skin thickness and echogenicity.

The parameters of age will be analysed to determine variations in echogenicity and skin thickness. The results indicate that the skin of the lower and upper lips is three times thicker than the skin of the upper eyelid. The discussion will include a study wherein healthy Japanese women were enrolled to determine the surface structure of facial skin at various anatomical sites. The structure and shape of the skin pores will be discussed. This section will also discuss a study that was conducted to observe the SC layer's skin condition for the estimation of skin hydration levels.

Highlights of Chapter 3

Chapter Three, “Skin TEWL Measurements,” examines TEWL at various anatomical sites on the facial skin. In this study, nine different anatomical sites of facial skin were included for TEWL determination. The ages of all human subjects were taken into

consideration to draw the results accurately. The first segment concerns the determination of variance between TEWL values at different anatomical sites of facial skin. However, the second segment includes a determination of the association of TEWL with age. The highest variance of TEWL is reflected for the neck and lip. This will determine the highest and lowest TEWL values for lip and neck skin. Hence, the presence of puckered skin and dehydration will be investigated.

Highlights of Chapter 4

In Chapter Four, “Skin Hydration Measurements,” Epsilon is discussed one of the most significant instruments for skin analysis. Section One includes an evaluation of variations in facial skin at various anatomical sites. In the second section, the Epsilon values for facial skin calculated before and after exercise in both genders are presented. According to the results obtained, the under-eye skin reflected the highest mean Epsilon value. However, the mean Epsilon value of lip skin was determined to be the lowest. The mean Epsilon value for under-eye skin and lip skin will also be calculated in this chapter. Skin structure and composition vary from one anatomical site to another. According to the experimental study, the highest mean value of Epsilon will be recorded for the eye-corner skin. The cheek and nose will also be assessed for their Epsilon values.

Highlights of Chapter 5

This chapter, “Skin Ultrasound Measurements,” will demonstrate that of all the anatomical sites of facial skin, the cheek has around three percent greater percentage of

the dermis than the rest of the anatomical sites. The chapter also provides numerous statistical studies based on the Welch test to determine which facial sites have similar width of each of the three skin layers; this can be considered a version of statistical face mapping. Finally, the feasibility to train a Machine Learning- based classifier of the facial sites based on the high-resolution ultrasound images of the sites was evaluated.

1.8.2 Prospective Exertion

The study revealed that the reasons for variation in values for different facial skin sites was the degree of corneocyte formation, lipid contents of SC, skin temperature, damaged barrier function, bodily health, and skin blood flow. The unequal sampling for the three methods of skin determination resulted in some limitations. Skin analysis is promising with respect to its potential applications in determining the optimum treatments for the body's physiological and pathological factors.

High TEWL values are associated with high pH values of the skin. The main reasons for the variations in TEWL values include blood circulation through the skin, damaged skin barrier function, skin temperature, lipid contents of different skin layers, skin temperature and degree of corneocyte formation. The second section involved in the determination of skin analysis by Epsilon considered the parameters of the exercise. A key limitation of the study was the inappropriate sampling in the three facial skin determination approaches. The decline in collagen and elasticity leads to skin sagging. Skin analysis will advance considerably in the near future and will provide personalised skincare to humans. The increasing ratio of ageing, collagen breakage, skin roughness, and wrinkles will decline in the future.

1.9 Chapter Summary

Individuals' self-consciousness with respect to their skin and health has contributed to the growth of the cosmetic industry. People are becoming more concerned about their skin's health and seek the most reliable solutions to their beauty concerns. According to face mapping, both are linked with each other. Face mapping is the art of identifying the underlying issues in the body from the face. The face reflects the body's inner condition and health. Hence, it can be used to optimise one's elegance, appeal and younger look. The aim and objective of this research study was to determine the hydration levels of skin at various anatomical sites. The study is also aimed at visualising the skin in depth as a means of analysing underlying issues. The method involves the use of the latest technology for skin assessment. Non-invasive technology is used to avoid any harm and obtain accurate results. Various factors were taken into consideration to determine their effect on skin characteristics, physiological properties and hydration. The study was conducted without any gender discrimination. Dermatology and cosmetology use ultrasonic techniques more frequently for the determination of skin health and integrity. The main reason for using such techniques for skin analysis is that they are non-invasive in nature. They visualise the skin optimally and provide information about skin scars, tissue inflammation, echogenic variations and epidermal thickness. Comparison of all these values with the standard value can help reveal the underlying cause. Face mapping divides the human face into 14 distinct zones, with each zone representative of a different body organ.

Chapter 2. Literature Review

2.1 Introduction

This chapter provides an general overview of skin research and skin measurement technologies. The experiments performed to measure hydration level, TEWL and the observations of ultrasound are formally given in corresponding chapters. Additionally the observations and conclusions are presented for each practical in easy terms comprehended from the arithmetic of corresponding results.

The role of Stratum Corneum (SC)in controlling hydration, the factors that cause water loss from facial skin and instruments that can effectively measure water loss from the facial skin and provide effective visualisations of facial skin. Hydration of the skin prevents the desiccation of tissues (Lambers, 2006). In dermatology and cosmetology, ultrasound techniques are becoming increasingly popular owing to their non-invasive nature in accessing scars, tissue inflammation, echogenic variations and epidermal thickness.

AquaFlux, Epsilon and Episcan are various instruments used to assess the various physiological properties of the skin, especially the facial skin, when the specific concern is cosmetic. AquaFlux and Epsilon are skin measurement instruments developed by Biox Systems Ltd, UK. AquaFlux can be used for skin TEWL measurements. Epsilon can characterise the human skin's physiological parameters up to a perceptible sensing depth (~20 micron). It can measure skin hydration based on the dielectric permittivity values, as the skin has different dielectric values for different layers(Feldman, 2009).See

Table 2.1

Layer	Permittivity ϵ	Layer width (μm)
Dermis	3.9	1000
Epidermis	3.2	350
SC	2.4	30

Table 2.1. Skin layers and Epsilon capacity of measurement

The Epsilon software displays colour-coordinated histograms that indicate hydration distribution for both the whole image and the region of interest (Bioxysystems, 2010). Finally, Episcan, developed by Longport Inc., USA, utilises ultrasound techniques with frequency band 20 to 50 MHz to display images of the skin's strata. It can detect variations in skin surface thickness and density through which it can indirectly measure TEWL and skin hydration. Subtle changes in thickness, density and fluid content can be clearly appreciated (Longport Inc., 2012).

2.2 Skin Analysis

Skin analysis is usually carried out to determine its condition and the most suitable treatments applicable to the observed skin structure. Conditions may include dryness, roughness, pore structure, blackheads, bumps, acne and sun damage. Before administering any treatment, a good dermatologist will always study the patient's skin and its various physiological parameters and then move to suggest a particular treatment method (Gunathilake, 2009). The analysis begins by removing any particle of face skin that could serve as an impediment **sample** to the study of **damaged** skin type, structure and organisation. To achieve the best results, all particulate matter and traces of cosmetic products should be removed before the analysis begins (Rawlings, 2003).

The skin is broadly divided into two types: glabrous skin and palmoplantar skin. Glabrous skin is present on the palms and soles; it is also called non-hairy skin. By contrast, palmoplantar skin covers most of the body and plays an essential role in maintaining the hydration state of our skin (Hillebrand, 2001). It is generally accompanied by a thick SC with a gentle and soft surface texture. It maintains a high surface (skin) barrier function compared to the glabrous skin and support our existence in the dry terrestrial environment (Berardesca, 2006).

2.2.1 Facial Skin Analysis

The facial skin is the most delicate part of the body as it is exposed to rough weather conditions, sunburn, pollution and humidity, which catalyse the ageing process of the facial skin as compared to elsewhere on the body (Chu, 2011). To develop a holistic model for facial skin analysis, it is important to consider various morphological and visual parameters of the facial skin. A brief discussion on facial skin is included hereunder:

2.2.2 Facial Skin Thickness and Echogenicity in Different Anatomical Locations

A study was performed by Giovanni and Stefania to study variations in facial skin thickness and echogenicity with respect to different anatomical sites and age. The study concluded that skin thickness measured in (mm) is significantly higher on the upper and lower lips, chin and infraorbital regions than on the central forehead, lateral forehead and cheeks, given in Figure 2.1. In elderly subjects, an increase in facial skin thickness was observed on the forehead, cheeks, lips, chin and nose, and a thinning on the infraorbital regions, compared with younger subjects. The increase in skin thickness values was statistically significant in the lateral regions of the forehead, upper and lower

lips and the nose. On the other hand, skin echogenicity was higher on the upper part of the face (forehead, infraorbital regions and cheeks) than on the lower part (lips and chin) (Giovanni, 1999).

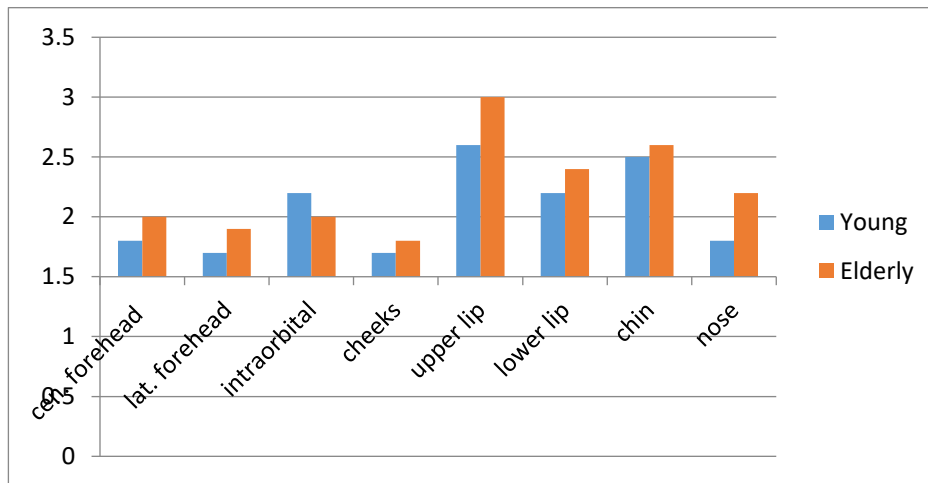


Figure 2.1. Facial Skin Thickness (mm) in different anatomical locations

Another study by Adams used biopsy specimens at 15 facial sites identified as clinically relevant locations: upper lip vermilion, lower lip vermilion, philtral column, chin, upper eyelid, lower eyelid, brow/forehead, right cheek, left cheek, right neck, left neck, malar eminence, nasal dorsum and nasal tip. Skin thickness measurements were evaluated by analysis of variance, and ratios of skin thickness were calculated using the upper eyelid as a referent site. The ratios suggested changes in dermal and epidermal thickness along with various anatomical locations. It was concluded that the relative thickness index served as a quantitative guide for differences in skin thickness between various areas of the face. By using the relative thickness index, surgeons have a template that describes

the nasal tip skin thickness to be approximately 3.3 times thicker than that of the upper eyelid (Adams, 2005).

2.2.3 Variation of Facial Skin Colour with Age, Gender and Environmental Conditions

Numerous studies have focused on the relationship between race, ethnicity and gender and skin colour (Leung, 2002). However, there is a dearth of studies analysing the effect of environmental concerns on facial skin colour (Wei L, 2007). A study was conducted to analyse skin colour at four facial skin sites in 409 volunteers comprising 219 males and 190 females aged 20–79 years. By comparing the skin colour of Chinese individuals living in different environments, some factors did not exhibit explanatory power of the skin brightening. The study concluded that gender is an important factor affecting facial skin colour. Females with an average intermediate facial skin colour tended to be fairer than males with an average slightly dark facial skin colour. The study found that age has a significant influence on facial skin colour.

2.2.4 Facial Pore Characterizations

Facial pore openings are not typically observed at a young age, but pores tend to become more open with ageing and do not appear to close again in older skin as the tissue structure around the pore keeps the pore open (Inomata, 2007). Thus, the tissue structure around the pores might affect structural immobilisation (Koji Mizukoshi, 2013). In addition, in the case of inner skin structures, the skin surface structures around the pore might have different structures from those in the other skin areas (Mizukoshi, 2009).

A study was performed to analyse the skin surface structure of 248 healthy Japanese women. Subjects' ages ranged from 10 to 50 years, with ~50 subjects in each decade group. The results showed that the ratio of the pore area increased with age (Sugiyama-Nakagiri.O, 2010).

The traditional methods of pore visualisation have limitations. These methods cannot account for small and invisible pores (see Figure 2.2), so for facial pore characterisation; a study was carried out using image analysis tools. The study found that the image analysis method was able to measure pore colour, shape and orientation in addition to size and count, facilitating a holistic study of facial pores (Bandara Dissanayake, 2019).

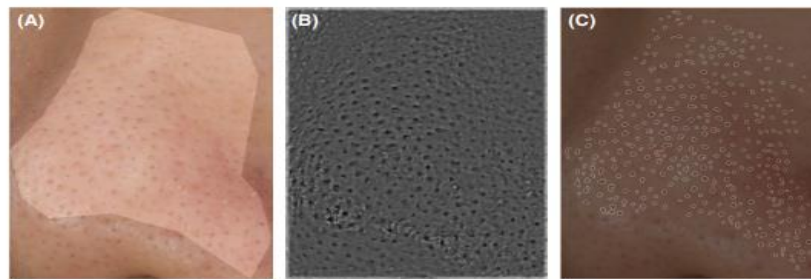


Figure 2.2. Image Analysis of Pores in the Nasal Region (Dissanayake & Miyamoto, 2019)

2.3 Facial Skin Mapping

Face mapping stems from an ancient Chinese belief that a person's skin reflects their inner health (Healthline, 2010). Face mapping is a revolutionary approach to skin analysis that was developed by the International Dermal Institute. Rather than analysing the skin in general terms, face mapping divides the skin into 14 distinct zones, each with its own set of potential problems and unique needs (LogicalSkincare, 2012).

The classification of each zone is explained in the following Figure 2.3.

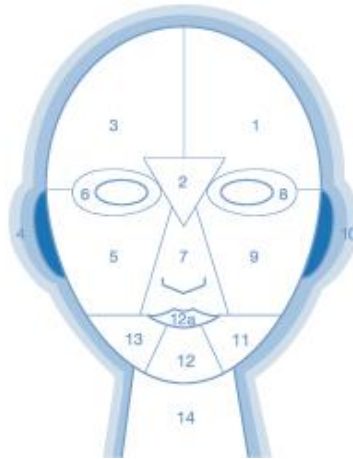


Figure 2.3. Pictorial Representation of Face Mapping Zones (LogicalSkincare, 2012)

Zones 1 and 3 are regarded as ‘sisters’ to the bladder and digestive system. If one frequently breaks out in these zones, then higher water intake is recommended. Zone 2 between the eyebrows is related to the liver. Congestion in this zone indicates intake of alcohol or any food allergy. Zone 4 and 10 are related to the kidneys. If the ears appear red, then caffeine and alcohol intake should be monitored.

Zones 5 and 9 indicate distress in the respiratory system. If dark circles surround zones 6 and 8, the body is suffering from excessive dehydration. Zone 7 indicates the nasal region and upper lip area. A reddened nose can indicate heightened blood pressure or early stages of rosacea. Congestion around the upper lip can occur as a result of comedogenic lipstick or liner use.

Zones 11 and 13 can breakout due to dental surgery. For women, this area is related to the ovaries and breakouts can occur due to menstruation. In zone 12, breakouts can indicate hormonal imbalance, possibly caused by stress. Finally, adrenal stress can often lead to flushing in zone 14.

A comprehensive mathematical treatment given in subsequent chapters, continuous colour mapping analysis of facial skin hydration, barrier function, skin surface pH and sebum has highlighted inter-ethnic differences in these parameters that are unexpected based on other published single-point measurement data (Lopez, 2000).

2.3.1 Capacitance and Trans Epidermal Loss Mapping

An observational study was conducted among 16 young females (21.8 ± 1.1 years old) without visual signs of photo aging, all living in Pretoria (Voegeli, 2015). SC capacitance was measured using a Corneometer CM825 and basal TEWL was assessed using an AquaFlux AF200 on 30 predefined sites on the left-hand side of the face, as shown in Figure 2.4.

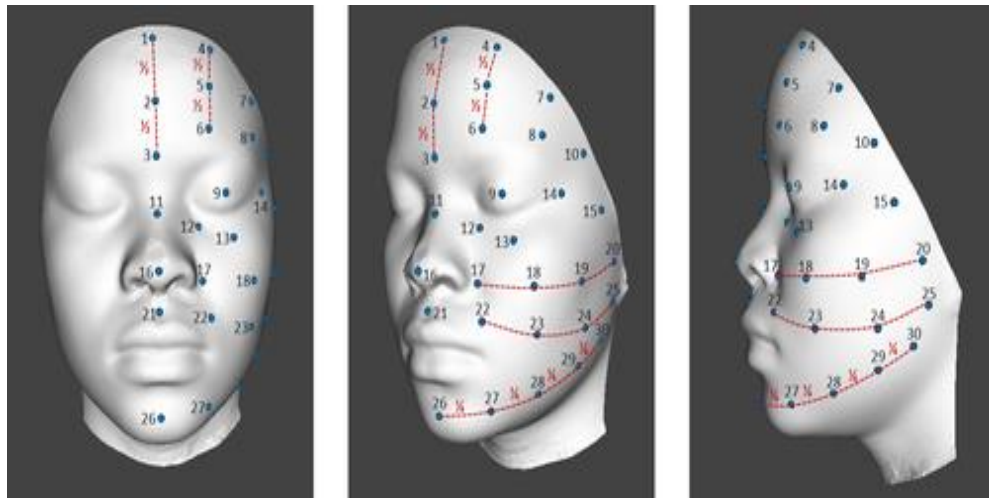


Figure 2.4. Thirty predefined sites for Skin Mapping (Voegli, 2019)

Although a certain level of heterogeneity was expected, the complexity of facial hydration and barrier properties was surprising, as Figure 2.5 illustrates. Remarkable skin hydration and TEWL gradients were observed. On some areas of the face, subtle differences were found, particularly in the Chinese subjects, but in others, steep

gradients were observed within short distances. Related mathematical models, observations and analytics are given in next chapters.

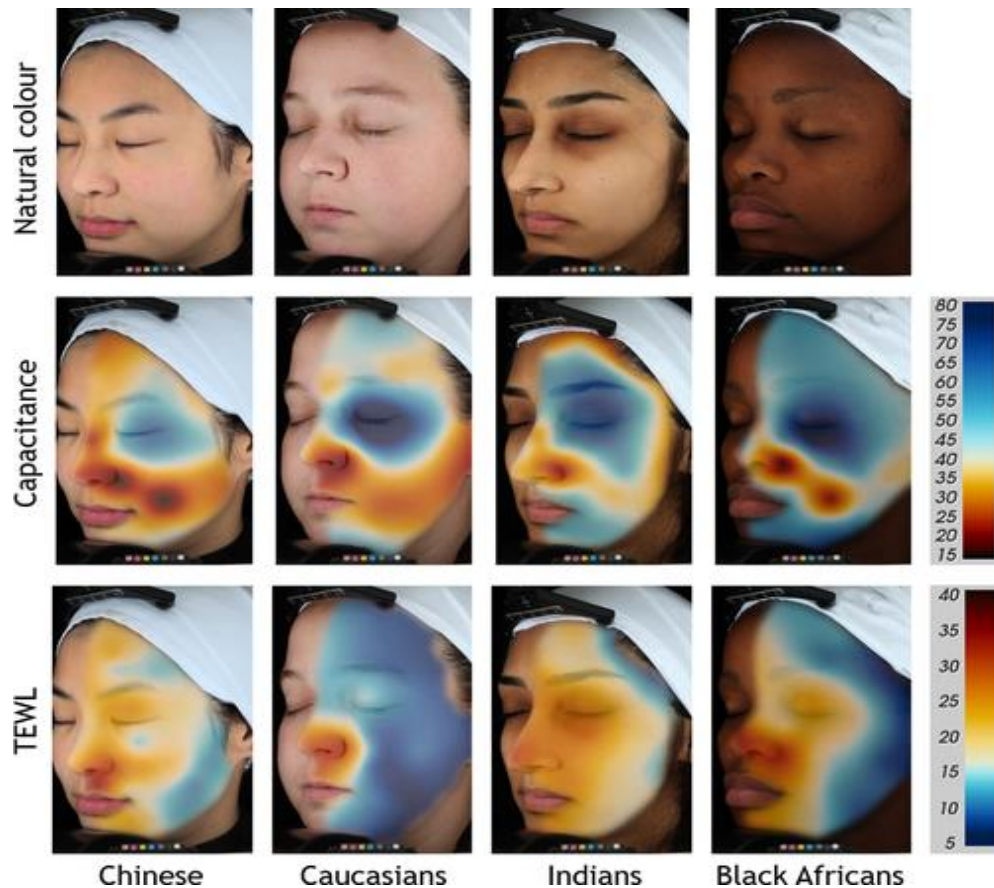


Figure 2.5. Interethnic Skin and Capacitance Mapping (Voegli, 2019)

2.3.2 Study of Moisturising Using Skin Mapping

Moisturising (hydration level) is measured as dielectric constant of the skin. The measurement time is short at only 1 second minimizing occlusion effects. The depth of the measurement is 10-20 μ m. A study was performed to observe the effects of miniaturisation on people from different ethnicities. The study comprised a three-day conditioning phase and a longitudinal 28-day application phase. During the conditioning phase, the subjects did not apply any dermatological or cosmetic products. During the

application phase, a moisturising cream containing saccharide isomerate, niacinamide and glycerine was applied twice daily, one in the morning and next in the afternoon under normal conditions of use. The evaluations on day 28 were taken at least 12 hours after the last application of the moisturising cream. The facial mapping of different subjects is shown in Figure 2.6.

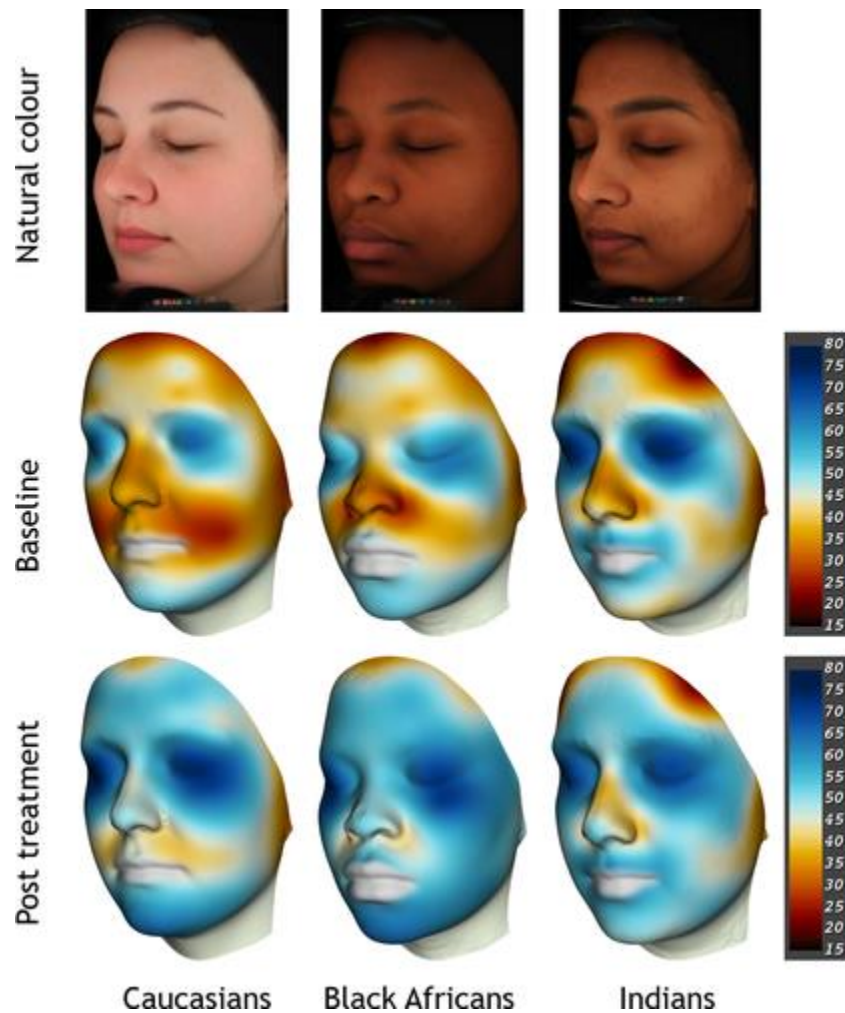


Figure 2.6. Moisturisation Skin Mapping (Rogiers, 2001)

No statistically significant differences were observed between the ethnicities when the overall baseline skin hydration values were considered, and in all subject groups a significant improvement was observed after four weeks of treatment (Rogiers, 2001).

2.4 Stratum Corneum (SC)

The SC is the transparent skin layer that inhibits water loss from the facial skin into the atmosphere. It has a barrier function that can be quantified by calculating the TEWL measured as grams of water per square meter per hour ($\text{g}\cdot\text{m}^{-2}\cdot\text{h}^{-1}$) (Alexander et al, 2018). The water content of the SC is necessary for proper maturation and prevention against peeling. Increased TEWL impairs the enzymatic functions required for normal desquamation, resulting in the visible appearance of dry and flaky skin (Bonté, 2007).

Compared with other body parts, the SC of the face is usually thinner in size and consists of smaller layers of corneocytes (Berthaud & Boncheva, 2011). The thickness of SC also varies in different regions of the face; for instance, nose, cheek, eyelids and perioral regions have different SC characteristics (Tagami, 2008; Tagami & K., 2003). However, these features do not remain stagnant but vary according to age, gender and demographics (Ya-Xian, 1999). Lipids and corneocyte size have a direct bearing on the barrier function of SC. The corneocytes are produced in the lowermost SC layer; however, they are gradually transferred into the upper SC layer, where they form a covalent bond with the intercellular lipids, as shown in Figure 2.7, via the esterification of glutamine or glutamate residues of involucrin, periplakin and envoplakin composing the SE that firmly covers their cell body (Wang, et al., 2018). This forms a hydrophobic

formation on the SE of mature corneocytes, and intercellular lipids become well organised, making a significant contribution to the barrier function. (Kashibuchi, 2002)

The characteristics of SC layer are not uniform across the entire facial skin; therefore, hydration also varies. The eyelid skin is distinct from the skin in other areas because its SC is composed of a poor skin surface lipid and a thin SC cell layer of large corneocytes that brings about a high surface hydration state and consequently a poor barrier function, whereas the vermilion borders of the lips that are covered by an exposed part of the oral mucosa exhibit remarkably poor barrier function and a low hydration state (Koch, 2006).

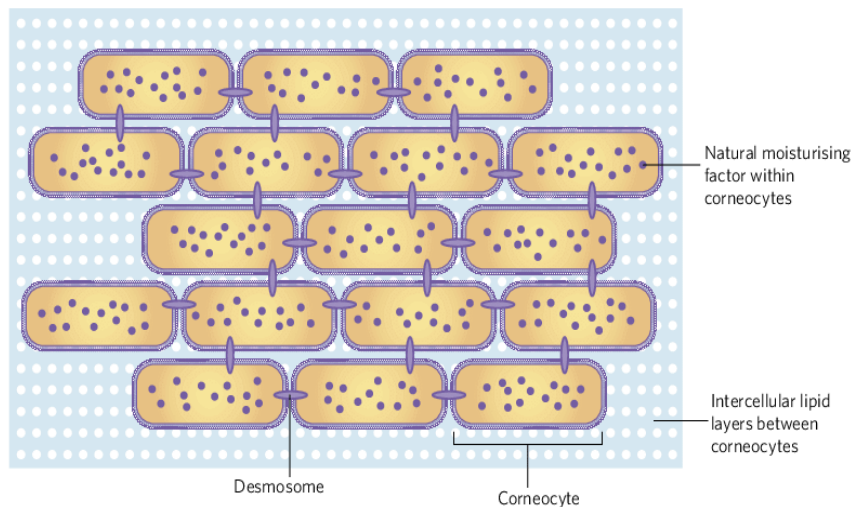


Figure 2.7. Structure of Stratum Corneum (Beekman & Campbell, 2015)

2.4.1 Functional Characterisation of SC

A functional characterisation of facial skin along different age groups can give us some indication of the variation of SC (Kim, 2006). The characteristics of facial skin studied in adults appear to be morphologically and functionally distinct from those of the skin

elsewhere on the body. Babies' skin is less exposed to harsh environmental conditions. At birth, their skin undergoes a transformation from a fully hydrated state and later develops an SC that is morphologically and functionally unique to each region. Interestingly, from the data available so far, babies' facial SC barrier function evaluated with TEWL seems to be the best, being almost at a level similar to that of the adult flexor forearm (Tagami, 2003). In contrast to children, elderly individuals' SC consists of thicker SC cell layers and shows slow turnover, a well-maintained barrier function, and a remarkably low SC hydration state if not accompanied by inflammation (Hara, 1993).

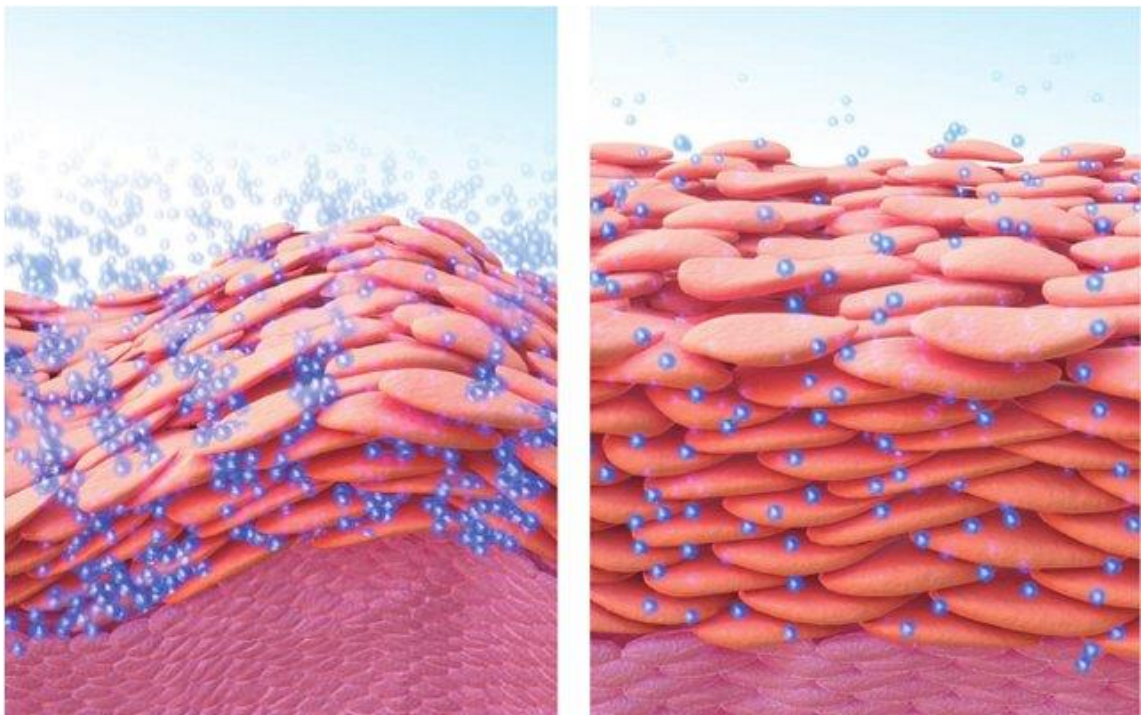


Figure 2.8. The SC of infant skin (a) and adult skin (b) is hydrated (small blue spheres) under normal conditions. (Telofski, 2012)

Infant SC is more hydrated but also loses water at higher rates than adult SC (Telofski, 2012), see Figure 2.8. A study to determine the influence of ageing on biophysical

parameters by collecting data regarding TEWL, high-frequency conductance, and size of superficial corneocytes on the cheeks, nasolabial folds, and chins of 303 healthy Japanese female volunteers of different ages was conducted. The results showed that the SC's barrier function was best on the cheek, presenting the lowest TEWL, which was significantly higher on the nasolabial fold and chin than on the cheek (Gross, 2016).

2.5 Factors Affecting Skin Hydration

2.5.1 Facial Skin Hydration and pH

The human SC has a pH gradient from an acidic pH to a neutral pH (Ohman, 1994). Therefore, the circadian rhythm in the skin surface pH may reflect circadian variations in enzyme function in the human SC. A high pH is frequently correlated with high TEWL (Patrick, 1988), but in our study, no correlation was observed between the circadian rhythms in TEWL and those of the skin's pH (Yousiovipch, 1998).

An increased skin pH raises the rate of enzymatic reaction at the rate of SC's lipid metabolism. This might contribute to the formation of a skin barrier, which is normally observed. Syndets are now preferred due to their bacteria-regulating properties and the skin's favourable tolerability profile. Acidic syndets are of value even for persons with healthy skin and for skin cleansing in patients with seborrheic-type diseases.

2.5.2 pH-meter

A pH meter is an electronic instrument used to measure the acidity or alkalinity of any substance. It can also be used to measure the aforementioned properties of the skin. It consists of an electrode that is connected to an electronic display. When the electrode

touches the skin, the pH is indicated on the electronic display. The pH electrode must be standardised before used by immersion in a standardised solution of pH 4.0 and 7.0.

2.5.3 Facial Skin Hydration and Temperature

The temperature of the skin is distinct from the internal optimal body temperature of 37°C. Skin temperature is often influenced by various environmental factors, such as circulating air, ambient temperature and humidity, which can cause body temperature to vary significantly. The variations in the skin temperature can result in decreased or increased chemical flux across the skin. Skin permeability is dependent upon the temperature such that an increase in temperature would result in increased permeability. Simply, high temperature triggers increased fluidisation, resulting in increased diffusion and osmotic coefficient of drugs. Therefore, it is important to determine whether different areas of the facial skin show abnormal variations with respect to temperature. For this purpose, infrared imaging techniques should be used. An Infrared Thermometer is a device that measures temperature or temperature gradient from the thermal radiation of the object.

2.5.4 Thermal Imaging Camera

Thermal imaging cameras use infrared radiation in their operations, with the difference that they produce a temperature profile of a larger skin area, in some cases the entire body. Thermal imaging cameras are mainly used to sense certain characteristics in the environment.

The transmission of infrared radiation must also be efficient. The FLIR T420 uses optical fibre, a vacuum or the atmosphere for effective transmission. Moreover, optical lenses help to effectively converge and focus the infrared radiations. This largely

involves optical lenses made from polyethylene fresnel, quartz, germanium and silicon. Detecting radiation is an important process in the functioning of the camera. The infrared detectors contribute significantly to making it a reality.

The detection of skin temperature is one main function of this camera in medicine. This is realised using a non-invasive no-touch technique whereby the infrared portion of the spectrum emits heat energy. The human skin enhances its functionality by functioning as an excellent blackbody radiator. Thus, the thermal imaging system produces a high-quality image of the skin.

2.5.5 Skin Hydration and Natural Moisturising Factor (NMF)

Natural moisturising factor (NMF) maintains the skin in a properly hydrated state. Adequate hydration of the SC serves three major functions: (1) it maintains plasticity of the skin, protecting it from damage; (2) it allows hydrolytic enzymes to function in the process of desquamation (Jacobi, 1959); and (3) it contributes to optimal SC barrier function (Serup, 1992).

Due to the positive influence on the barrier function of the facial skin, NMF decreases TEWL. NMF components are highly efficient and can effectively draw atmospheric water into the corneocytes. This process can occur even at a relative humidity as low as 50 percent, allowing the corneocytes to maintain an adequate level of water in low-humidity environments (Horii I, 1989). The water absorption is so efficient that the NMF essentially dissolves within the water it has absorbed. Hydrated NMF forms ionic bonds with keratin fibres, reducing the intermolecular forces between the fibres and thus increasing the elasticity of the SC (Wellner K, 1993).

2.6 In-Vivo Measurement of Skin Hydration

2.6.1 Electrical-Based Methods

Because the lower portion of the SC can receive an ample supply of water from the underlying hydrated living epidermal tissue, it is the water content in the superficial portion of the SC—only several microns in depth—that keeps the skin smooth and soft. To evaluate the hydration of the skin's surface, it is conventionally using high-frequency impedance measurements of the skin (Tagami, 1980). In contrast to capacitance and conductance, skin impedance evaluates the resistance of skin, which increases with dehydration of the SC layer and is influenced by the skin's composition and metabolic activity. In capacitance and conductance measurements, the dielectric constant of water differs from that of other substances.

Thus, water is much more powerful at enhancing the capacity of a capacitor, leading to the assumption that skin capacitance is directly proportional to skin water content and that the higher the hydration level in the SC, the higher the capacitance (Walters & Roberts, 2007). Of the two components of high-frequency impedance, (i.e., conductance and capacitance), conductance is more suitable for measuring the skin surface's hydrated state (Hashimoto-Kumasaka, 1993).

2.6.2 Differential Scanning Calorimeter

Differential scanning calorimetry (DSC) is a thermal technique that is used to determine the energy of thermal transitions and that permits quantification of their temperature dependence. A typical thermogram of the SC is composed of several peaks. The first peak is not always apparent and can disappear if an organic solvent is added to the SC sample due to the melting of sebaceous lipids on the skin's surface (Agache, et al.,

2004). The second peak is assumed to reflect the melting of hydrophobic chains present in the lipid bilayers, and the third, although difficult to interpret, has been suggested to relate to the changes imposed by heat in the lipid-protein complex between the intercellular lipid and corneocyte membrane (Golden, et al., 1986). Moreover, this peak is highly sensitive to hydration, and when the SC water content increases, its transition temperature and area are reduced (Khan & Kellaway, 1989). The fourth and final peak is thought to be linked to thermal denaturation of intracellular keratin, which is irreversible and is also seen in lipid-free SCs (Golden, et al., 1987).

2.1.3 Trans-epidermal Water Loss (TEWL)

Trans-epidermal water loss (TEWL) is characterised by the constitutive evaporation of water that initiates from the deeper, more hydrated layers of the epidermis and dermis and then moves towards the more superficial SC layer in the absence of sweat gland activity. Measurements of TEWL are often employed in regulatory testing and to claim support for cosmetic products (EEMCO Group., 2001). Some claim support parameters for which TEWL readings have been used include reduction of irritating skin reactions, skin mildness, modulation of SC barrier function, increase in skin hydration, and protection against sun damage. TEWL can be measured through four different mechanisms:

2.6.4 Open Chamber

The open chamber mechanism follows the basic theory of Fick's law of diffusion and is the traditional method for TEWL measurements. The setup consists of a chamber made up of two pairs of temperature and humidity sensors, placed inside a hollow cylinder.

Commercially available instruments include the Tewameter R, DermaLab R, and the evaporimeter R.

2.1.5 Closed Chamber

This system is composed of humidity and temperature sensors placed in a closed cylindrical chamber. Upon application on the skin, the relative humidity (RH%) increases and is used to detect the rate of TEWL (Nuutinen, et al., 2003). A popular device of this type is the VapoMeter, which has been proven through comparative studies (De Paepe, et al., 2005) to give more accurate and rapid readings (Chilcott & Price, 2008).

2.1.6 Ventilated Closed Chamber

This approach follows the flow principle and measures the humidity of ambient air flowing into a closed chamber. The closed chamber is placed onto the skin's surface with air passing through it, which causes TEWL to be removed (Bennett, S., Jones, C., Matheson, J.R., 2005). Air humidity is calculated before it is released back into the surroundings, and thus, the rate of TEWL is determined by estimating the difference in humidity before and after contact with skin.

2.6.7 Condenser Chamber

This is a more recent method where in a closed chamber contains a cold plate that condenses moisture into ice using a Peltier system (Zhai, et al., 2007). The system eliminates the accumulation of moisture by removing it from the chamber, a problem that normally occurs in unventilated chambers. The Biox AquaFlux is an example of this technique, which uses a diffusion gradient to give TEWL readings.

2.6.8 Raman Spectroscopy

The use of Raman Spectroscopy (RS) to examine the lateral packing and conformational order of SC lipids is well established, as well as in evaluations of SC water profiles (Lee, et al., *Skin Res. Technol*) and determinations of lipid/protein ratio through calculations of lipid and protein intensity peaks. A study conducted in summer using RS to investigate age-dependent variations in SC hydration revealed large individual differences in the depth profile of water content in the forearm skin of aged individuals (Egawa, 2008). By contrast, the SC of their cheek skin retained its thinness, as did that of younger people, indicating that no such thickening of the SC occurs in the facial skin even with ageing, which contrast sharply with the skin on the lower halves of their bodies (Janssens, et al., 2014) as given in the following figure. The SC consists of keratin- and NMF-rich corneocytes, a lipid matrix in the intercellular water (Darvin, 2017).

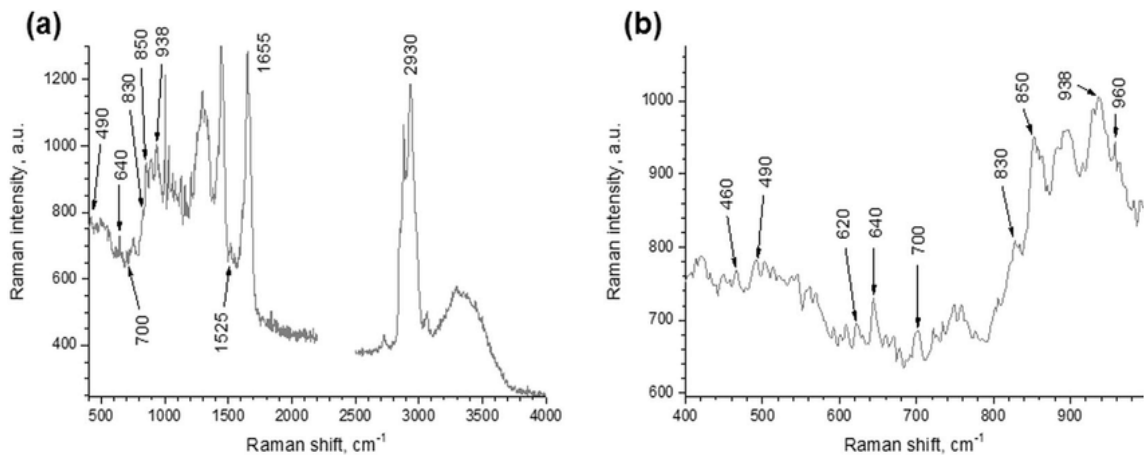


Figure 2.9(a) Raman spectrum of forearm skin at a depth of 8 μm (male, age 27). (b) Detailed depiction of the same spectrum in the depth of 400-1000 cm⁻¹ range (Darvin, 2017).

2.6.9 Photothermal Radiometry

Photothermal Radiometry, also termed Opto-Thermal Transient Emission Radiometry (OTTER), is a non-invasive, non-occlusive method that uses excitation and thermal emission wavelengths that are strongly absorbed by the top few microns of the SC and are specific to the spectral properties of water (Bindra, et al., 1994). Excitation and radiation from deeper layers of the skin do not affect measurements due to the skin's low thermal diffusivity, and the effects of optical scattering are also negligible owing to the dominance of absorption and the low turbidity of the skin at the long wavelengths used (Imhof, et al., 1984).

Further studies on SC hydration concluded that OTTER is capable of measuring water content at the skin's surface as well as the water concentration gradient within the SC (Xiao, et al., 2012), water status in the SC, SC thickness and SC swelling during hydration (Xiao & Imhof, 1996).

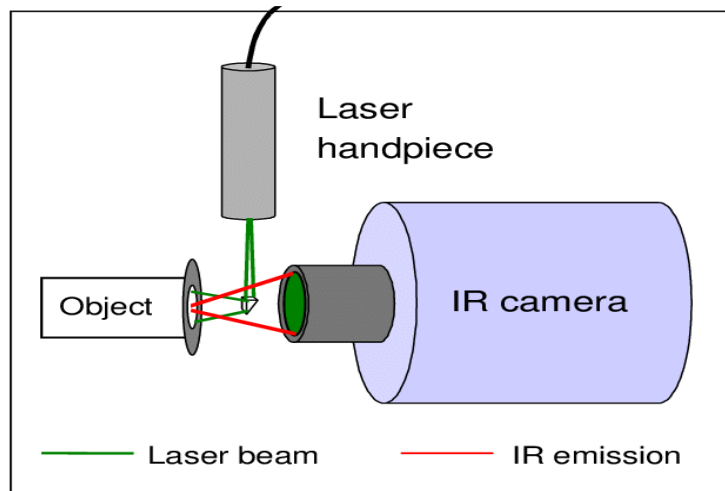


Figure 2.10. Schematic diagram of the Photothermal Radiometry setup (Majaron & Choi, 2003)

2.7 Analysis of Instruments to Measure Skin Hydration

The traditional techniques, such as TEWL and Electrical-Based Instruments estimate barrier function based on the SC's water content and hydration state. However, it is important to evaluate the entire intercellular structure for a detailed description of the SC hydration state. Traditional instruments perform simplistic analyses and do not provide information about the phenomenon that is occurring at the cellular level. For this purpose, several spectroscopic and imaging techniques have been employed in recent years.

The capacitance/resistance-measuring probes which determine skin moisture by means of skin conductivity or impedance are often occlusive, which can lead to inaccuracies resulting from water build-up at the examination site, as per (Hansen & Yellin, 1972). According to their theory of operation, the flow of electrical current through the SC is associated with its water content, but this flow is also influenced by alterations in ion movement and by reorientation of protein dipole moments (Kilpatrick-Liverman, et al., 2006). Similarly, TEWL and mechanical-based devices have proven excellent in highlighting the SC's biomechanical nature, but nonetheless, they do not provide direct measurements of skin hydration or barrier function and merely serve as indicators of changes in these parameters (Ablett & Burdett, 1996).

2.8 Epsilon

The Epsilon is a novel instrument for measuring near-surface dielectric permittivity (ϵ) and contact imaging of the skin. Its proprietary electronics and signal processing

algorithms to map the sensor's nonlinear signals onto a calibrated scale for measuring properties such as SC hydration and TEWL. The Epsilon differs from other similar systems (e.g., Skin Chip, L'Oréal France, Moisture Map, CK Technology sprl Belgium) in its calibrated, linear response to near-surface dielectric permittivity. This works because the dielectric permittivity of water is much higher ($\epsilon \sim 80$) than that of other constituents of the skin. The linear response is important because hydration is linearly related to permittivity. The calibration ensures consistency in all its instruments and use cases. (Wei Pan, 2014).



Figure 2.11. Epsilon Hand-held probe and parking stand (Anon, n.d.)

Hydration and TEWL Measurements

The SC's water content can be measured using the Epsilon (Epsilon E100, Biox, UK). The Epsilon can measure the calibrated dielectric permittivity (dielectric constant, ϵ) and consists of a probe of 76,800 sensors with a sensing area of 12.8×15 mm, a depth resolution of $20 \mu\text{m}$ and a spatial resolution of $50 \mu\text{m}$ (Imhof, 2017). It can process images without alteration from inconsistent contact, hair, micro-relief and wrinkles and

surface water from imperceptible perspiration. The multiple sensors allow skin surface hydration to be mapped, taking skin relief and the variable distribution of sweat glands into account (Anon, 2014).

Logger conducted a study to measure the effectiveness of Epsilon over the traditional Corneometer. Fifteen healthy Caucasian volunteers (9 women and 6 men; median age 26 years; range 21–62 years) participated in this explorative study. Hydration and TEWL were measured for five different anatomical sites. In this case, only the measurements obtained on the facial skin were used (Logger JGM, 2019).

Figure 2.12 shows the literature-based reference values of the water content obtained using a single-sensor Corneometer. In general, the single-sensor Corneometer showed higher water content values than the Epsilon.

Study	Device	Population	Skin Location (Cheek)
O’Goshi K, 2005	Corneometer CM820	53 healthy volunteers	74 (38-122)
	Corneometer CM82		72 (29-113)
	Corneometer CM810		78 (41-131)

Table 2.2. Hydration and TEWL Measurements Tools

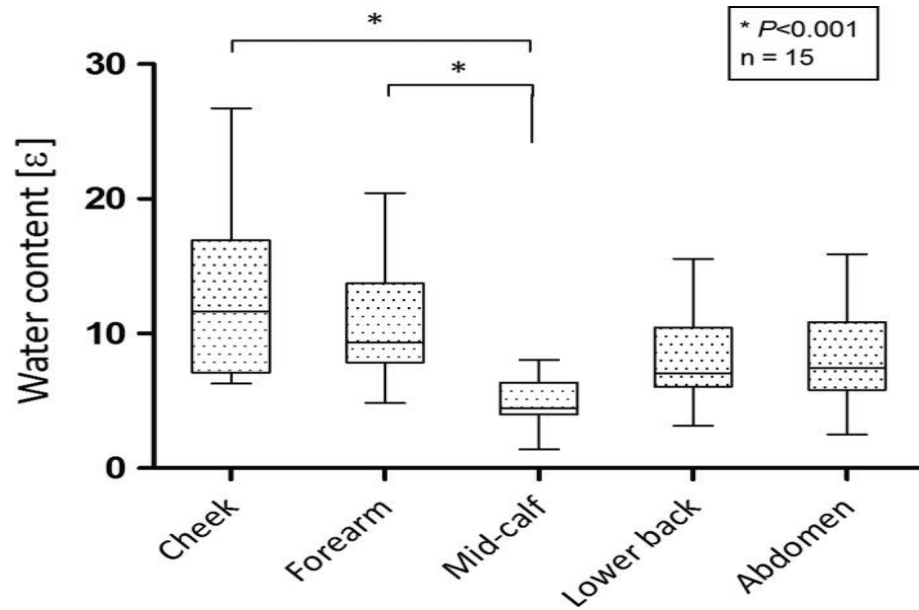


Figure 2.12. Water content at five body sites measured with the Epsilon (Mlosek et al, 2013)

The Epsilon's measured water content values were lower than those of conventional corneometers, as Figure 2.12 illustrates. It is important to notice that Epsilon measurement units are displayed using a calibrated dielectric permittivity scale (ϵ) rather than an arbitrary scale as used in conventional corneometers (Robertson & Rees, 2010). As both instrument types use the same capacitance measurement principle, they are expected to correlate well; however, in view of the Epsilon's multisensory character, the sensing depth will probably be more superficial than that of conventional Corneometers, which makes a single large electrical loop through the skin. Therefore, owing to the Epsilon's "skin mapping" characteristics, the number of values in one measurement can be averaged, potentially leading to more accurate water content values (van Logtestijn MD, 2015).

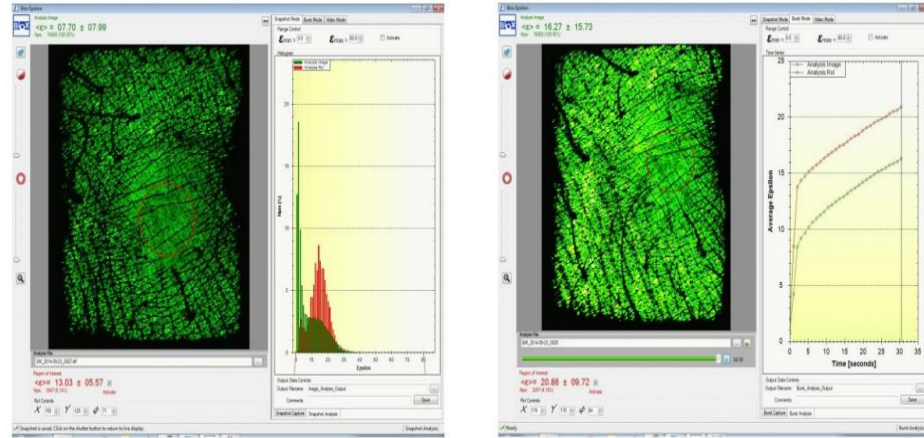


Figure 2.13. Ultrasound Image (Biox Systems Ltd, 2014)

The main image processing technique for hydration measurement is the ϵ -filter in Epsilon, in which thresholds can be set to remove measurement artefacts associated with low ϵ (bad contact) and high ϵ (surface water). In Figure 2.13 (Left), the low ϵ dark area around the periphery is due to bad contact, and the high ϵ bright spots represent surface water at sweat gland openings. The filter's action is clearly visible in Figure 2.13 (Right), where the removed pixels are indicated by the dark and light grey areas for low and high ϵ , respectively (Biox Systems Ltd, 2014).

A pilot study was conducted to measure TEWL and skin hydration using four different instruments (Logger JGM, 2019). Water content was measured using the Epsilon, a state-of-the-art corneometer using multi-sensor skin mapping technology with correction for skin occlusive effects (Zhang, et al., 2018). The Epsilon's sensing depth is restricted to the less hydrated SC, in contrast to earlier model conventional corneometers that measure the deeper, more hydrated epidermis (Wa & Maibach, 2010); this potentially yields more accurate water content values. The Epsilon showed significant variations in water content at different anatomical skin locations (Levine & Markowitz, 2018);

however, the size of the probe head (4 cm × 3 cm) that restricts measurements to non-recessed body parts.

2.9 AquaFlux

The AquaFlux is the top-performing evaporimeter for TEWL. AquaFlux is provided in a rough aluminium case, complete with guidance manual, instrument identification, alignment frill, estimation and USB link. The power packs are qualified for clinical use that accompany US, European and/or UK fittings and supply connectors for different outlets.

AquaFlux, Fig 2.14, is an infrared distant-detection innovation for non-contact and non-damaging surface examination of discretionary samples. It is used to calculate Transepidermal Water Loss (TEWL) that is observed as flux of water through the Stratum Corneum (SC) from wet Epidermis to the dry skin surface. Its applications include estimating skin hydration, skin shades, transdermal medication conveyance, warm diffusivity, and torment covering thickness. Its primary advantages are that it is a surface innovation bringing about simple profundity profiling, short estimation time, inhumane towards shading, and spectroscopic in nature. The dark elastic plug in the stopping repository is used to close the estimation chamber when the test is not being used. A typical setup of AquaFlux comprises the segments stated below:



Figure 2.14. AquaFlux Instrument.

The software of the product provided with the instrument runs on a Personal Computer which can be connected through a USB connector. The software runs on latest editions of Windows; see prerequisites of use available in the documentation. The company provides new software updates free of cost for licensed clients.

The software product gives functions that allow estimation, adjustment, show and capacity. All functionalities are reached by means of tabs and drop-down menus. Information is saved consequently in Excel format viable, tab-isolated qualities (TSV) design. The guidance material is far-reaching, and backing is only an email away.

Condenser Chamber

AquaFlux utilises the condenser-chamber technique to estimate water vapour motion.

The figure below shows the schematic chart of the AquaFlux estimation chamber.

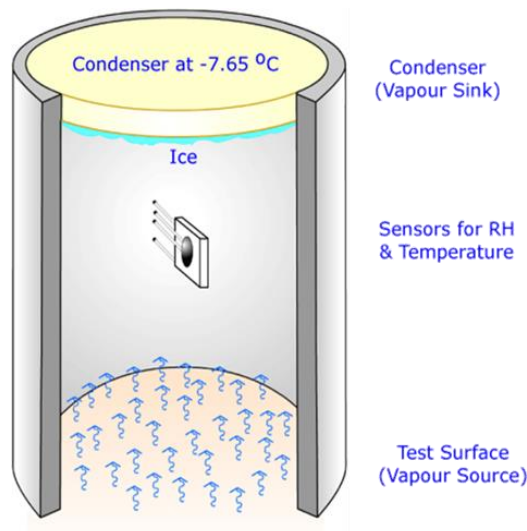


Figure 2.15. Cut-out view of the AquaFlux condenser chamber.

AquaFlux utilises the condenser-chamber estimation standard. This is a blend of Nilsson's dispersion angle estimation standard, yet with a closed chamber to eliminate disruptive influence from encompassing air developments. It has the following functionalities:

- Condenser @ - 7.6°C with Fume Sink, controls the microclimate.
- RH and T Sensors are utilised to detect vapour motion.
- Skin surface is near the vapour source

The dispersion gradient is determined from the RHT sensor readings and condenser thermodynamics.

Properties of device

- It has the highest repeatability, precision and affectability.
- Does not require recuperation time between estimations.

- Measurements of autonomy of administrator and area
- It is undisturbed by surrounding air developments.
- Supports optional multilingual on location preparation.
- User comfort: The probe is applicable on any site, any point and any place on the body.
- Calculation of Skin Surface Water Loss (SSWL) and desorbed water.

Specifications

- Measurement covers are adjustable to 180°C temperature.
- It is compatible with Windows 7, 8 and 10.
- The operating temperature is around 15–28°C.
- Probe with Start/Stop press button.
- Operating humidity is less than 80% RH.

Applications

- TEWL of skin, lips and nails.
- Efficacy and case support.
- In vivo, in vitro, and in-culture connectors.
- Zoological creature wellbeing.
- Medical research.
- Membrane uprightness testing.
- Perspiration contemplates
- Desorption estimations

2.10 Skin Ultrasound and Episcan

2.10.1 Skin Ultrasound

Ultrasounds are sound waves with non-audible frequencies above 20,000 Hz that are generated using crystals that have the ability to emit these waves in response to an electrical stimulus and to convert the reflected echoes of these ultrasounds into electrical signals; this is known as the piezoelectric effect (Tikjøb G, 1984).

Piezoelectric crystals, which are located in transducers or probes, emit electrical signals to the processing unit. This unit converts electrical signals into greater or lesser intensity points on a screen (B-mode image) (Lehman PA, 2014).

B-mode images represent a longitudinal or transverse line based on the probe's orientation with respect to the structure being examined. The greater the frequency of the ultrasound, the lower its ability to penetrate the tissue and the greater the ability to distinguish echoes from adjacent structures (Yano T, 1987). Dermatologists look for the parallel structures on skin therefore it is common practice in dermatology that skin surface is probed with high frequency of more than 7.0 MHz. This involves very high resolution echoed images at different depths.

Since ultrasound waves are greatly attenuated when transmitted through air, a gel or a stand-off must be placed between the skin and the transducer to facilitate transmission (Dines KA, 1984). Unlike conventional ultrasound, skin ultrasound assesses surface structures and is performed by lightly positioning the transducer on the gel placed over the skin without applying pressure (Flynn, 1990).

2.10.2 Episcan

The Episcan I-200 (shown in Figure 2.16) is a high resolution skin ultrasound instrument from Longport Inc, USA. With ultrasound frequencies in the range of 20 to 50 MHz, corresponding to spatial resolution from 80 to 32 μm (Bezugly, 2021), it can easily facilitate the visualisation of the skin's anatomy and many of the diseases, injuries and treatments that impact the dermis and underlying soft tissues (Helvig EI, 2012).

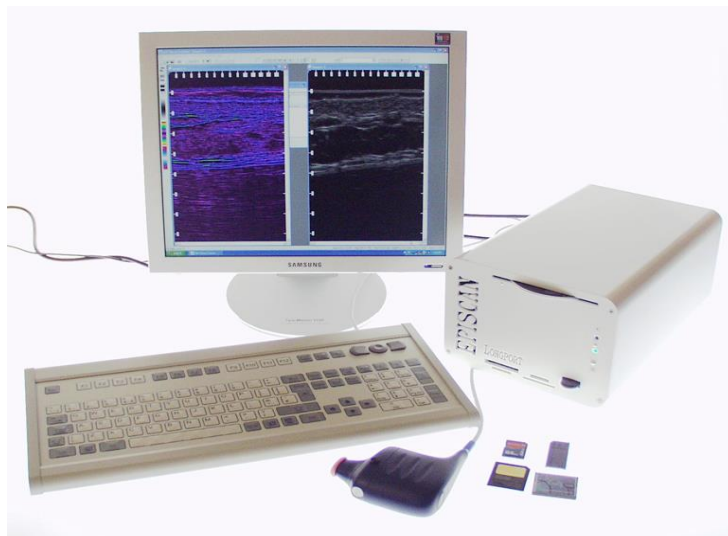


Figure 2.16. Episcan (Anon, 2014)

The Episcan creates high-resolution images of the skin that can typically be seen in the following biopsy in Figure 2.17. The Episcan can visualise many of the diseases and injuries that impact the skin and underlying soft tissue, but unlike tissue damaging biopsies (JM, 2005), it can also track changes with treatment and over the time at the same site (Longport., 2007). Episcan has a high imaging resolution that distinguishes it from other ultrasound imaging systems in the market, which provide more in-depth

imaging capabilities but significantly lower resolving power than Episcan. As a result, subtle changes in the density, fluid content, and thickness of the skin can be appreciated owing to Episcan's capability (Landis J, 1977). The system is designed in such a way that it offers users very high clarity, resolution and provides a user-friendly interface.

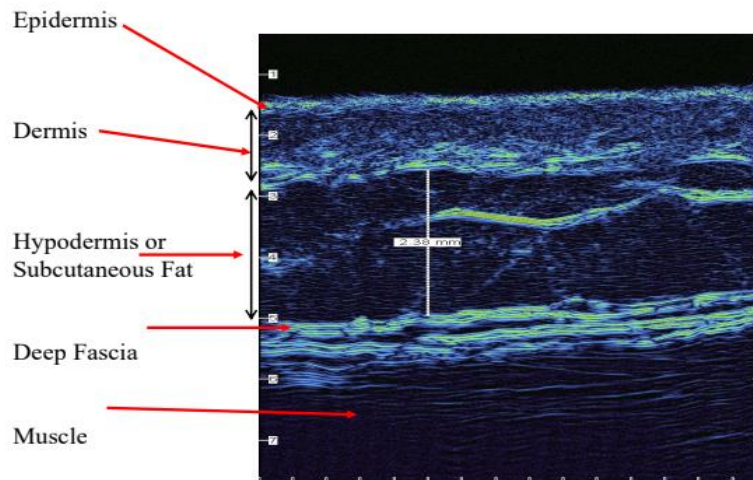
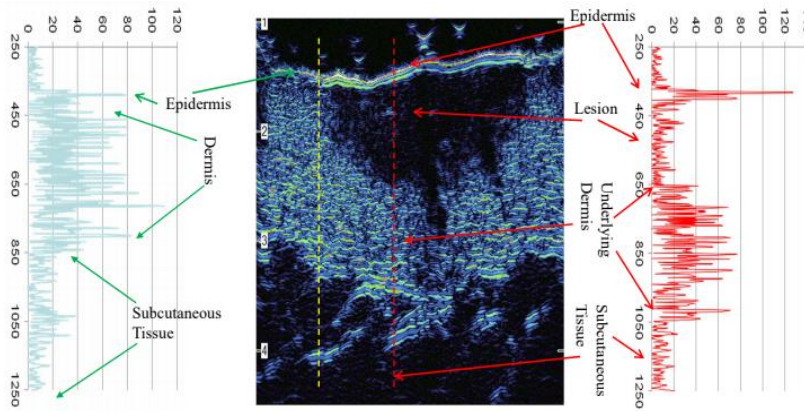


Figure 2.17. 35 MHz Image of Superficial Soft Tissue through Episcan (Black J, 2007)

The ultrasound images are normally viewed as brightness or B-scans; these scans are constructed from numerous amplitudes or A-scans. The Episcan allows the user to view and export any of up to 1024 A-scans that make up a B-scan (SA, 2009). Ultrasonic waves are reflected at boundaries where the acoustic impedances of the materials or tissue types on each side of the boundary differ. This difference is commonly referred to as the impedance mismatch. The greater the impedance mismatch, the greater the percentage of energy that will be reflected (Fornage BD, 1993). Thus, the larger signal at the top of the A-scan in Figure 2.18 from the entire echo at the epidermis is a result of the comparatively large impedance mismatch between the epidermis and the coupling gel and the epidermis and dermis. While the smaller signal from subcutaneous tissue in

the lower part of the A-scan is indicative of a lack of interfaces and/or boundaries, and those that occur have small acoustic impedance mismatches (Rohrbach, 2014).



The A-Scan on the left shows normal tissue, taken from the yellow dotted line, while that on the right goes through the lesion, red dotted line.

Figure 2.18. Two A-Scans showing the difference between Normal Tissue and Skin Lesion (Andersen ES, 2008)

Many of Episcan's applications require linear dimensions to be measured on the scans. This can be readily performed to high accuracy. Several groups have reported on the measurement accuracy. An Anglo-Greek study reported "a highly significant, positive association between the ultrasonographic (Episcan) and histological measurements ($P < 0.001$) of skin thickness" (Mantis, 2014).

Skin Thickness

The Episcan cannot measure TEWL or skin hydration directly. However, it can measure changes in dermal thickness, of which can be related to changes in skin TEWL or skin hydration. Changes in dermal echogenicity reflect alternations in dermal water content associated with inflammation. High-frequency ultrasound (HFUS) dermal echogenicity and skin water content using nuclear magnetic resonance were evaluated, and HFUS

was shown to be a sensitive method for assessing dermal hydration and skin pathology associated with oedema formation (Gniadecka, 1996).

The measurement precision of a 20 MHz ultrasound dermal scanning system, Episcan, was investigated for its use in the measurement of skin thickness. Results from measurements of relatively ideal homogeneous, uniformly thick plastic plates indicate that the scanner can accurately measure to depths of 8–34 mm from the surface of the transducer or approximately 18 mm from the surface of the latex probecover with a high level of precision (Kong, 2007).

2.11 Mathematical Analysis

To understand the results taken from measurements by different skin sensing machines, different statistical expressions have been used. This activity is called Data Analytics which have been recently used in data intensive systems to get the meaningful results from the resulting data. Since the data used in this thesis cannot exceed some hundreds of samples therefore only some of the statistical tools are given whereas the advanced mathematical and computing techniques were not required. Moreover, data used in experiments are discrete therefore nonparametric statistical methods have been applied, for example means and standard deviation (SD). The (sd) suggests how well the results taken from skin analysis are evenly spread over the mean values when compared from different samples. Higher (sd) values are the indicators of poor skin quality in hydration and thickness, whereas lower (sd) values indicate higher quality of skin that is mapped from its parameters. The machines used for skin analysis compute these values

automatically just after taking the outer and inner images of skin regions. Simply by pressing the buttons the values obtained are compared by the software provided by these machines. Moreover, the comparison graphs are also generated by these software which can be further seen on computer screen.

2.12Chapter Summary

This chapter provided a general overview of skin research and skin measurement technologies. It reviewed various studies that have been conducted on skin analysis. The association of skin health with diseases can be estimated from skin quality and the underlying integrity of skin tissues. Face mapping clearly indicates the organ that is suspected of being in distress based on the results of skin assessment. Hence, the dermatologist assesses the skin in detail and recommends the most appropriate and rational treatment. Giovanni and Stefania conducted a study to evaluate facial skin thickness and Echogenicity. They considered the parameter of age to determine the variation of echogenicity and skin thickness. The results indicated that the skin of the lower and upper lips shows high thickness levels. It was concluded that the nasal tip's skin thickness was about 3.3 times thicker than the skin of the upper eyelid. In a study, 248 healthy Japanese women were enrolled to determine the surface structure of facial skin at various anatomical sites. The results obtained from the data concluded that pore size and area ratio increased with ageing. The structure of the skin's pores changed and was shown to be convex in shape. Ageing is the key aggravating factor leading to the opening of facial pores. Various factors play a role in skin determination. These include skin pH, temperature and own moisturising factors. A study was conducted to observe

the SC layer's skin condition for estimation of skin hydration levels. The SC water profiles of young human subjects were studied using RS.

Chapter 3. Skin TEWL Measurements

3.1 Experimental Results of Transepidermal Water Loss (TEWL)

The primary purpose of this chapter is to present the study and its results, to formulate a relationship between the TEWL values at various anatomical sites on the facial skin. The TEWL was measured by using AquaFlux instrument, under the normal ambient laboratory condition ($\sim 21^{\circ}\text{C}$, $\sim 40\%$ relative humidity(RH)), at 9 anatomical skin sites of 48 healthy volunteers (10 male, 38 female, age between 18–70 y), amounting to a total value of 501 measurements. The subjects' ages were also noted to determine the variance of TEWL at different anatomical sites in response to ageing.

Anatomical site	Count	Mean [g/m ² h]	Standard deviation
Neck	27	15.67	10.57
Cheek	107	20.36	11.85
Eye corner	37	22.88	9.53
Forehead	86	26.66	18.28
Under-eye	72	29.02	13.77
Chin	64	32.31	15.45
Nose	51	37.43	15.03
Upper lip	11	51.77	23.74
Lips	46	70.89	22.06

Table 3.1. TEWL values measured at 9 (501 instances) anatomical sites as grams of water per square meter per hour ($\text{g}\cdot\text{m}^{-2}\cdot\text{h}^{-1}$)

The study is divided into two segments. In the first segment, the discussion largely concerns to the causes of the variance between TEWL values. In the second segment,

the relationship between TEWL and age is discussed in relation to our subjects. The locations at which TEWL values were noted are given in Table 3.1 and Figure 3.1 along with their count, mean and standard deviation.

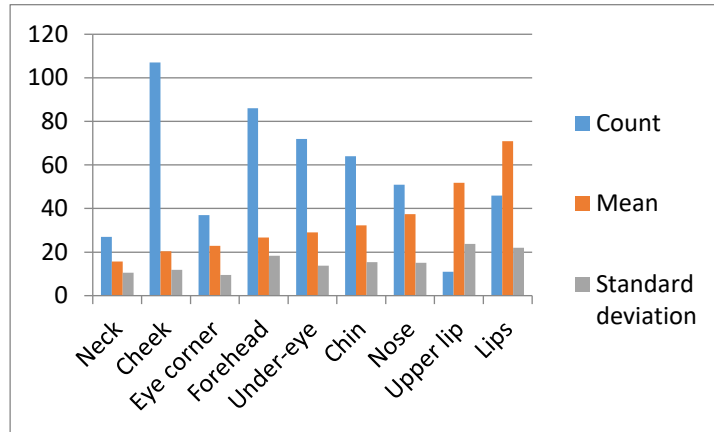


Figure 3.1. Graphical illustration of TEWL with Mean and SD

The lip has the highest mean TEWL value, and the neck has the lowest mean value. The difference in TEWL levels may be attributable to several reasons, such as skin blood flow, damaged barrier function, skin temperature, the SC's lipid content and the degree of Corneocyte formation. Moreover, ethnicity and age may also have a bearing on the result. The detailed discussions each of them will be presented in the following sections.

3.2 Causes of High TEWL on the Lip and Upper Lip

In our study, the mean value for TEWL for the lip is 70.89. This higher value can be attributed to the different characteristics of lip skin as compared to other parts of facial

skin. The lips represent a specialised transitional region from the skin to the oral mucosa. The region where the facial skin meets the external lip is known as the vermilion border, see Figure 3.2 (Bhairy, 2016). This vermilion zone consists of a connected underlying tissue that has greater flexibility compared with the connective tissue of most regions of the skin and a thin orthokeratinised epithelium.

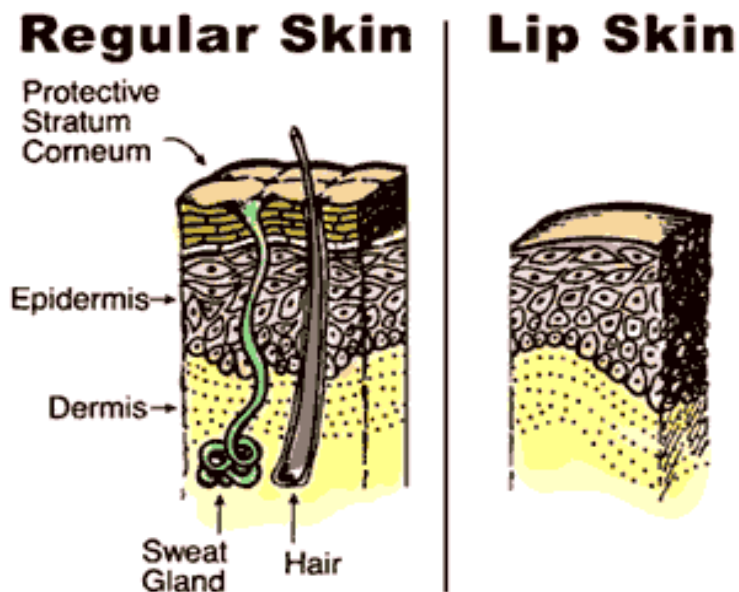


Figure 3.2. SC Thickness Comparison between Lip & Facial Skin (Bhairy, 2016)

The SC of the lip has the same types of ceramides and cholesterol found in other parts of the epidermis, but has a weak barrier function compared to other facial skin sites, allowing comparatively high TEWL. The lips' characteristics change with increasing age as the sebaceous follicles in the underlying connective tissue provides sebaceous lipids to the lip skin. The area of the corneocytes on the vermilion zone is greater than that of the cheeks, so TEWL through the lip is greater than TEWL through the cheek.

The change from the exterior keratinised epithelium of the vermilion zone and the internal non-keratinised epithelium is sudden; however, the portion of the vermilion zone closest to the oral mucosa is sometimes referred to as the submucosa. So, the hydration of the submucosa is less as compared to the entire external vermilion zone. Therefore, TEWL of the upper lip is lower than that of the lip.

Moreover, the SC of the lip is thinner compared to other areas of the facial skin. Therefore, the barrier function of the SC is lower, hence greater TEWL as compared to other parts of the facial skin. Also, the standard deviation value is on the higher side in this case. This indicates a greater spread of data from the mean value. Hence, the data set is the least accurate of all the data collected from other anatomical locations.

3.3 Eye Corners and Under-Eye TEWL Difference

The TEWL value for the eye corner was 22.88, as per the results tabulated in Table 3.1, while the under-eye portion had a mean TEWL of 29.02. Despite the close proximity between the eye corner and under-eye areas, there is a significant difference between their mean values. To account for this difference, the underlying skin structure must be examined for both areas.

The skin around the eyes is ten times thinner than the skin on the face. As people age, the skin loses its elasticity and becomes even thinner due to a breakdown of collagen. This can be further aggravated by sun exposure, smoking and other environmental exposures. This accounts for greater TEWL in the under-eye area than in the eye corners.

3.4 Nose and TEWL

A high TEWL on the nose is associated with a damaged barrier function. In our case, the mean TEWL for the nose was 37.43, which was slightly higher than that for other parts of the facial skin. The condition of the nose skin can shed light on the high TEWL values. Every person experiences cold multiple times during his lifetime. The use of handkerchief can damage the barrier function of the nose, leading to high TEWL values. Moreover, the porous structure of the nose also contributes to an increase in TEWL, as the pores allow more water to be lost in the atmosphere as compared to other anatomical sites on the facial skin.

3.5 Neck and TEWL

Regarding the facial skin, the neck has the lowest TEWL value. The neck skin is quite sturdy in structure, as it houses some of the body's most important organs. It also has a large corneocyte layer compared to other parts of the facial skin. Consequently, the water cannot leave the skin surface easily. Hence, it has the lowest TEWL value for facial skin in terms of the data that have been analysed.

3.6 Forehead and TEWL

The mean value for the TEWL for the forehead was calculated to be 26.66. This is a smaller value than those of the other anatomical sites, as the forehead skin mainly comprises features such as the skull, scalp and bones. The movement of muscles in the forehead skin constitutes facial expressions rather than releasing water via the skin.

Wrinkles are one of the major results of these expressions. The T-zone (includes your chin, nose and forehead) and particularly the forehead skin are mostly oily owing to their high sebum content. This is a reason for the low rate of TEWL from the forehead skin.

3.7 Chin and TEWL

The chin constitutes another oily region of the face in major skins around the world. However, its average TEWL content was found to be 32.31. Moreover, this value increases as a person ages, as demonstrated by the results obtained in the later part of this study. Recent research on the development of chin skin also shows that it does not evolve by mechanical forces, such as chewing, but through adaption, evolving and changing in shape as a person ages. As the diagram below illustrates, the chin has fat compartments as part of the first layer, which may resist the loss of TEWL from that area.

3.8 Cheek and TEWL

The cheeks are a relatively drier region of the face than the nose, T-zone and chin. Most of the blood supply to the face is performed by a network of arteries and veins connected with the cheeks. The skin at cheeks is also thicker compared to the other regions of the face. It is found the average TEWL value of cheeks in adults and youngsters to be 20.36. The cutaneous and subcutaneous permeability barrier of children is immature compared to that of adults. This increases TEWL and percutaneous penetration of topical compounds from the cheek skin. The skin barrier matures during the initial years of life and continues to change thereafter. As a person ages, anatomical

and physical alteration occurs in the cheek skin, increasing its exposure to sunlight and pollution. This contributes to the increasing TEWL values with age.

3.9 Variance of TEWL with Age for Different Anatomical Sites

In this section, TEWL's dependency on age is analysed. For the purpose of this study, age 35 have been taken as the dividing line to compare the impact of ageing on TEWL values.

3.10 Welch t-TEST

The first summary study compared average TEWL per location using the Welch test. This test was used because readings for different areas were taken independently and equality of variances per location for under and over 35 could not be assumed. This was done to determine whether any statistically significant relationship existed between age and the rate of TEWL from different anatomical sites of the human face.

To conduct our test, a table was constructed below that shows measurement averages, their standard deviations, and corresponding Welch t-statistics for the null hypothesis that averages are different. Given the large number of implied degrees of freedom for all cases except for the neck, the statistic effectively follows a normal distribution in these cases. Therefore the 3-sigma point corresponds to the 0.27% level of significance of the two-sided test.

Moreover, it can be seen from the table that the average TEWL values for the neck, eye corner and forehead are almost the same as the values of cheeks and under-eye areas closer to them. However, the nose and lips generated higher TEWL values, and

therefore they can be considered outliers in the data represented. The lower standard deviation values for eye corners indicate that they are closer to the mean; therefore, the null hypothesis cannot be rejected for this anatomical site.

Area	Under 35			Above 35			Welch t-stat	No. of DF	Different?
	Average [g/m ² h]	Study	Count	Average [g/m ² h]	Study	Count			
Neck	19.35	15.02	11	13.15	5.16	16	1.32	11	FALSE
Cheek	15.58	6.11	22	21.59	12.67	85	3.17	93	TRUE
Eye corner	19.61	6.04	8	23.79	10.18	29	1.47	22	FALSE
Forehead	19.46	9.73	22	29.14	19.87	64	2.99	124	TRUE
Under-eye	24.74	12.17	16	30.25	14.05	56	1.54	28	FALSE
Chin	23.11	4.74	15	35.12	16.50	49	4.52	309	TRUE
Nose	40.08	18.09	16	36.22	13.53	35	0.76	23	FALSE
Lips	61.60	25.26	15	73.84	20.99	31	1.62	24	FALSE

Table 3.2. TEWL values measured under the age 35 and above of 125 instances as grams of water per square meter per hour (g·m⁻²·h⁻¹)

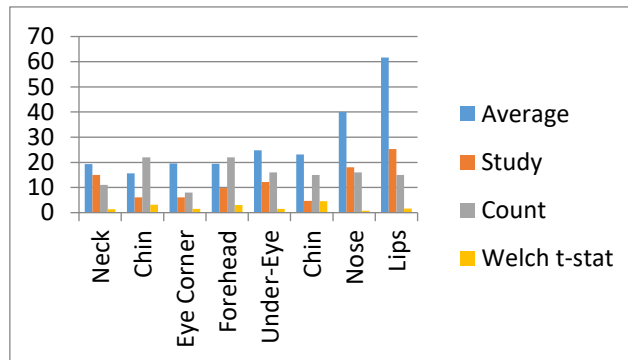


Figure 3.3. Welch t-TEST under age 35

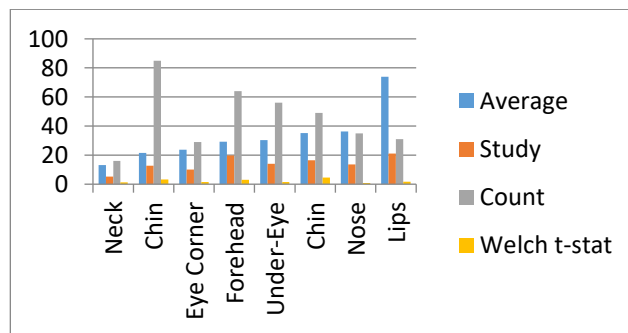


Figure 3.4. Welch t-TEST above age 35

As such, the hypothesis that averages are different only for cheeks and chin was not rejected. For forehead, the hypothesis can be rejected at a 0.28% level of significance for the two-sided test. For this reason, it is also considered that the null hypothesis cannot be rejected for forehead

3.11 Age Based Variance in TEWL

3.11.1 Neck

TEWL was measured for neck skin from a wide range of people from different age groups. This was performed to assess the relationship between age and water loss from the skin. For this purpose, a total of 27 measurements were taken for TEWL on the neck. The average was calculated by dividing the data set among age groups. Eleven people under the age of 35 had an average of 19.35, while 16 of them were above 35 years had an average of 13.15.

Neck	Count	Average [g/m ² h]
Below 35	11	19.35
Above 35	16	13.15

Table 3.3. Variance in TEWL of Neck less than 35 and above 35, as grams of water per square meter per hour (g·m⁻²·h⁻¹).

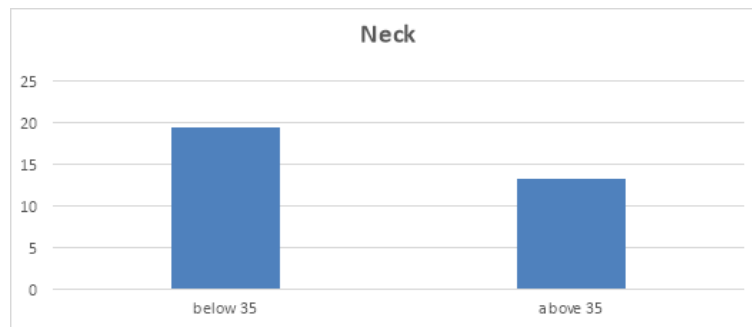


Figure 3.5 TEWL measurements performed on the Neck of below 35 (n= 100 subjects) and above 35 (n = 100 subjects) are represented in grams of water per square meter per hour ($\text{g}\cdot\text{m}^{-2}\cdot\text{h}^{-1}$)

There exists a statistical difference between the two data sets, as shown by their averages. Therefore, it can be concluded that age does affect the TEWL on the neck skin, as indicated from the average values listed in the table below. As people age, laxity occurs in the neck due to less support from connective tissue and muscle. This leads to a “waddle” or “turkey neck” and looks like loose skin under our chin. This may be one of the reasons for the drop in TEWL values for elderly people, as the following table illustrates.

3.11.2 Lips

TEWL was measured for the lips of a wide range of people from different age groups to assess the relationship between age and water loss from the skin. For this purpose, a total of 46 measurements were taken for TEWL on the lips. It is found that 15 people who were aged below 35 had an average of 61.6, while 31 aged above 35 had an average of 20.99. Although the sample size for people below 35 is lower than that of people above 35, there exists a statistical difference between the average TEWL measurements of both. It can be explained by looking at the effect of age on lip

structure. The structures that give our lips plump shape begin to erode with time. A permanent frown results in dropping of the mouth's corners, with the result that the lips lose their fullness and definition. Therefore, there is a chance that TEWL may decrease with age.

Lips	Count	Average [g/m ² h]
Below 35	15	61.6
Above 35	31	20.99

Table 3.4. Variance in TEWL of Lips, as grams of water per square meter per hour (g·m⁻²·h⁻¹)

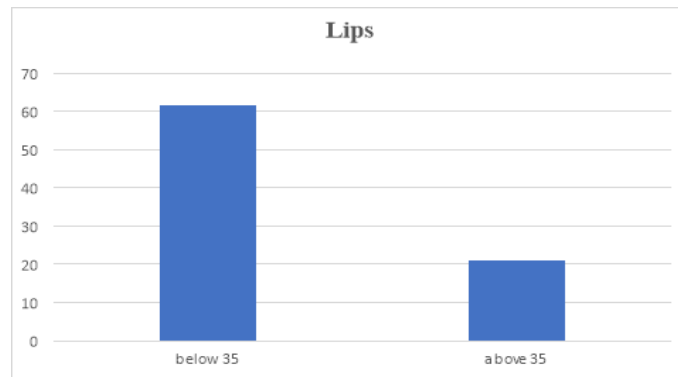


Figure 3.6. TEWL measurements performed on the Lips below 35 (n= 100 subjects) and above 35 (n = 100 subjects) are represented in grams of water per square meter per hour (g·m⁻²·h⁻¹)

3.11.3 Nose

TEWL was measured on the nose skin for a wide range of people from different age groups to assess the relationship between age and water loss from the nose skin. For this purpose, a total of 51 measurements were taken for TEWL on the nose skin. Sixteen people under the age of 35 had an average of 40.08 while 35 aged over 35 had an average of 36.22. A double difference was observed between the values of the sample sizes for age, which eventually affects the average TEWL value. People aged under 35 have a high rate of water loss from their nose skin, while as they age, the TEWL value

starts to decrease. Hence, a statistically significant relationship may be said to exist between age and TEWL in the nose skin. Decreased TEWL with increasing age indicates an improvement in barrier function as the person ages. This may be attributed to the fact that our nose grows in shape and size during the ageing process. Various skin parameters like the dermis, epidermis and hypodermis develop with age for the nose skin. Therefore, it is quite possible that TEWL values for the nose skin decrease during the ageing process.

Nose	Count	Average [g/m ² h]
Below 35	16	40.08
Above 35	35	36.22

Table 3.5. Variance in TEWL of Nose, as grams of water per square meter per hour ($\text{g}\cdot\text{m}^{-2}\cdot\text{h}^{-1}$)

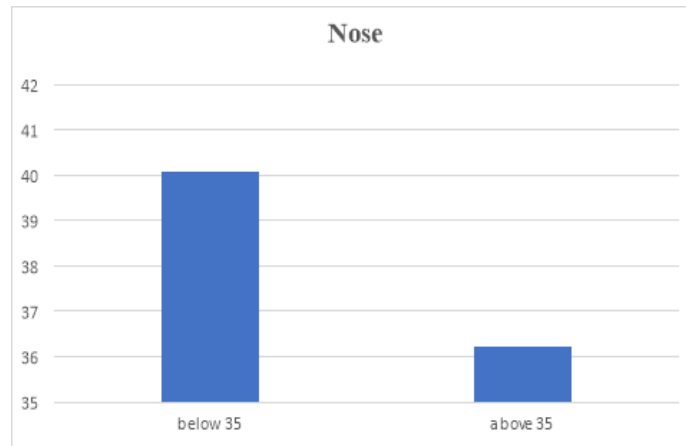


Figure 3.7. TEWL measurements performed on the Nose below 35 (n= 100 subjects) and above 35 (n = 100 subjects) are represented in grams of water per square meter per hour ($\text{g}\cdot\text{m}^{-2}\cdot\text{h}^{-1}$)

3.11.4 Under-Eye

TEWL was measured on under-eye skin for a wide range of people with different age groups to assess the relationship between age and water loss from the under-eye skin. A total of 72 samples were taken from the under eyes. Sixteen of them aged under 35 had an average of 24.74, while 56 aged over 35 had an average of 30.25. Despite the huge difference between the sample sizes of the two age groups, the average TEWL values for both were similar. A small difference was observed between their averages. This may be due to the fact that as people age, the under-eye skin deteriorates, as indicated by the presence of dark circles in most elderly individuals. The SC's barrier function is affected as a result.

Under-eye	Count	Average [g/m ² h]
Below 35	16	24.74
Above 35	56	30.25

Table 3.6. Variance in TEWL of Eyes, as grams of water per square meter per hour ($\text{g}\cdot\text{m}^{-2}\cdot\text{h}^{-1}$)

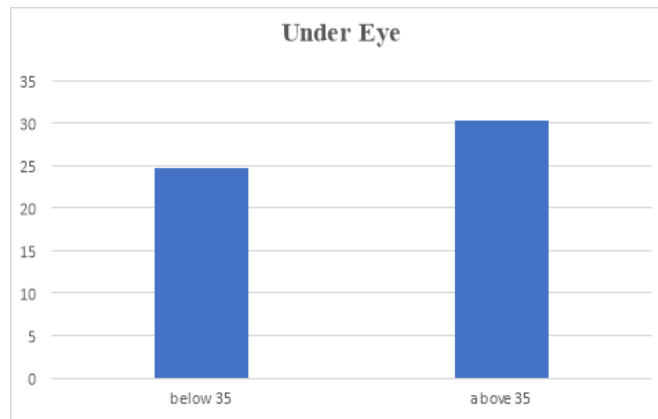


Figure 3.8. TEWL measurements performed on the Under Eye area of below 35 (n= 100 subjects) and above 35 (n = 100 subjects) are represented in grams of water per square meter per hour ($\text{g}\cdot\text{m}^{-2}\cdot\text{h}^{-1}$)

3.11.5 Eye Corner

TEWL was measured from the eye corners of a wide range of people with different age groups. This was performed to find a relationship between age and water loss in the eye corners. A total of 37 people were tested, and eight of them aged under 35 had an average of 19.61, while 29 of them above 35 had an average TEWL value of 23.79. A significant difference is again evident in the sample sizes; however, the TEWL rate is found to increase with age, as shown by the significant difference between the averages. Hence, it may be concluded that a relationship exists between age and the rate of TEWL on the eye corners.

Eye corner	Count	Average [g/m ² h]
Below 35	8	19.61
Above 35	29	23.79

Table 3.7. Variance in TEWL of Eye Corner, as grams of water per square meter per hour (g·m⁻²·h⁻¹)

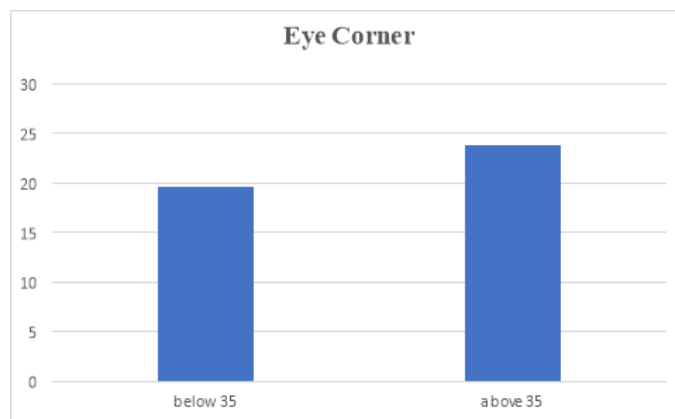


Figure 3.9. TEWL measurements performed on the Eye Corner below 35 (n= 100 subjects) and above 35 (n = 100 subjects) are represented in grams of water per square meter per hour (g·m⁻²·h⁻¹)

3.11.6 Forehead

TEWL was measured from the foreheads of a wide range of people from different age groups to assess the relationship between age and water loss from the forehead skin. A total of 86 TEWL measurements were taken from the forehead skin, and 22 of them aged under 35 had an average of 19.46. However, 64 of them who were aged over 35 had an average of 29.14. A huge statistical difference is observed between the sample size and the averages, so it is difficult to conclude any relationship between age and TEWL on the forehead skin. However, one fact may explain this difference: the length of the forehead increases with age, and this increase in length reduces the size of the corneocytes. Thus, TEWL may increase as one ages; however, the difference is not significant.

Forehead	Count	Average [g/m ² h]
Below 35	22	19.46
Above 35	64	29.14

Table 3.8. Variance in TEWL of Forehead, as grams of water per square meter per hour (g·m⁻²·h⁻¹)

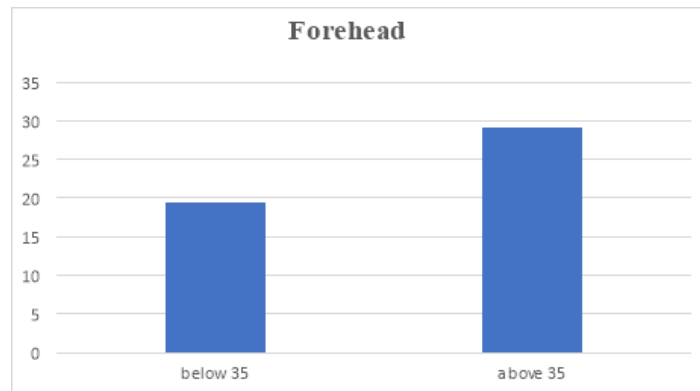


Figure 3.10. TEWL measurements performed on the Forehead below 35 (n= 100 subjects) and above 35 (n = 100 subjects) are represented in grams of water per square meter per hour (g·m⁻²·h⁻¹)

3.11.7 Cheeks

TEWL was measured on the cheeks of a wide range of people with different age groups to determine whether a relationship exists between age and water loss from the cheeks. A total of 107 samples were taken, which included 22 people below 35 years of age who had an average of 15.58, whereas 85 people who were above 35 had an average of 21.59. The sample sizes were not similar, yet the TEWL rate is observed increased with age, as demonstrated by the average values. This may be due to the fact that Ptotic cheek fat loosens to create a nasolabial fold, leaving a cheek concavity that is enhanced by malar fullness deletion. Ageing also brings changes to the cartilaginous nasal skeleton and soft tissue covering. Major changes occur in the glabella, nasion and upper dorsum, as shown in the following figure. Therefore, TEWL increases as the person ages, as the following table illustrates.

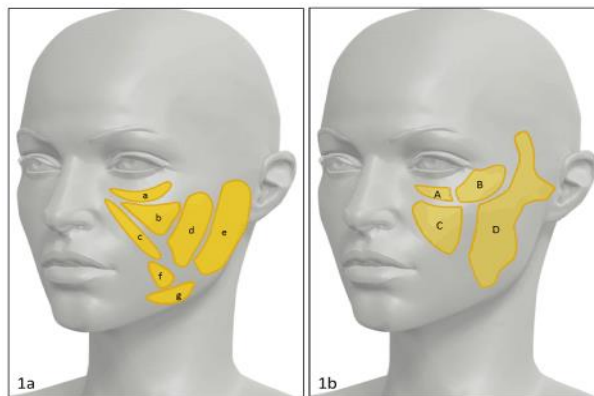


Figure 3.11: Cheek

Cheek	Count	Average [g/m ² h]
Below 35	22	15.58
Above 35	85	21.59

Table 3.9. Variance in TEWL of Cheek, as grams of water per square meter per hour (g·m⁻²·h⁻¹)

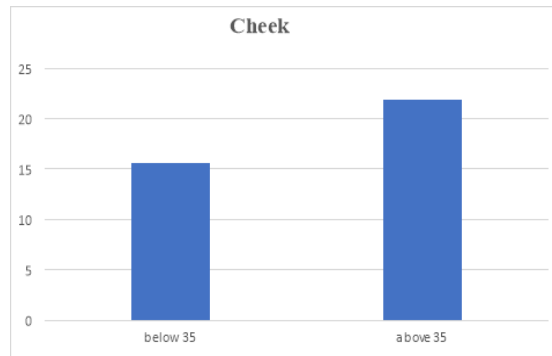


Figure 3.12. TEWL measurements performed on the Cheek below 35 (n= 100 subjects) and above 35 (n = 100 subjects) are represented in grams of water per square meter per hour ($\text{g}\cdot\text{m}^{-2}\cdot\text{h}^{-1}$)

3.11.8 Chin

TEWL was measured from the chin of a wide range of people with different age groups to determine whether any relationship exists between age and water loss from the chin. A total of 64 samples were taken. Fifteen aged under 35 years had an average of 23.11, while 49 aged over 35 had an average of 35.12. As shown by the average, the TEWL value increases with age.

Chin	Count	Average [g/m ² h]
Below 35	15	23.11
Above 35	49	35.12

Table 3.9. Variance in TEWL of Chin, as grams of water per square meter per hour ($\text{g}\cdot\text{m}^{-2}\cdot\text{h}^{-1}$)

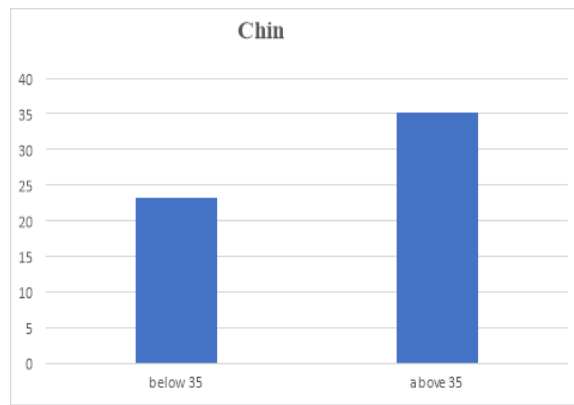


Figure 3.13. TEWL measurements performed on the Chin below 35 (n= 100 subjects) and above 35 (n = 100 subjects) are represented in grams of water per square meter per hour ($\text{g}\cdot\text{m}^{-2}\cdot\text{h}^{-1}$)

Loss of fat below the skin in the cheek area may result in loosening skin. Mostly around the mouth and chin, bone loss may become evident after age 60 and maybe the primary reason for the puckering of the skin around the mouth. Hence, it can be concluded that TEWL increases for chin skin as one ages.

3.12 Chapter Summary

This study focused on determining TEWL values at various anatomical sites on the facial skin. Nine different facial skin sites were included for TEWL measurement. The total of 501 readings were taken. All subjects' ages were taken into consideration when drawing the results accurately. The study was divided into two segments to extract the results more accurately and in greater depth. The first segment is linked to the determination of variance between TEWL values at different anatomical sites of facial skin. However, for the second segment, there was a determination of the association of TEWL with age.

Hence, all the participants were divided into two groups. One group included individuals aged under 35, whereas in group 2 all human subjects were aged over 35. All values were carefully noted, and statistical tools were applied to them for the calculation of mean and standard deviation. The highest variance of TEWL was reflected for the neck and lip. The highest TEWL value was recorded for the lip. However, the lowest mean value of TEWL was recorded for the neck skin. Welch's t-test was the statistical tool applied to the data. The 3-sigma point corresponds to the 0.27% level of significance of the two-sided test. With the advancement of age—particularly after 60—individuals begin to lose bone along with fat, resulting in the puckering of skin and dehydration. The results obtained supported the null hypothesis.

Chapter 4. Skin Hydration Measurements

4.1 Experimental Results of Epsilon

The primary purpose of this chapter is to present the study and its results to formulate the measurements and demonstrate skin hydration results and their relationship with several anatomical facial sites. The skin hydration was measured by using Epsilon instrument, under the normal ambient laboratory condition ($\sim 21^{\circ}\text{C}$, $\sim 40\%$ relative humidity(RH)), at skin sites of 48 healthy volunteers (10 male, 38 female, age between 18–70 y). The facial anatomical sites considered were the forehead, cheek, lip, chin, under-eye area and nose, and 1299 human subjects measurements were conducted by using Epsilon.

Anatomical site	Count	Mean (Dielectric Constant)	Standard deviation
Lip	86	21.42	5.75
Nose	116	23.13	4.65
Forehead	232	24.05	6.40
Chin	157	25.28	6.99
Neck	108	26.15	8.19
Cheek	239	26.46	7.36
Eye Corner	92	27.32	7.89
Under-eye	144	28.00	7.93

Table 4.1. Illustration of Epsilon values (dielectric constants) with mean and SD.

As an individual's age, there exist variations in the various anatomical sites of facial skin, these variations were also observed in response to exercise (Flament, et al., 2020).

The study was divided into two significant segments. The first segment of the experimental study included the reason for the variance between Epsilon values. However, the second segment of the study reflects Epsilon's relationship with exercise. Epsilon values (measured as dielectric constant or relative permittivity, no units) were determined for all human subjects at different anatomical sites. These values are provided in Table 4.1 along with other parameters that include their count, mean and standard deviation.

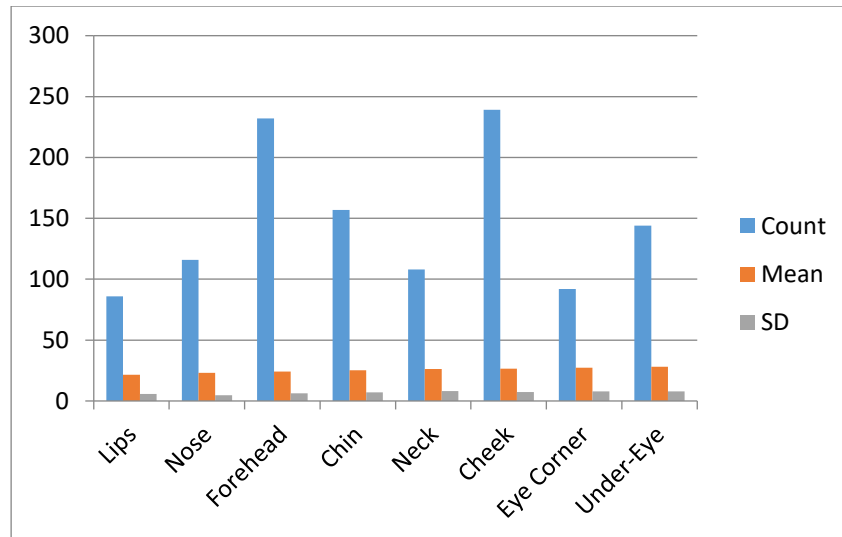


Figure 4.1. Graphical illustration of Epsilon values with Mean and SD.

Among all 144 facial skin sites, the under-eye area showed the highest mean value at 28.00, its graphical representation is given in Figure 4.1. Lips had the lowest mean value at 21.42. Several reasons contribute to these differences in Epsilon levels. The most significant reasons include the degree of corneocyte formation, lipid contents of SC, skin temperature, damaged barrier function, and skin blood flow (Logger, et al., 2019).

Additionally, age and ethnicity are the factors that are responsible for having an impact on experimental results. Besides this, exercise is also a valuable factor that seems to have a distinct impact on the Epsilon value of different anatomical sites of facial skin. The detailed study is discussed in the following sections.

4.2 Causes of High Epsilon Values on the Under-eye and Eye Corner

The experimental study demonstrates a high mean value for the Under-Eye for Epsilon, which is 28.00. The next highest value for facial skin belongs to the Eye Corner, with a mean Epsilon value of 27.32. These higher mean values are attributed to the different characteristics of the under-eye and eye corner skin; that is the reason the skin of under-eye area is relatively thinner than that of other facial sites.

The under-eye area is composed of various layers of skin and blood vessels and contains hypodermis, dermis, and epidermis. The hypodermis is the innermost skin layer that includes subcutaneous tissues. These tissues are composed of connective tissue and fat. The middle layer is known as the dermis, characterised by the sweat gland, hair follicles, and rigid connective tissues. The outermost skin layer of the under-eye area is the epidermis, which is exposed to the outer environment (Logger et al., 2019). It aims to provide a waterproof barrier for the skin and to contribute to the formation of skin tone.

The skin tone of the under-eye area is relatively dark owing to the presence of high levels of melanocytes. The under-eye skin can retain fluid, which is the main reason for the appearance of eye bags. Elastic breakdown or deficiency of collagen contributes to

ageing and ultimately leads to a loss of skin structure. The eye skin is about ten times thinner than other facial skin. Environmental exposure, smoking, and sun exposure are other factors that aggravate the thinning of the skin under and around the eye. Wrinkles at the sides of the eyes are typically represented by three prominent lines, commonly known as crow's feet.

4.3 Cheek in Epsilon Values

The Epsilon value for cheeks observed for human subjects in this study was 26.46. The skin of the cheek region is drier and thicker than other facial areas. In children, the permeability barrier in the subcutaneous and cutaneous skin layers of the cheek is immature. However, in adults, this barrier is found to be relatively mature. Ageing is the main factor leading to alteration in the cheek skin. This may be a physical and anatomical alteration that speeds up due to exposure to pollution or sunlight. Hence, with advancing age, the Epsilon value for the cheek skin increases (Zhao, et al., 2020).

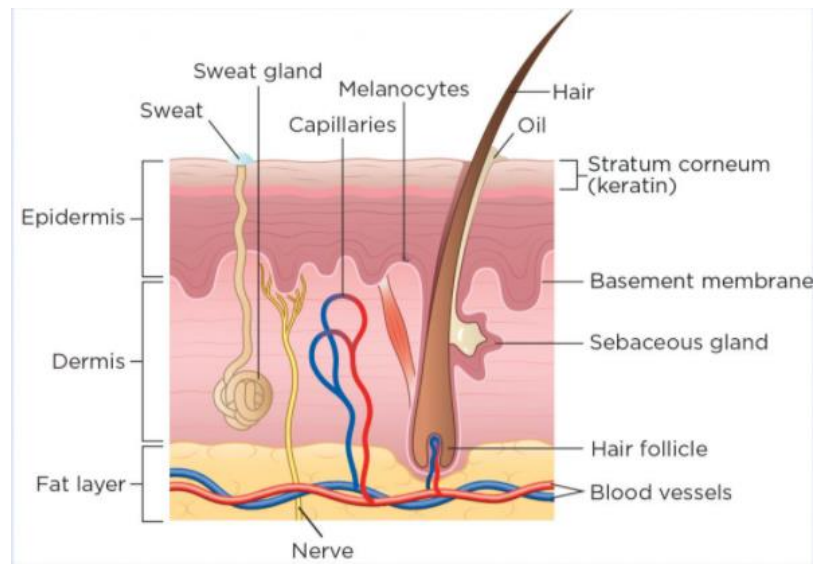


Figure 4.2. Cross-section of Cheek skin (Nursing Times, 2019)

The tough and rigid skin acts as a barrier to moisture loss and tries to retain moisture. Connective tissue fibres run throughout the cheek and connect the dermis to the Superficial Musculo-Aponeurotic System (SMAS) layer. These tissues and fats are the main constituents of the subcutaneous layer.

4.4 Neck in Epsilon Values

In this study, 108 human subjects were studied to determine the Epsilon values for the neck. The study revealed these values for the neck to be 26.15. The neck's skin is quite thick and rigid, as it has to support various essential body organs. In comparison to other facial skin, the neck's corneocyte layer is relatively large. This large layer is responsible for affecting the extensive path length for water efflux. Consequently, the neck's water content does not escape quickly. Hydrated muscles and tissues contribute to healthy skin conditions. Dehydration of the neck muscle and skin leads to itching and scaling.

Lifestyle modifications, such as quitting smoking, can help ensure the retention of high moisture levels in the facial skin (Chirikhina et al., 2020).

4.5 Chin in Epsilon Values

Table 4.1 illustrates the Epsilon value of the chin to be 25.28. The chin is one of the most prominent facial areas whose skin is comparatively oily. The Epsilon value for the chin increases with advancing age. It contains fat compartments in it, which are responsible for resisting the loss of water content from this section. It plays a significant role in the determination of facial profiles. Mentalis contraction is responsible for affecting the skin of the chin and lead to wrinkles. Mentalis are also known as the pouting muscles.

As the skin of the chin is oily, it retains moisture it for longer. On the contrary, the facial regions with thin skin or less water content are subjected to wrinkles. The double or triple chin reflects the heavy layers of skin below the chin. These layers can be removed by pushing your head to back side and look to the ceiling, then move the lower jaws forward to stretch the skin which is below the chin as much as possible. The rejuvenating power and high recovery are possible when the skin is highly hydrated and depicts high water content.

4.6 Forehead in Epsilon Values

The forehead is comparatively larger than other facial sites and contains various essential anatomical structures. The most significant of these include the bones, scalp and skull. Facial expressions convey human's personalities. All facial expressions rely on the movement of the forehead muscles. A common facial feature that cannot be ignored is wrinkles. Like the chin area, the forehead also contains oil. Adipose tissues have fat globules that accumulate to make fat. Excess sebum can lead to pimples, and hence, oily skin must be cleansed appropriately. The high sebum content of the forehead and T-zone area (chin, nose and forehead) prevents the skin from wrinkling while also staving off other signs of ageing for longer.

4.7 Nose in Epsilon Values

The mean Epsilon value calculated for the noses of 116 human subjects was found to be 23.13. The nose hydration level is relatively lower than those of other facial sites. The low Epsilon value is linked to damaged barrier function. All individuals experience colds on many occasions throughout their lives, and the use of handkerchiefs can affect the nose barrier function. Like the facial skin, it has a porous structure, but the nose's pores are relatively larger than those in other facial areas. Damage to the nose skin along with nasal colds also impacts the porous structure. Ultimately, it permits excessive water loss from the nose. Hence, it is found to be less hydrated than other facial skin sites.

4.8 Lip in Epsilon Values

The mean Epsilon value for lip skin was 21.42. Lip skin varies in structure from other anatomical sites, and these differences result in the lower hydration value. The lip skin is

soft and pliable. It contains a muscle layer, connective tissue and epidermis on its surface. The specialised transitional region of the lip moves towards the oral mucosa. The vermilion zone is the region where the outer lips join the facial skin. At the vermilion border, the facial skin's connective tissues have a high level of flexibility, and the epithelium contains a thin orthokeratinised layer. The SC of lip skin is different to that of other facial skin sites, but it contains the same ceramide types.

The blood vessels in the lip area are particularly visible due to the thinness of the lip skin; this is the reason for the lips' rosy appearance. The barrier function of lip skin is weak; hence, moisture evaporates from the lips easily, leaving them less hydrated. Due to ageing the structural and morphological changes appear in the lip skin. The submucosa is the region of skin that is closest to the oral mucosa, and it contains less hydration than the external vermilion zone.

4.9 Variance of Epsilon Values with Exercise for Different Anatomical Sites

This section of the experimental study will present the analysis of the Epsilon values of different facial skin sites in relation to exercise. Epsilon data was gathered for males and females before and after exercise to determine the impact of exercise on the level of hydration. The facial pores remain intact in normal conditions. However, any strenuous task or exercise causes the pores to open, ultimately leading to the evaporation of fluid from the skin. This evaporation results in the sweating. The more vigorous the exercise is, the more the individual will sweat. Hence, it is recommended that the body be kept hydrated during exercise to prevent dehydration. Fluid consumption or contact with

moisture through wet towels or facial sprays helps to regain moisture and keep skin hydrated.

Female subjects were engaged in exercise for the purpose of comparing their Epsilon values before and after exercise, see table 4.2. Their Epsilon values for various facial skin sites were monitored. These include the forehead, under-eye R, under-eye L, nose, cheek R, cheek L, chin, and lips. After the values of these sites were recorded, the women were instructed to consider different types of exercise, including walking, working out, cycling, minor weight lifting, running, etc. Afterward, the participants' hydration levels were noted with an Epsilon corneometer to evaluate the impact of exercise. The following table illustrates the Epsilon values of the participants' facial skin before and after exercise.

FEMALE	Epsilon Values Before Exercise (Dielectric Constant)			Epsilon Values After Exercise (Dielectric Constant)			Difference of Averages
	Min	Average	Max	Min	Average	Max	
Forehead	30.5	31.4	33.4	30.7	33.5	35.4	2.1
Under-eye R	31.4	33.2	34.9	31.8	33.5	34.7	-0.3
Under-eye L	31.6	33.1	34.7	32.6	33.9	34.8	0.8
Nose	20.8	23.3	29.9	27.9	29.9	32.4	6.6
Cheek R	26.2	27.1	29.2	29.6	32.1	35.3	5
Cheek L	25.7	26.9	30.5	30.4	32.4	35.4	5.5
Chin	28.2	29.3	31.8	29.8	32.2	33.7	2.9
Lips	27.4	29.5	32.8	27.7	30.2	32.2	0.7

Table 4.2. Illustration of Epsilon values of female before and after exercise

The maximum average Epsilon value before exercise was found for the facial skin of Under-eye R in females. After exercise, however, the maximum average Epsilon value was calculated for the skin of Under-eye L. Comparison of the Epsilon values for facial skin before and after exercise showed the highest value for the nose, with an increase of 6.6. The Epsilon value for nose skin was 23.3, which increased to 29.9 while depicting an enhanced value of 6.6.

Male participants were also instructed to exercise in order to gather their Epsilon values for different anatomical sites before and after exercise. Epsilon values for males before and after exercise were found to be greater than those for females, see table 4.3.

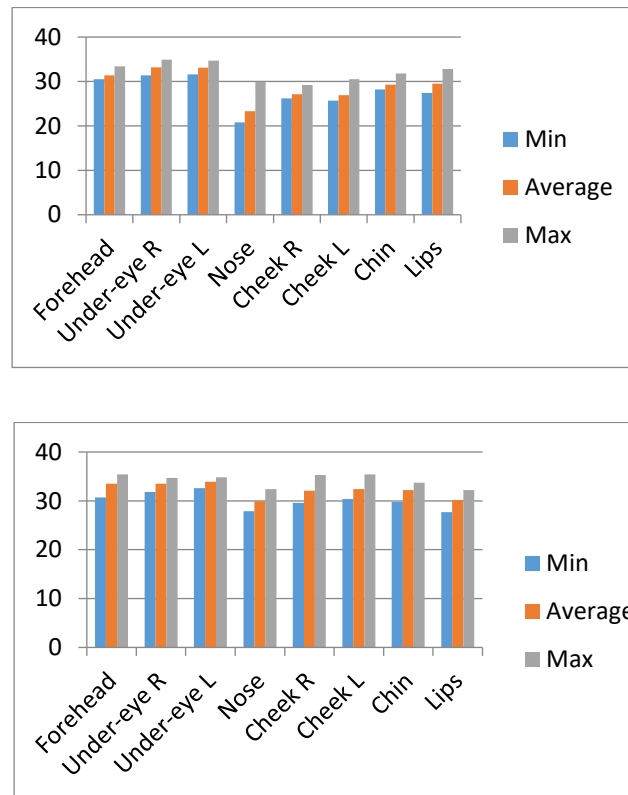
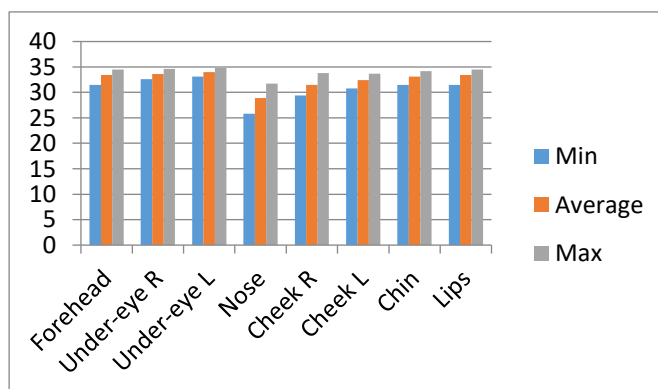


Figure 4.3. Graphical illustration of Epsilon values of female before and after exercise

Men's sweat contains a greater amount of lactic acid than that of women. Lactic acid is a natural humectant that has a greater capacity to retain moisture. Hence, men's skin is more hydrated than women's skin. Additionally, men's pH levels tend to be lower than those of women (Song, et al., 2019). In the next sub sections, each of the facial regions is discussed individually before and after the exercise for both of male and female.

MALE	Epsilon Value Before Exercise (Dielectric Constant)			Epsilon Value After Exercise (Dielectric Constant)			Difference of Averages
	Min	Average	Max	Min	Average	Max	
Forehead	31.5	33.4	34.5	31.5	33	35.6	0.4
Under-eye R	32.6	33.6	34.6	31.4	33	34.4	-0.6
Under-eye L	33.1	34	34.8	30	32.5	34.7	-1.5
Nose	25.8	28.9	31.7	31	32.8	34.2	3.9
Cheek R	29.4	31.5	33.8	30.1	31.6	33.2	0.1
Cheek L	30.8	32.4	33.7	32.3	33.2	33.4	0.8
Chin	31.5	33.1	34.2	31.8	33.2	34.4	0.1
Lips	31.5	33.4	34.5	31.5	33	35.6	-0.4

Table 4.3. Illustration of Epsilon values of male before and after exercise



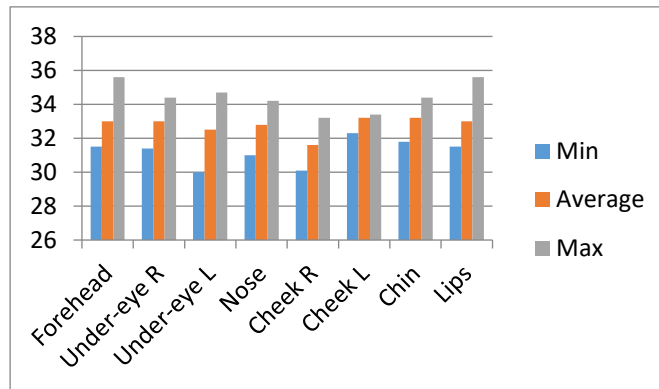


Figure 4.4. Graphical illustration of Epsilon values of male before and after exercise

4.10 Forehead

The average Epsilon value for forehead skin in males was found to be reduced after exercise. However, in females, the average Epsilon value for forehead skin increased from 31.4 to 33.5. Changes in the Epsilon values of different facial sites are observed after exercise. This is because the facial skin undergoes various changes in response to exertion. Skin structure, the nature and number of pores, skin thickness and skin elasticity are the key factors contributing to the differential Epsilon values before and after exercise. During exercise, the body's heat dissipates, and so does that of the facial skin. The facial skin cools down as the heat is eliminated from the skin. The process includes enhanced blood flow to the face and enhanced sweat secretions. The high blood flow is responsible for nourishing the skin cells, which improves the skin's hydration. Blood includes numerous nutrients and oxygen that it carries throughout the cells. In response to exercise, the delivery of nutrients and oxygen to the different facial skin sites increases and the regions that receive these quickly exhibit higher hydration levels than others.

Forehead	Male (Dielectric Constant)	Female (Dielectric Constant)
Before exercise	33.4	31.4
After exercise	33	33.5

Table 4.4. Illustration of Epsilon values of male and female before and after exercise

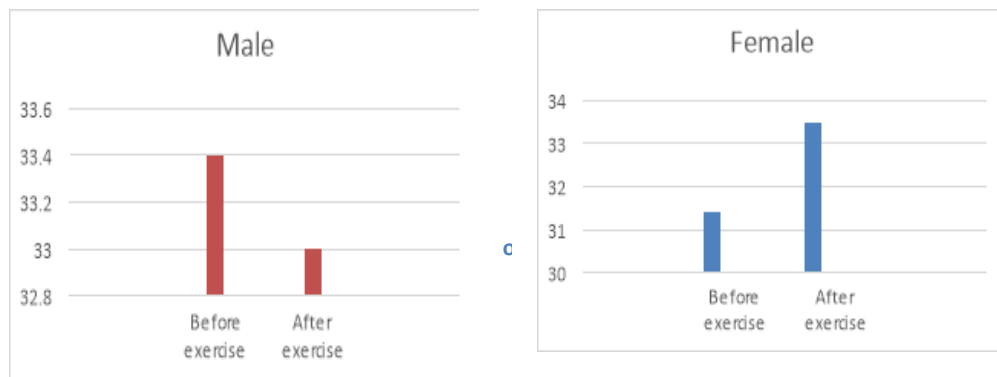


Figure 4.5. Illustration of Epsilon values of male and female before and after exercise

4.11 Undereye Right and Undereye Left

In men, the average Epsilon value indicates a reduction after exercise for both the right and left under-eye. By contrast, female participants' Epsilon values show elevated readings after exercise for both the left and right under-eye areas. Testosterone is the male hormone that contributes to the enhanced thickness of male skin, and is the main reason that male skin is approximately 25% thicker than that of females. Hence, when they practice high-intensity exercise, they sweat more and lose hydration from their

facial skin. Unlike females, the average values of the right and left under-eye areas in men indicate reduced Epsilon values.

Under-Eye R	Male (Dielectric Constant)	Female (Dielectric Constant)
Before exercise	36.6	32.2
After exercise	36	33.5

Under-Eye L	Male (Dielectric Constant)	Female (Dielectric Constant)
Before exercise	34	33.1
After exercise	32.5	33.9

Table 4.5. Illustration of Under-eye R and Under-eye L values of male and female before and after exercise

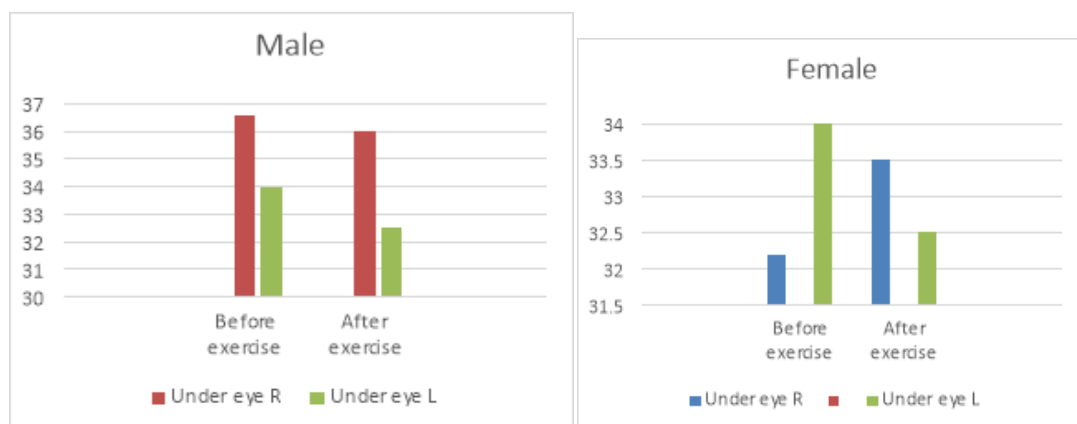


Figure 4.6. Illustration of Under-eye R and Under-eye L values of male and female before and after exercise

4.12 Nose

The average Epsilon value for nose skin in females shows a massive increase after exercise. Before exercise, it was 23.3, which increased to 29.9 after exercise. Likewise, male participants also showed an increase in their average Epsilon value for nose skin, from 28.9 to 32.8. The nose indicates elevated hydration as a result of exercise. The impact of working out on the nose skin in both males and females was optimum. The difference between their averages was calculated for before and after exercise in males and females as 3.9 and 6.6, respectively. Nose skin contains sebum, which prevents fluid loss, and blood circulation to the nose skin improves with exercise. Compared to other facial sites, it is the area that is least prone to signs of ageing.

Nose	Male (Dielectric Constant)	Female (Dielectric Constant)
Before exercise	28.9	23.3
After exercise	32.8	29.9

Table 4.6. Illustration of Nose values of male and female before and after exercise



Figure 4.7. Illustration of Nose values of male and female before and after exercise

4.13 Cheek Right and Cheek Left

The average Epsilon value for the right and left cheeks shows an increase after exercise for both males and females. For the left cheek, the Epsilon value in males increased from 32.4 to 33.2 after exercise. In females, the Epsilon values for the right and left cheeks were 27.1 and 26.9 before exercise, respectively. However, they increased after exercise, with Epsilon values of 32.1 and 32.4 for the right and left cheeks, respectively (Kim, 2006).

Cheek R	Male (Dielectric Constant)	Female (Dielectric Constant)
Before exercise	31.5	27.1
After exercise	31.6	32.1

Cheek L	Male (Dielectric Constant)	Female (Dielectric Constant)
Before exercise	32.4	26.9
After exercise	33.2	32.4

Table 4.7. Illustration of Cheek R and Cheek L values of male and female before and after exercise

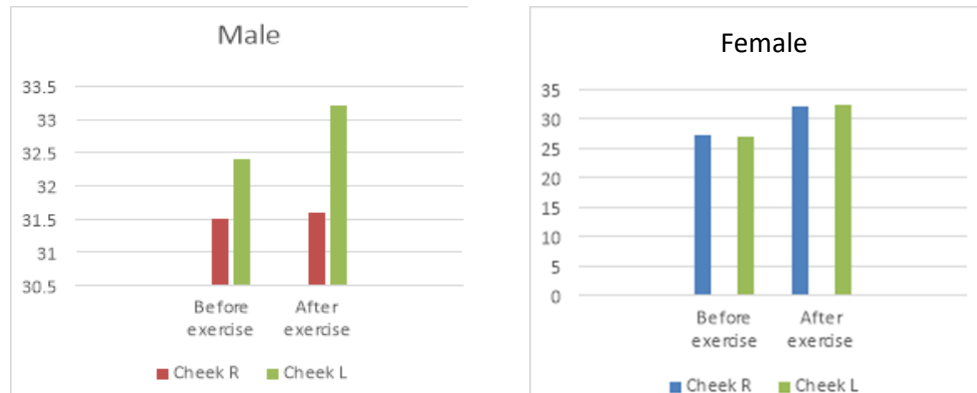


Figure 4.8. Illustration of Cheek R and Cheek L values of male and female before and after exercise

4.15 Chin

Loss of moisture from the chin region in males was negligible. However, in females, the Epsilon value for chin skin before and after reflects a vast difference. The average Epsilon value before exercise was 29.3, which increased to 32.2 after exercise. The hydration level was observed to be higher in women chins than men, who lost hydration after exercise. The improved hydration level contributes to plump skin and reduces the risk of cracks.

The chin's skin is thick and contains a protective SC that helps retain fluid. The facial sites of that release more sweat are subject to greater fluid loss. However, the removal of heat from the facial skin as a workout or exercise contributes to replacing the body fluids loss due to sweat (Song et al., 2019). In this way, the facial skin becomes hydrated, particularly at sites that receive a high blood circulation levels and contain sebum to prevent fluid loss.

Chin	Male (Dielectric Constant)	Female (Dielectric Constant)
Before exercise	33.1	29.3
After exercise	33.2	32.2

Table 4.8.

Chin values of males and females before and after exercise

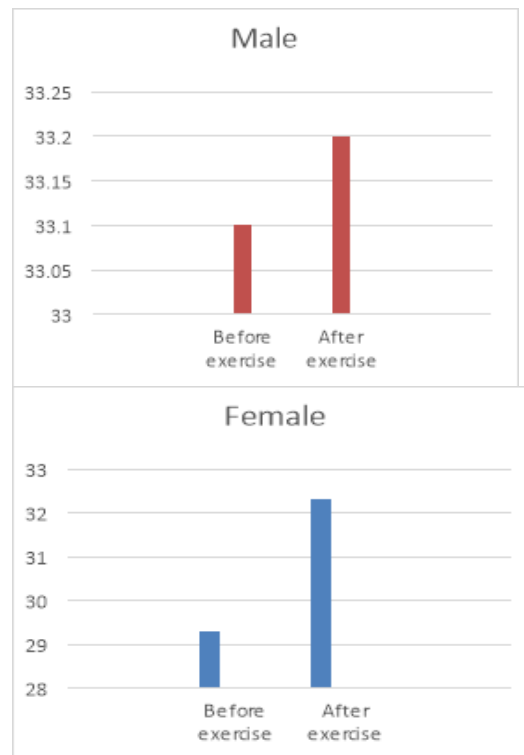


Figure 4.9. Chin values of males and females before and after exercise

All facial skin sites have pores, and sweat evaporates through these. The replacement of fluid by enhanced circulation reduces the risk of heat stress. It optimises the functionality of the human body and ensures enhanced energy levels when performing

tasks. The combination of improved circulation and hydration is responsible for glowing facial skin.

4.16 Lips

In men, the average Epsilon value for lip skin was 33.4 before exercise, which declined to 33. It reflects the loss of moisture from lip skin. By contrast, in females, the Epsilon value was detected to be 29.5, which was increased after exercise. After exercise, the average Epsilon value for lip skin in females was 30.2. As light increase was observed in the Epsilon value for lip skin in females, while in males, the Epsilon value for lip skin obtained after exercise was lower. Dehydration of lip skin causes it to crack. In severe cases, skin dehydration on the lips leads to bleeding. Both men and women must ensure that their lips are adequately hydrated. Thin skin at the lips is a weak barrier for the prevention of water loss. Chapped lips occur for several reasons, including cold, consumption of spicy foods, licking of lips, irritation or exposure to the environment. Sun damage and cold are the most significant causes of damaged lip skin.

Epsilon values for the different facial sites vary between males and females, with lower Epsilon values calculated for males. Gender impacts the Epsilon values for facial skin. Men require more hydration than women, as their skin is drier and tougher. Men's skin also contains less fat that can function as a barrier preventing moisture loss (Voegeli, et al., 2019). However, females have more hydrated skin with sufficient fat levels at different sites. Men's energy expenditure is higher than that of women, leading to greater loss of moisture.

Lip	Male (Dielectric Constant)	Female (Dielectric Constant)
Before exercise	33.4	29.5
After exercise	33	30.2

Table 4.9. Lips values of male and female before and after exercise

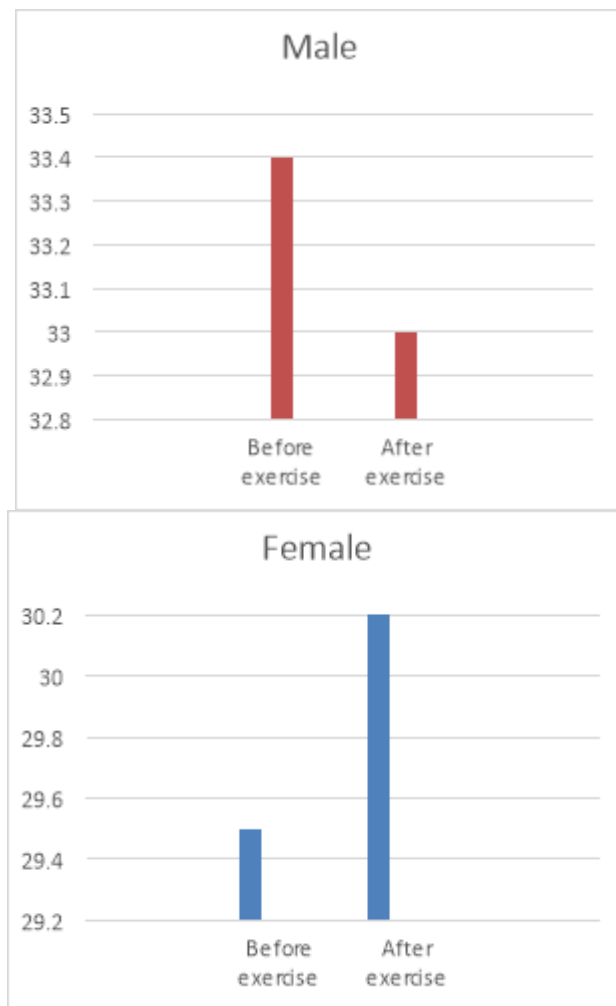


Figure 4.10. Lips values of male and female before and after exercise

4.17 Hydration-based Face Mapping

By placing the Epsilon images on the corresponding part of face, it is possible to create a hydration-based face mapping. Below are several examples of hydration visual face maps, obtained using Epsilon from people of different sexes, ages and ethnicity. One can clearly observe significant differences in both hydration and texture among the different volunteers.



Figure 4.11. Hydration visuals of different Caucasian females of age: top 41 and 51, bottom 53 and 33.

4.18 Chapter Summary

Epsilon is one of the most significant instruments used in skin analysis. This in-vivo method of skin analysis was used in the present study to formulate the results. The experimental study using Epsilon was divided into two sections. One section included the evaluation of variations in facial skin at various anatomical sites. It includes 1299 humans who were tested to determine variations in the skin at different anatomical sites. In the second section, the Epsilon values for facial skin were calculated before and after exercise in both genders. According to the results obtained, the under-eye skin showed the highest mean Epsilon value. However, the mean Epsilon value of lip skin was determined to be the lowest. The mean Epsilon values for under-eye skin and lip skin were calculated at 28.00 and 21.42, respectively.

The major reasons behind these values are blood flow, degree of corneocyte formation, lipid contents of SC, and skin temperature. Skin structure and composition vary from one anatomical site to another. Environmental factors, age and exercise play a significant role in skin health. Highly vigorous exercise induces sweating and aggravates hydration loss. The next highest mean Epsilon value was recorded for the eye corner skin at 27.32. The cheek showed a mean Epsilon value of 26.15. Before exercise, the Epsilon value for nose skin was 23.3, which subsequently increased to 29.9. Hence, it reflected a huge change in value, with a difference of 6.6 in females. A Hydration-based Face Mapping has also been created by placing the Epsilon images on the corresponding part of face.

Chapter 5. Skin Ultrasound Measurements

The primary purpose of this chapter is to measure the skin ultrasound using Episcan and to demonstrate the significance of Episcan in determining the skin issues at various anatomical sites. Episcan helps illustrate the facial skin in considerable detail by providing internal imaging. These include the illustration of skin layers, such as the dermis, epidermis, subcutaneous tissue and deep fascia, along with the probe membrane. Episcan is among the latest high-resolution techniques to bring about massive innovation in medicine, aesthetics, and dermatology. This imaging system is popular owing to its high-resolution ultrasound (HRUS) characteristics (Mandava et al, 2013). The ultrasonic waves of the Episcan instrument range from 20 MHz to 50MHz. These frequencies can generate skin images with spatial resolutions from 80 to 32 μm (Bezugly, 2021), and can help to demonstrate the in-depth imaging of skin to provide a clearer view (Reginelli, et al., 2020). The highest frequency of Episcan is 50 MHz, which ensures that skin imaging is visible to the clinicians and dermatologists until the skin's underlying soft tissues (Xiao, et al., 2020). Moreover, the instrument's interface is user-friendly; hence, it does not cause any irritation or disturbance to the subject while they were subjected to the experimentation results with Episcan.

High-resolution and precise imaging was obtained from Episcan to analyse the skin condition and its hydration. Both males and females were enrolled in the experiment, ranging in age from 20 to 70. Different anatomical facial skin sites were analysed, including the eyelid, forehead, chin, nose, cheek, lip, neck and arm. The adult males and females were Black, Indians or Americans. Episcan's wide-ranging clinical applications make it a worthy and reliable tool for research and development. The examination of the

facial skin, as given an example in Figure 5.1, facilitated by Episcan includes a view at the microscopic level, proving to be an alternative solution to biopsies (Chirikhina et al., 2020).

The images obtained during the experimentation revealed different sites of the skin. These define the skin's properties in detail, including fat content, thickness, density and water content. Colour images are necessary to distinguish the different sites from one another. Monochrome presentation can be confusing and lead to loss of information. In this study, it is demonstrated and calculated various human skin factors from the anatomical sites and compared them for the purpose of confirming or rejecting the hypothesis.

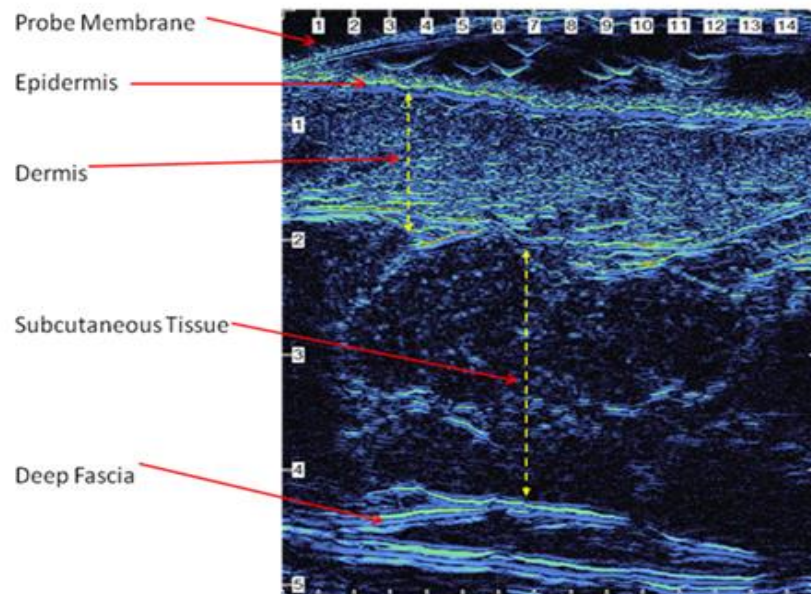


Figure 5.1. Cross-sectional Illustration of Skin (Longport, 2018)

Episcan's non-invasive nature makes it a likeable and popular part of aesthetic and beauty care. It offers imaging for all kinds of injuries and wounds. Moreover, it has

proven to be an early and rapid detection source for underlying pressure ulcers. This skin assessment aid can be used as a complementary means of confirming and elaborating on skin conditions to prevent any possible future hazards (Borzdynski, et al., 2016).

The advanced software's cost-effective approach improves the presentation and processing of data with optimum flexibility (Zhang, 2020). It offers rapid data up to a speed of about 200MSPS (200 million samples per second), allowing the system to capture as much information as possible. Probes of various resolutions and depths can be used.

Comprehensive detailing with a friendly interface is Episcan's main feature. Besides this, it allows the tiling of multiple images on the scanner screen along with an illustration of the progression of conditions, thus making comparison quick and flexible. Any suspected damage to skin tissues can be diagnosed using Episcan. High-frequency ultrasonic waves facilitate estimation of changes and damages to the skin. Clinical skin assessment has become easier and quicker with such advanced tools.

5.1 Variance of Episcan in Skin Layer Assessment for Different Anatomical Sites

Episcan was used to assess the skin layer thickness of chin, nose, cheek, forehead, lip, neck, eyelid, and arm of healthy volunteers (aged 18–70, both male and female, Caucasian and Asian). According to the obtained results, the cheek contains the highest percentage of dermis among all facial sites, see table 5.1. The dermis percentage of the

cheek was about 95.3%, while the neck's dermis percentage was the lowest at 92.0%. The dermis is the skin's inner layer and is comprised of hair follicles, nerves, sweat glands, sebum glands, blood vessels and connective tissue. The papillary dermis is the upper thick layer, while the reticular dermis is the lower, thin layer. The dermis percentages of the lip, arm and eyelid were observed to be 92.5%, 90.7%, and 94.5%, respectively. However, the dermis percentages for the chin, nose and forehead were all 95.2%. The standard deviation was highest for the cheek at 0.437. By contrast, it was lowest for the forehead at only 0.173.

	Count	Full skin (mm)	Standard deviation	Stratum Corneum (mm)	Epidermis (mm)	Dermis (mm)	Dermis %
Arm	498	1.306	0.194	0.024	0.047	1.185	90.7%
Eyelid	453	1.309	0.226	0.025	0.052	1.238	94.5%
Neck	490	1.378	0.187	0.026	0.054	1.267	92.0%
Lip	477	1.426	0.294	0.027	0.064	1.320	92.5%
Forehead	451	1.647	0.173	0.028	0.065	1.569	95.2%
Cheek	551	1.690	0.437	0.032	0.074	1.611	95.3%
Nose	487	1.912	0.316	0.033	0.077	1.821	95.2%
Chin	339	1.929	0.271	0.038	0.083	1.837	95.2%

Table 5.1. Episcan results of Skin Layer Thickness (mm) at Various Anatomical Sites.

The full skin measurement indicated the maximum values for the chin 1.929mm, while the lowest value 1.306mm was recorded for the arm. The full skin is basically the combination of all skin layers with their thickness, density, features and several other aspects, see Figure 5.1 for example. The epidermis and SC values measured using Episcan for the determination of different facial skin sites was noted. The value for the

SC was found to be highest for the chin, at 0.038mm. However, it was lowest for the arm, which was merely 0.024mm. Likewise, the epidermis measurements recorded for the arm and chin was lowest and highest, respectively. It was 0.047mm for the arm, while for the chin the value noted was 0.083mm. A deviation from the mean indicates poor skin condition. The risk of skin damage will be higher when the standard deviation is high. It represents a move away from the ideal skin conditions that the ultrasonic dermal scanner can detect easily (Chirikhina et al., 2020).

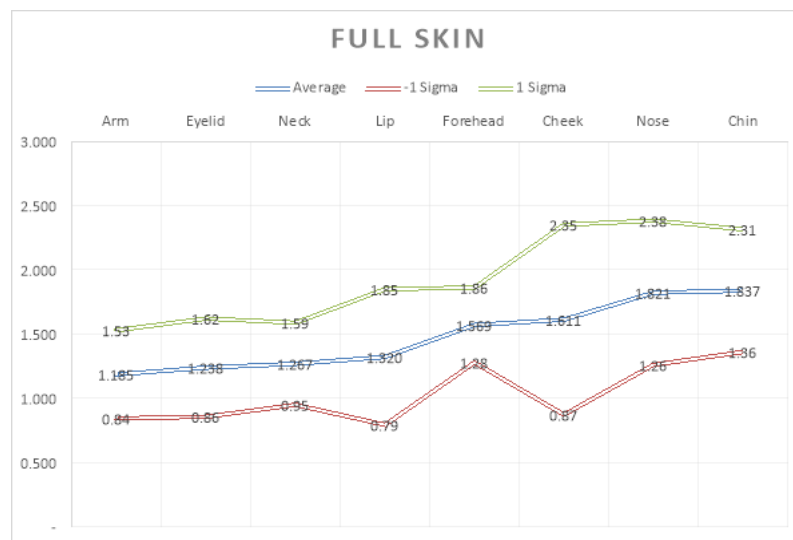


Figure 5.2. Sigma Values of Dermis Skin Layers

In this experimentation, the standard deviation was found to be higher for the cheek, at 0.437mm, which indicates a deterioration of conditions at this particular site. The next highest value for the standard deviation after the cheek was found to be for the nose, which was 0.316mm. However, the least subtle changes were observed in imaging the anatomical site of the forehead skin, whose value is 0.173mm. The graphical

representation Dermis layer of human skin for the different anatomical sites, along with its average and sigma values is given in Figure 5.2.

The average value or mean for the arm dermis was lowest, at 1.185mm. It was found to be highest for the chin, at 1.837mm, as given in the Figure 5.2. The dermis mean values of the eyelid and neck remained closer to the mean value of the arm. However, a drastic gap was observed between in the mean values of the arm and chin. The highest sigma value was observed for the chin, which is 1.36mm for -1 sigma. While, for +1 sigma, a higher value was found for the nose. Forehead values in-1 sigma were close to the chin and were found to be 1.28mm, while the lowest value was for lips, which were found to be 0.79mm. Values closer to the mean are beneficial for the skin, while a greater deviation from the mean suggests pathological conditions.

Here, the cheek and lip are shown to have negative and positive maximum standard deviations from the mean, respectively. The thickness of the cheek skin plays a key role. It is a broad area of skin that comprises various layers and is considerably exposed (Raj, et al., 2017). Its skin is somewhat rigid compared to that at other facial sites. However, the pores, the pore structure, and sebum levels vary in this area. Acne and other facial issues are much more prominent in this area. Flawless, healthy skin is possible when it has optimum elasticity and freshness. Likewise, the lips are sensitive and require frequent moisture. Upon exposure to harsh conditions or any health issues, the lips and cheek become moisture-deprived, and the cracking and bleeding may ultimately ensue. However, nutritional deficiencies can cause poor health conditions for the cheek and lip

skin (Watanabe, et al., 2019). Lip skin comprises stratified squamous epithelium. The sensitivity of the lips' skin is due to the sensory cortex, which is located in the mucous membrane. The vermilion border is the main area that separates lips from rest of the facial skin. It is located at the lips' edges and is reddish in colour. It functions as a transition layer for the lip and the inner mucous membrane, hair-bearing tissue and outer mucous membrane. This sensitive area comprises three layers—the oral mucosa, muscle and skin. The skin here is thinner than at any other site.

The delicate and thinner skin has a thickness of only 3–5 layers, while the skin at other facial sites is thicker, for approximately 16 cell layers. For this reason, these elements require more care and attention. Moreover, it contains apparent blood vessels, which contribute significantly to the area's red or pink colour. The cheek skin comprises the subcutaneous layer, which contains connective tissue fibres and fat. These are present in the skin throughout the face and connect the dermis with the SMAS layer. The layering and organisation of the fat are responsible for determination of the subcutaneous tissue that the cheek contains.

Visibly traumatised skin is indicated by peeling, scaling, irritation, enlarged pores, dull tone, etc. However, internal damage can be detected using an imaging system with optimum resolution (Whitney, et al., 2020). Damaged skin manifests in various ways, including hyperpigmentation, swelling, burning, pain, oozing, boils, blisters, rash, itching and redness. Clear and flawless skin maintained with good hydration ensures that the skin layers have the appropriate density and better immunity against hazards.

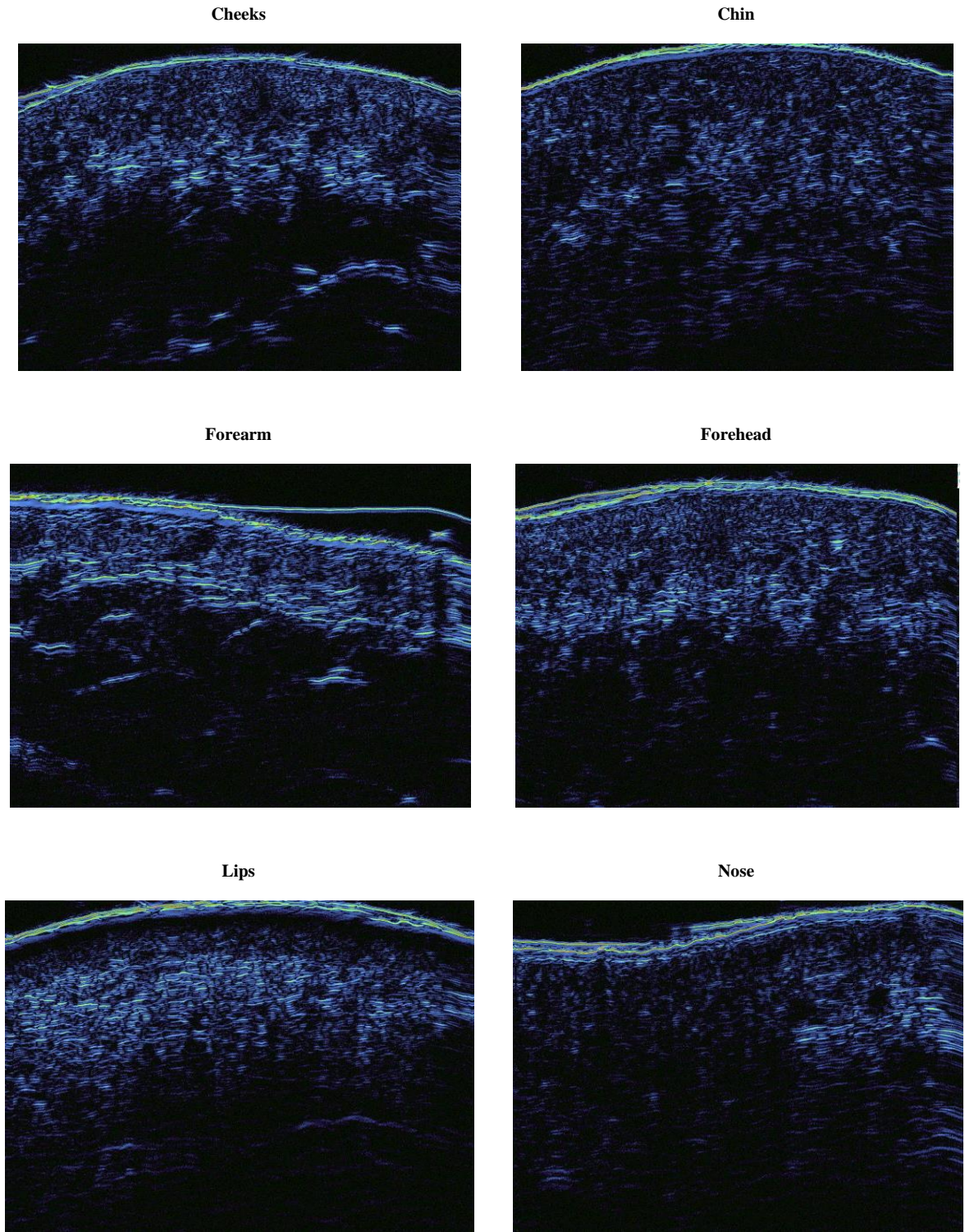


Figure 5.3. The cross-sectional high-resolution ultrasound images for cheeks, chin, forehead, arm, lips, and nose

Underlying skin that is subjected to hormonal changes, poor blood flow, or ruptures can lead to worsening skin health and appearance. Dermatologists can examine the inner skin closely with using advanced tools, such as Episcan, to recommend appropriate products or treatments. The images produced by Episcan for healthy subjects in the present study are presented in Figure 5.3.

This figure shows the results of microscopic imaging for different anatomical sites of human skin. The uppermost layer covering the entire section indicates the epidermis. The layer below the epidermis is dermis. The chin's dermis content was calculated as high. Moving downward from the dermis reveals the subcutaneous layer. The enhanced subcutaneous fat offers protective cushioning to the skin. The final layer underneath the subcutaneous layer is the deep fascia.

The black portion of the image represents the fluid content, while the white portion indicates the fat content in the images. Fat content is necessary to protect and cushion the skin. Facial skin contains fat and sebum for its protection. The sebum protects it from various pathological conditions and prevents dryness in harsh conditions as well as preventing early signs of aging. However, low fluid content, ruptured skin layers, low thickness, and absence of sebum indicate poor skin condition (Hameed, et al., 2019).

Such skin is prone to injury, bruising, or damage. The epidermis density is higher for the chin and lower for the arm. The epidermis is the avascular layer that originates from the ectoderm and contains keratinocytes and melanocytes. The dermis is the next layer to the epidermis and is vascular, containing blood vessels that run through it and provide

nourishment to the skin. It originates from the mesoderm and comprises skin appendages and an extracellular matrix (Gilaberte, et al., 2016).

The superficial layer of the dermis is known as the papillary layer, which is rich in vascularisation. The deep layer is known as the reticular layer and is less vascular. The specialised cells of the dermis are macrophages, adipocytes and fibrocytes. Besides these, it also contains collagen fibrils, mast cells, Langerhans cells, lymphocytes, and phagocytes. The primary purpose of the skin layers is to provide immunity defence and protection against extreme temperatures, pathogens and hazards. The subcutaneous layer is the hypodermis, which lies beneath the dermis and works as a shock absorber, insulator and calorie reserve and provides cushioning to the skin (Sriram, et al., 2018).

The microscopic evaluation has revealed the SC's structure in detail. The SC must have at least 15% to 20% water content. The density of the water in this range reflects a healthy skin condition. It ensures adequate skin hydration levels and helps prevent water loss. Its structure resembles bricks (protein from skin cells) and mortar (lipids and important fats), which aim to lock the water content inside the skin. The high-resolution images obtained from Episcan were subjected to transformation, including the removal of gel, which may interrupt the actual results or lead to manipulation. Likewise, the curvature of the images was also a critical element that was subjected to algorithmic removal.

The distribution of the skin's layers and their arrangement in the anatomical sites are responsible for their peculiar functionality and protective properties. The greater thickness of the dermis ensures protection against pathogens and wounds. Superficial

skin analysis facilitates estimation of the skin's condition, but cross-sectional analysis can provide greater detail regarding existing and potential issues in the target area (Oltulu, et al., 2018). In-vivo assessment of the skin in different regions provides information about abnormalities in the underlying skin. These include the formulation of clusters, lesions, etc., within the skin's layers.

The human skin's biophysical properties play a significant role in the diagnosis of various diseases. It is central in restorative surgery, cosmetics, beauty treatments, medical treatments, forensics and other fields. High-resolution ultrasonic imaging has revealed indistinguishable areas. Lip skin varies from regular skin cells, as it contains a thin barrier as compared to other skin. It contains a thin layer of epidermis as a barrier and does not have hair follicles, sweat glands, and sebaceous glands. Lack of hydration leads to tightening and shrivelling of the lip skin. Fresh and healthy lips should appear sponge-like, and microscopic imaging has shown them to be widespread, with more fluid content inside. These plump up through the absorption of water and prevent chapped lips (Watanabe and Saga, 2019).

The internal connective tissue that is responsible for sheet or band formation is known as fascia. The deep fascia supports nerves, vessels and muscles. The neck contains deep cervical fascia and super cervical fascia to support its structure. Lesions, such as melanocyte lesions under the skin, can be evaluated through HRUS imaging, which has proven to play a significant part role in the diagnosis of diseases. Prevention of skin ulcers and skin cancer is possible with early detection using an imaging system. Removal of the green-coloured gel layer provides a clear view of the outermost

protective barrier, while the thickness of the dermis is directly related to the health condition of the facial skin in a given area.

The shrinking of cells, tissues or layers is associated with low fluid content, leading to dehydration. The strongest arrangement of skin layers indicates optimum skin density. The breakage of lines in the topmost area of the microscopic images represents damage to the epidermis and dermis. Growths or holes in the images facilitate the identification of lesions and assessment of their frequency and size (Phillips, et al., 2020).

5.2 Variation in Skin Assessment Through Welch-T-Test

Statistical tools offer a more vivid understanding of the skin's condition and health at different anatomical sites. One of the most popular tools for the statistical investigation of data is the Welch T-Test. It is the test that basically compares two populations to determine whether they have the same mean. Hence, it is a powerful tool for accepting or rejecting the hypothesis. A great deal of ultrasound imaging systems is a part of the healthcare system.

The Welch t-test given in Table 5.2 was considered for all the skin layers of eight different anatomical sites of human skin and was applied to the epidermis, dermis and subcutaneous layers of all these regions. Each anatomical site was analysed against all other sites. For instance, there was determination or comparison between arm to chin, arm to neck, arm to lip, arm to forehead, arm to cheek, arm to nose, and arm to eyelid. The results were noted for all the anatomical human skin sites for the different skin layers, including the epidermis, dermis and SC. The results obtained for all anatomical sites for different races are given as follows.

	Eyelid	Forehead	Chin	Nose	Cheek	Lip	Neck	Arm
Eyelid	-	0.42	1.61	2.12	2.62	5.27	6.36	8.48
Forehead	0.42	-	1.29	1.83	2.35	5.13	6.29	8.45
Chin	1.61	1.29	-	0.49	0.96	3.79	4.63	7.04
Nose	2.12	1.83	0.49	-	0.46	3.36	4.14	6.64
Cheek	2.62	2.35	0.96	0.46	-	3.00	3.75	6.33
Lip	5.27	5.13	3.79	3.36	3.00	-	0.29	3.19
Neck	6.36	6.29	4.63	4.14	3.75	0.29	-	3.21
Arm	8.48	8.45	7.04	6.64	6.33	3.19	3.21	-

Table 5.1. Welch T-test on the SC of Anatomical Sites

The Welch t-test was initially applied to the SC layer of all eight anatomical sites with the lowest value of 0.42 corresponding to the eyelid and forehead. By contrast, the highest values of the Welch t-test for the SC analysis were for the arm and eyelid. It was noted to be 8.48, which was close to the Welch t-test value for the Episcan of the forehead to the arm. For the forehead to arm, it was found to be 8.45. Proximity to the mean value is indicative of healthy skin. The anatomical values with higher values from the mean should be given special attention. These often show higher values than the mean in cases of drastic skin diseases, such as psoriasis, melanoma or skin ulcers, etc. The mean value obtained for the arm was 0.038; however, the deviation is significant. The positive and negative sigma values for the SC arm were 0.06 and 0.02, respectively as given in Figure 5.5. The above graph shows that the facial skin study reveals the highest variation or deviation for the arm and lip in the SC layer.

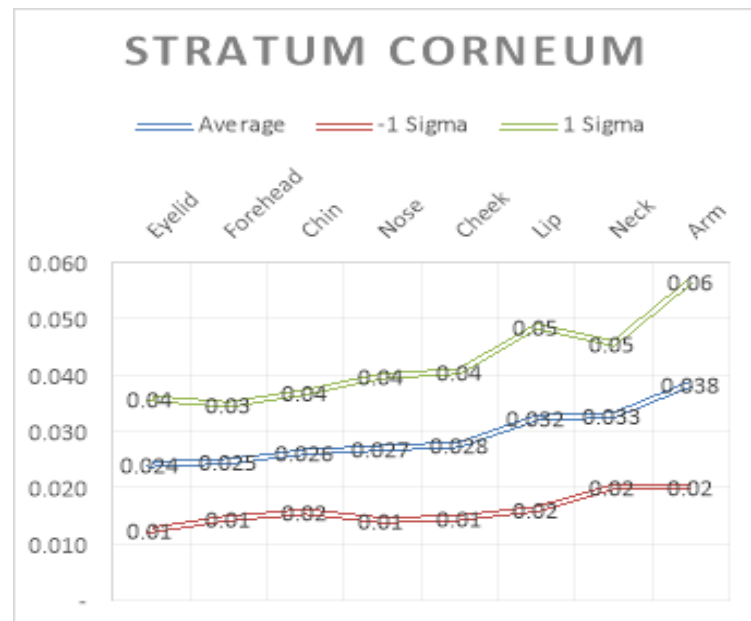


Figure 5.4. Sigma Values of SC Skin Layers

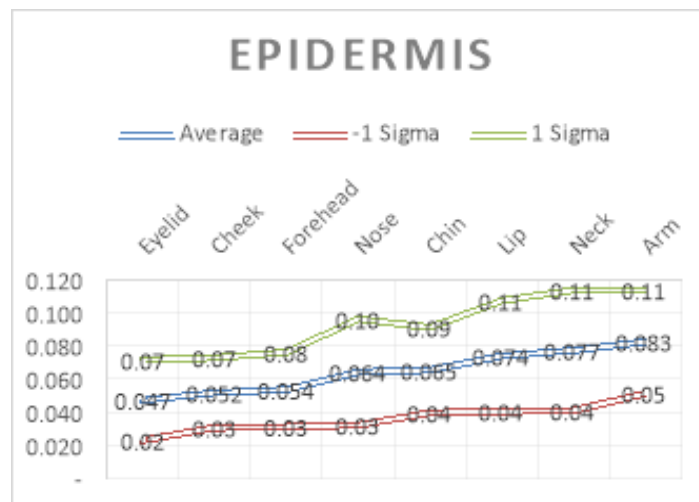


Figure 5.5. Sigma Values of Epidermal Skin Layers

Similarly, the epidermis layer has greater variation in the arm region. For the average value of the arm, 0.083, the deviation value for -1 sigma and +1 sigma to be 0.05 and 0.11, respectively. Likewise, the deviation for other anatomical sites is demonstrated in

the graph, which reflects changes or modifications in skin health. The cheek skin deviation is minimal in the epidermis, at 0.03 (-1 sigma) and 0.07 (1 sigma).

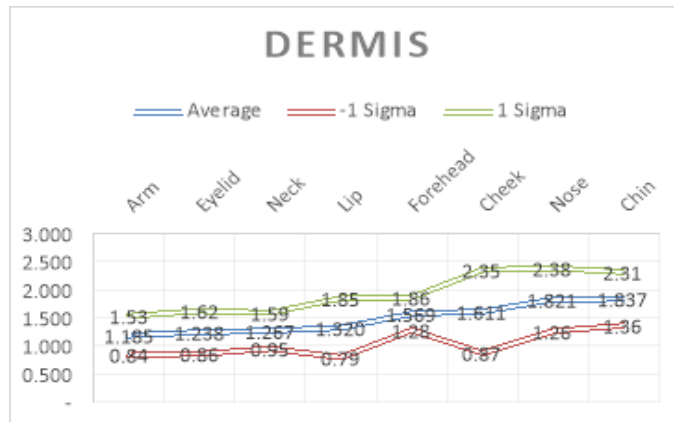


Figure 5.6. Sigma Values of Dermis Skin Layers

In the graph plotted for the dermis layer of different anatomical sites of human skin, the maximum +1 sigma value was found for the cheek, it was noted to be 2.35. However, it reflected the -1 sigma value of 0.87. The lip showed the lowest variation.

	Eyelid	Cheek	Forehead	Nose	Chin	Lip	Neck	Arm
Eyelid	-	1.71	2.27	5.22	5.69	7.99	8.56	11.22
Cheek	1.71	-	0.77	4.21	4.72	7.25	7.87	10.81
Forehead	2.27	0.77	-	3.37	3.82	6.28	6.95	9.55
Nose	5.22	4.21	3.37	-	0.34	2.68	3.47	5.34
Chin	5.69	4.72	3.82	0.34	-	2.39	3.21	5.10
Lip	7.99	7.25	6.28	2.68	2.39	-	0.90	2.49
Neck	8.56	7.87	6.95	3.47	3.21	0.90	-	1.44
Arm	11.22	10.81	9.55	5.34	5.10	2.49	1.44	-

Table 5.2. Welch T-test of the Epidermis of Anatomical Sites

Results of the Welch t-tests for the epidermis layer of all anatomical human skin sites under study were found to vary from theSC results. In this calculation, the lowest value of the Welch t-test was found for the chin to nose or nose to chin. However, the higher Welch t-test value was found for the arm and eyelid. The arm and eyelid values were close to those of the arm and cheek and arm and forehead.

The final skin layer that was considered was the dermis. All anatomical sites were subjected to analysis through Episcan for the determination of skin quality and health. It revealed the health status and condition of all skin layers.

The dermal value calculated was lowest for the chin to nose, or nose to chin at 0.26, given in Table 5.4. However, the highest value obtained through the Welch t-test was for the chin to arm or arm to chin with a maximum of 12.21.

	Arm	Eyelid	Neck	Lip	Forehead	Cheek	Nose	Chin
Arm	-	1.28	2.22	2.62	10.66	7.08	12.00	12.21
Eyelid	1.28	-	0.76	1.55	8.66	6.07	10.69	10.92
Neck	2.22	0.76	-	1.05	8.88	5.83	10.72	10.95
Lip	2.62	1.55	1.05	-	5.04	4.22	7.97	8.18
Forehead	10.66	8.66	8.88	5.04	-	0.72	4.95	5.23
Cheek	7.08	6.07	5.83	4.22	0.72	-	3.00	3.22
Nose	12.00	10.69	10.72	7.97	4.95	3.00	-	0.26
Chin	12.21	10.92	10.95	8.18	5.23	3.22	0.26	-

Table 5.3. Welch T-test of the Dermis layer of Anatomical Sites

These results were analysed and compiled to determine the results for all the skin layers of anatomical sites under study, including the cumulative results for all the skin layers. Figure 5.5 shows values for all skin layers. According to this table, the Welch t-test value obtained for arm and eyelid was shown to be 0.20 similar to the value obtained for the comparison of eyelid and arm. The results depicted the least obtained values for the arm and eyelid.

The values for the same anatomical site comparison were null. However, the highest value obtained was for the arm to chin or arm, at 36.42. The value for the skin analysis of the cheek to the forehead was also lower at 2.11. Likewise, the comparison of nose skin with chin skin revealed the low values too. It was found that the chin to the nose, or nose to chin values for the Welch t-test were a mere 0.82. Hence, the relationship of arm and eyelid, chin and nose, and forehead and cheek computed to the lowest Welch t-test values. Low values confirm low significance and good skin health conditions.

The closeness to zero confirms the null hypothesis. Skin analysis revealed that the values for the chin to arm, chin to eyelid and chin to neck were highest. These were calculated to be 36.42, 34.12 and 32.44, respectively. The greater variation from zero reveals greater distress in the underlying skin. The chin experienced much more variance than the skin of other anatomical sites. The chin is one of the most prominent parts of the human face. Besides the chin, the other anatomical areas of the lower human face include the jaw and lips (Nguyen & Duong, 2019).

Changes in the damage to the human skin at a particular site may occur due to several factors, such as hormonal changes. For instance, in the case of acne that covers the face, the most targeted areas are the cheek and chin. Itching may occur along with peel and

bleeding that aggravates the condition. Human skin is highly protected against pathogens due to the presence of an epidermal barrier. Hence, it has the ability to fight against harm and damage. Hormonal fluctuations or an unbalanced diet can lead to drastic conditions. The endocrine system is responsible for maintaining good health, and any disturbance in it can be easily reflected due to face mapping. Changes that occur in the skin that are not immediately visible can be seen with the assistance of Epsican. Excess androgen is the main contributor that disturbs hormonal balance and causes clogged pores and excessive stimulation of the sebaceous glands.

Skin that has elasticity and sebum remains younger-looking for longer. However, skin areas that lose their elasticity and collagen start to decline in appearance and continue to sag. Skin sagging is a sign of ageing, that can be delayed with the use of free radicals, a balanced diet, good moisturisers, organic meals, sufficient sleep and exercise. Thicker skin contains higher fat content and collagen to benefit the skin. Sagging skin in the regions of the jawline or chin is known as jowls. Unhealthy skin suffers from such signs of ageing relatively early (Hameed et al., 2019).

Various anatomical sites are free from skin tension lines, including the arm and nose among others. Various factors cause these sites lacking skin tension lines. Collagen and Elastin are the intrinsic elements that contribute to the formation of skin tension lines. A decrease in these elements is detrimental to skin health. The underlying muscles demand regular exercise and blood flow to ensure optimum health conditions for the human face. Nutraceuticals and collagen supplements aid in rejuvenating the skin and improving its health for longer (Pearson, 2018).

	Arm	Eyelid	Neck	Lip	Forehead	Cheek	Nose	Chin
Arm	-	0.20	5.89	7.50	28.65	18.69	36.14	36.42
Eyelid	0.20	-	5.05	6.85	25.25	17.78	33.78	34.12
Neck	5.89	5.05	-	3.07	22.94	15.28	32.08	32.44
Lip	7.50	6.85	3.07	-	14.03	11.48	24.67	25.17
Forehead	28.65	25.25	22.94	14.03	-	2.11	16.04	16.72
Cheek	18.69	17.78	15.28	11.48	2.11	-	9.43	10.05
Nose	36.14	33.78	32.08	24.67	16.04	9.43	-	0.82
Chin	36.42	34.12	32.44	25.17	16.72	10.05	0.82	-

Table 5.4. Welch T-test of all skin layer for Different Anatomical Sites

The highest standard deviation value from the mean was observed for the dermis layer of the cheek, which is 0.053, given in Table 5.6. However, the lowest standard deviation value from the mean was observed for the SC layer of all anatomical sites, which is 0.001. Skin diseases can be caused by viruses, allergies, bacteria, fungal infections, etc. These are relatively common compared to other diseases. Technological advancement has provided cost-effective and rapid pathways for diagnosing skin conditions.

New techniques have expanded the possibilities for diagnosis and have made dermatology and cosmetology screening considerable easier. Episcan can present an image of the skin on a computer screen, which dermatologists can use to identify existing or upcoming diseases in the near future.

Colour imaging has the additional benefit of revealing the particular zone affected by harm. Disease intensity and its spread can be controlled using such techniques (Xiao et al., 2020).

Location	Layer	Count	Average	Standard Deviation	Z-score
Forehead	SC	152	0.025	0.001	30.027
	Epidermis	141	0.054	0.002	28.274
	Dermis	158	1.569	0.023	67.610
Under-eye	SC	159	0.024	0.001	26.078
	Epidermis	136	0.047	0.002	22.692
	Dermis	158	1.238	0.030	40.707
Cheek	SC	184	0.028	0.001	28.784
	Epidermis	175	0.052	0.002	32.409
	Dermis	192	1.611	0.053	30.157
Nose	SC	169	0.027	0.001	27.368
	Epidermis	164	0.064	0.003	25.668
	Dermis	154	1.821	0.045	40.224
Lip	SC	165	0.032	0.001	25.639
	Epidermis	165	0.074	0.003	28.369
	Dermis	147	1.320	0.044	30.288
Arm	SC	168	0.038	0.001	27.289
	Epidermis	174	0.083	0.002	34.857
	Dermis	156	1.185	0.028	43.077
Neck	SC	159	0.033	0.001	32.482
	Epidermis	165	0.077	0.003	27.302
	Dermis	166	1.267	0.025	51.079
Chin	SC	116	0.026	0.001	26.642
	Epidermis	114	0.065	0.002	27.055
	Dermis	109	1.837	0.046	40.168

Table 5.5. Mean, SD, and Z-score of Skin Layers of Different Anatomical Sites

The z-score values, see Table 5.6, for the forehead SC, forehead epidermis and forehead dermis were calculated to be 30.027, 28.271 and 67.610, respectively. The highest z-score value for the SC was for the forehead (30.027) and the lowest was for the lip (25.639). Likewise, the highest z-score values for the epidermis and dermis were for the forehead, at 28.274 and 67.610, respectively. However, the lowest z-score values for the epidermis and dermis were found for the under-eye area and cheek, at 22.692 and 30.157, respectively. The z-score is the standard score that defines the points of data that reflect deviations from the standard. The lower the deviation, the closer the data will be to the standard. Variability and deviations are considered to be significant as the parameters that assist in assessing the skin at targeted anatomical sites.

5.3 Skin Site Classification by Machine Learning

It is often possible for an expert to determine what facial site does represent an Episcan image. But for large number of images, it is slow and cumbersome to analyse the images manually, it is better to automate the process by using modern Machine Learning (ML) techniques. The aim of this section is to investigate the feasibility of classifying skin ultrasound images from different skin sites by using ML algorithms. Specifically, a subset of the standard classifiers in the sklearn Python package will be used (Scikit, n.d.). Details of the classifiers are available in the package documentation.

The sample raw images for different sites are shown Figure 5.7. It is worth noting that those images were not originally intended to be used for ML-based classification, therefore measurements were not as systematic (e.g. not exactly same point on the facial site was measured for different people). It is clear that though pictures are somewhat distinct, there is lots of noise that needs to be dealt with first.

Expert evaluation of the images allows formulating the following observations /

hypothesis

1. Areas of different colours correspond to different elements of the skin
2. Density of the elements may only depend on the depth. As such any two-dimensional patterns will not be looking for and the problem is essentially one-dimensional.
3. Colours of the images is essential, so moving to monochrome representation will lose information.

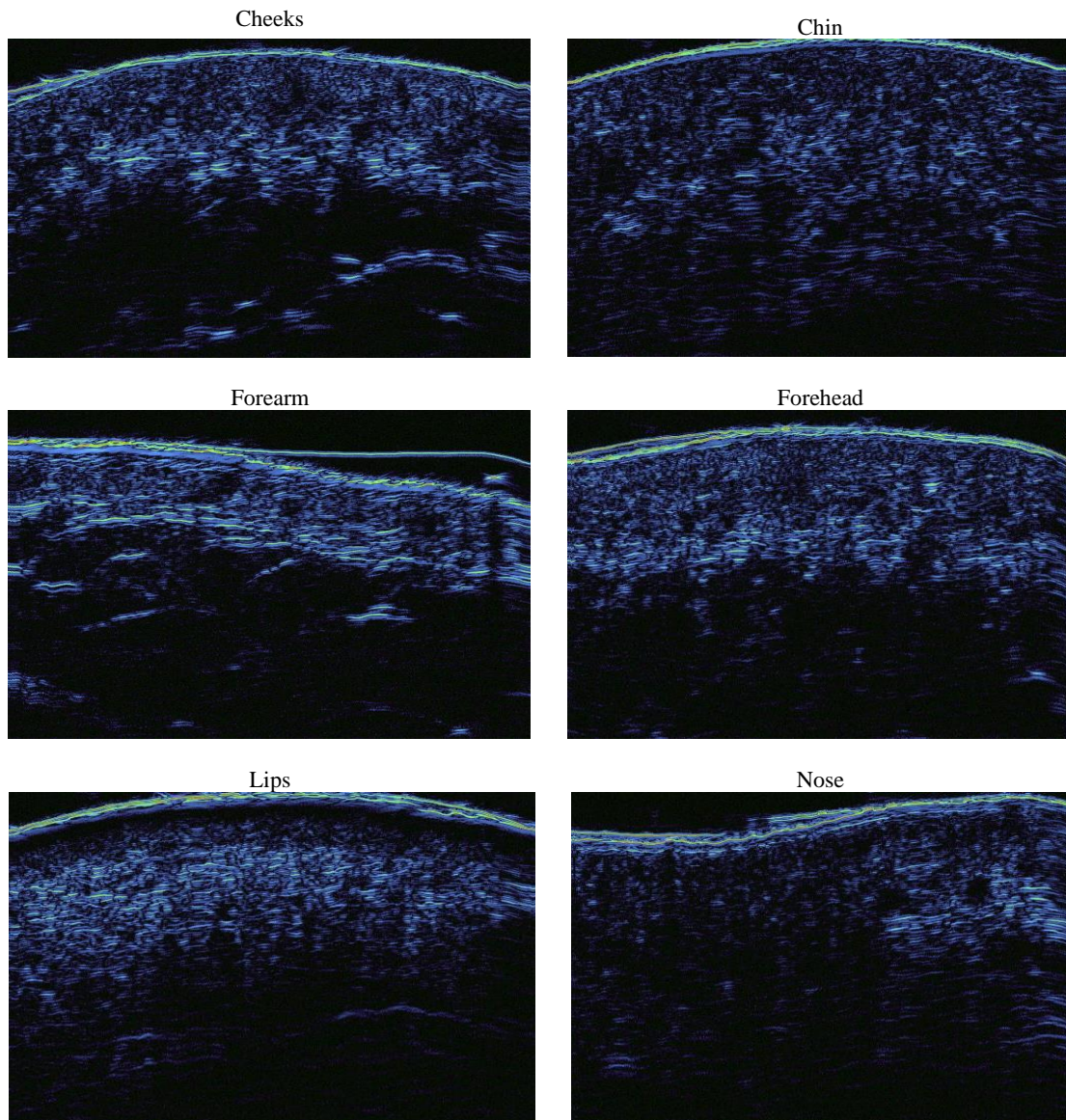


Figure 5.7 Sample raw Episcan images to be used in the

The table below summarizes the trading dataset; the original set of 409 images was modified to remove outliers per site.

Site number (code)	Site	Number of images
1	Cheeks	57
2	Chin	50
3	Forearm	46
4	Forehead	60
5	Lips	36
6	Nose	38
7	Undereye	81
Total		368

Table 5.6 Facial sites used for ML-based classification

All subjects were women of age 20-70 and mostly Caucasian or Asian race.

Data pre-processing

There are three major issues with the input images

1. The large empty area on top, which is not perfectly black.
2. The natural curvature of skin.
3. Possible presence of the gel layer.

As such three transformations of the images were performed

1. Gel layer was manually removed if present by editing the image
2. Curvature was removed algorithmically.
3. Nearly black area on top, if present, was removed algorithmically and only 50% of the image vertical area was kept.

The pictures below illustrate the transformations performed.

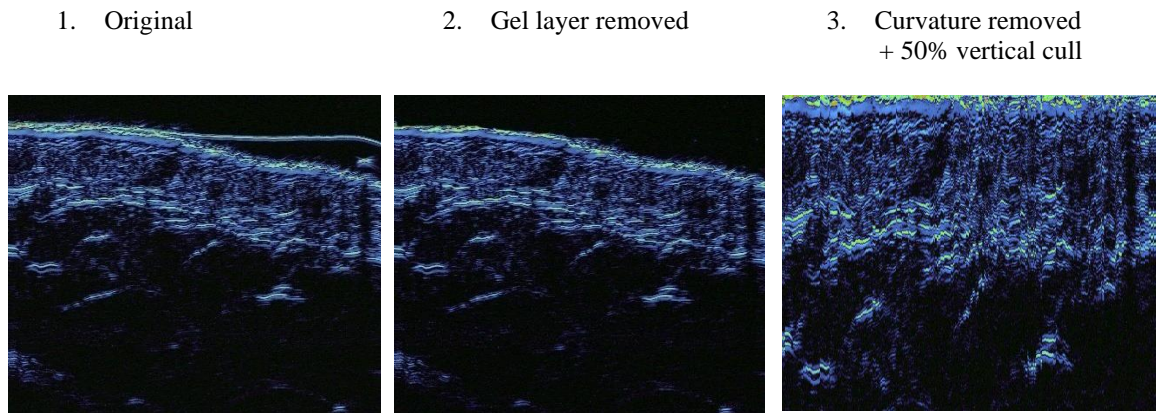


Figure 5.8 Image Transformation for ML-Based Classification

Factor specification

The pre-processed images were used as input for the training algorithms. Images were first represented as three matrices of luminosity values from 0 to 255, each matrix representing red, green or blue channels.

Due to the relatively small number of observations, the following features were chosen for classification per channel.

1. Mean luminosity value.
2. Standard deviation of luminosity value.
3. Median luminosity value.
4. Tail of the luminosity histogram with bin values [150, 170, 200, 256].

As such there were 6 factor values per channel and 18 factors per overall image. Values of those 18 factors were then used as the explanatory variable for the classification. The output variable was a number from 1 to 7, coding the facial site.

Three out of box classifiers were used, which were invoked with the following additional parameters, given in following table 5.8.

Classifier	Parameters
Logistic	<code>solver="lbfgs", max_iter=30000</code>
Nearest neighbour	<code>n_neighbors=3, leaf_size=10, algorithm="kd_tree"</code>
Neural net	<code>solver="adam", activation="relu", max_iter=5000</code>

Table 5.7 ML classifier parameters

Training was repeated 10 times and on each iteration the set was split randomly into 20% and 80% groups, representing testing and training sets. Score and accuracy across all runs were then aggregated.

	Score			Accuracy		
	min	avg	max	min	avg	max
Logistic	0.57	0.61	0.64	0.43	0.50	0.59
Nearest neighbour	0.62	0.65	0.68	0.30	0.39	0.42
Neural net	0.16	0.34	0.45	0.16	0.30	0.43

Table 5.8 ML training output

The table 5.9 presents a typical average output; the maximum score that has been observed was 0.68. Score represents the quality of training, while accuracy represents the quality of classification on the testing set.

It can be concluded that Logistic classifier performs best. It is expected its performance could be improved for larger sample sizes and more rigorous systematic measurements. Random Forest has also originally been tried, but it appeared constantly overfit and underclassify.

5.4 Chapter Summary

Skin analysis with Episcan is beneficial, as it clearly illustrates the skin's inner depths. Among all the facial skin sites, the cheek was found to have a greater percentage of the dermis. It was calculated to be 95.3%, which was higher than the rest of the anatomical sites.

The research study revealed more standard deviation for the cheek, which reflects the worsening skin condition in that peculiar area. It was found to be 0.437. The high-resolution images obtained from Episcan were subjected to modification or transformation for optimising the clarity. The transformation in these images includes the removal of the gel to avoid interruption and confusion. Additionally, the curvature of the images was also removed algorithmically. The excessive black region at the top of the images was removed to make the image more vivid and understandable.

The highest z-score value was found for the forehead, at 30.027. However, the lowest z-score value was noted for the lips, at 25.639. The z-score value noted for the forehead dermis was 67.610, while those for the forehead epidermis and forehead corneum were 28.271 and 30.027, respectively. The under-eye epidermis and cheek dermis reflected

the lowest z-score values, which were 22.692 and 30.157, respectively. The differences in the variation from standard values indicate poor health conditions.

Finally, the feasibility to train standard Machine Learning classifiers to identify the facial site based on the pre-processed Episcan picture was evaluated. It is considered the result a moderate success with lots of room to improve accuracy by having a more systematic measurement setup.

Chapter 6. Conclusions & Future Work

6.1 Conclusions

The combination of AquaFlux, Epsilon and Episcan provides details about skin health by covering various aspects. The reason for variation in values for different anatomical sites of facial skin was the degree of corneocyte formation, the lipid contents of the SC, skin temperature, damaged barrier function, bodily health and skin blood flow. The unequal sampling for the three methods of skin determination represents a limitation of this study. Skin analysis will have wide-ranging applications in the future for assessing the body's physiologic and pathological factors to identify the appropriate treatment. This would ensure a personalised skincare experience, as people will be able to obtain multidimensional images of their facial skin via email.

Rejuvenated, fresh skin is crucial to human beings' confidence levels. The skin's condition can make an individual appear younger or older. The business of the aesthetic market and beauty clinics is enhancing with each passing year. Skin is the body's main barrier against the environment. This strong barrier contains five different layers: the SC, stratum lucidum, stratum granulosum, stratum spinosum and stratum basale. The skin's resistive properties are due to its keratinized and specialised skin cells.

Facial skin has biophysical properties that distinguish it from the rest of the body. The skin is the body's largest multifunctional organ, reflecting variations in temperature, pH, sebum, blood flow, capacitance and TEWL. The use of face mapping science reflects conditions of the body's internal organs for the purpose of providing better care and

beauty enhancement. This technique finds its roots in Traditional Chinese Medicine and Ayurveda teachings. With advancements in science and technology, face mapping has also improved and has been proven to be an excellent aid to medical science. It has distinguished itself as a road map to swift diagnosis of underlying body issues. Skin analysis is the initial step in assessing the body's condition. Hence, it is further confirmed and estimated with clinical tests.

After successful analysis, the dermatologist recommends the best clinical treatment out of the various treatments available. Facial skin is subject to various issues, such as acne, irritation, dryness, blackheads, open-pore structure and roughness. It is essential that moisture be locked in the body. Flaky and dry skin clearly indicates a compromised or damaged lipid barrier. Hence, it leads to the escape of moisture from the skin, resulting in dehydration. High TEWL values are associated with high pH values. High pH values optimise enzymatic reactions, leading to lipid metabolism. The main reasons for variations in TEWL values include blood circulation through the skin, damaged skin barrier function, skin temperature, lipid contents of different skin layers, skin temperature and degree of corneocyte formation.

Epsilon is one of the most significant instruments used in skin analysis. This in-vivo method of skin analysis was used in this research study to formulate the results. The experimental study using Epsilon was divided into two sections. One section included the evaluation of variations in facial skin at various anatomical sites. The second section involved the determination of skin analysis by Epsilon considering the parameters of the exercise. Epsilon values for facial skin were calculated before and after exercise in both genders.

A limitation of the present study was the inappropriate sampling in the three facial skin determination approaches. Variations in sample characteristics can affect the results. According to the microscopic evaluation of the SC, it appears to have a bricks-and-mortar-like structure that locks fluid or water content inside the skin. The high-resolution images obtained from Episcan were subjected to modification or transformation for optimising the clarity. The transformation in these resultant images includes the removal of gel, which may confuse, disrupt or manipulate the actual outcomes.

A decline in collagen and elasticity leads to skin sagging. This is a sign of ageing that may be aggravated by skin dehydration. It can be controlled or reduced through exercise, adequate sleep, organic food, free radicals, a balanced diet and good moisturisers. Thick skin contains higher fat content, which works to maintain hydration levels for longer.

6.2 Future Work

Future advancements in skin analysis could potentially lead to the development of an app capable of diagnosing body issues based on images of the skin. Modern face mapping technology will be accessible to people at home so that they can improve their health. Online results and guidance would eliminate the need to wait for the detection of diseases or skin assessment. The diseases will be controlled much earlier before their progression, and hence the ratio of improved quality of health will increase.

In future dermatology and cosmetology, people will rush to have their skin assessed in clinics and to obtain the treatments accordingly. The increasing ratio of ageing, collagen breakage, skin roughness and wrinkles will decline. Hence, both aged and adult people will have flawless skin, which will ultimately optimise their health and confidence levels. Technological advancement will provide speedy and robust evidence of underlying illnesses. Dermatologists will be able to share live recordings of skin assessments, whereby the machine will highlight areas of concern. It may even provide details regarding disease stage and thereby assist in the judgement of prognosis.

Patient care settings in hospitals will be enhanced when these technologies are an effective part of the healthcare sector. Delays in disease detection will be overcome with such techniques, and they will be used as complementary aspects of other healthcare settings. Skin allergies are common among individuals and can cause considerable suffering. This study will assist in the future detection of allergens that are more likely to be involved in causing the particular allergy. This study yields more profound insights into human skin with particular respect to the pathological conditions that impact beauty and skin integrity.

Original Contribution to Knowledge

The main original contribution to knowledge of this study is to the conduction of a systematic study on the skin TEWL, skin hydration and skin layer thickness by using three state of the art instruments, the following are the details:

- Conducted a systematic, thorough investigation of skin TEWL, skin water content, and skin layer thickness measurements on faces and different skin sites of different volunteers, with the consideration of gender, age and skin colour.
- Quantified the effect of the physical exercise on the face skin properties.
- Applied Welch t-test to study similarities between different areas of the facial skin in terms of thickness of the skin layers.
- Evaluated the feasibility of training ML-based classifiers of the facial sites based on the high-resolution images.

List of Publications

Chirikhina, E., Chirikhin, A., Dewsbury-Ennis, S., Bianconi, F. and Xiao, P. 2021. Skin Characterizations by Using Contact Capacitive Imaging and High-Resolution Ultrasound Imaging with Machine Learning Algorithms. *Applied Sciences*. 11 (18), p. e8714. <https://doi.org/10.3390/app11188714>

Chirikhina, E., Chirikhin, A., Xiao, P., Dewsbury-Ennis, S. and Bianconi, F., 2020. In Vivo Assessment of Water Content, Trans-Epidermal Water Loss and Thickness in Human Facial Skin. *Applied Sciences*, 10(17), p.6139.

Zhang, X., Bontozoglou, C., Chirikhina, E., Lane, M.E. and Xiao, P., 2018. Capacitive imaging for skin characterizations and solvent penetration measurements. *Cosmetics*, 5(3), p.52.

Pan, W., Zhang, X., Chirikhina, E. and Xiao, P., 2014. Skin hydration measurement using contact imaging. *SCC Showcase*, New York, pp.11-12.

Bianconi, F., Chirikhina, E., Smeraldi, F., Bontozoglou, C., Xiao, P., Personal identification based on skin texture features from the forearm and multi-modal imaging, *Skin Research and Technology*, 23(3), pp. 392-398, 2017.

X. Zhang, C. Bontozoglou, E. Chirikhina, M.E. Lane, P. Xiao, Capacitive Imaging for Skin Characterizations and Solvent Penetration Measurements, *Cosmetics*, 5(3), 52, DOI: 10.20944/preprints201806.0331.v1, June 2018.

W. Pan, X. Zhang, E. Chirikhina, C. Bontozoglou and P. Xiao, “Measurement of Skin Hydration with a Permittivity Contact Imaging System”, *IFSCC Conference 2015*, Zürich, Switzerland, 21–23, September, 2015.

References

- Abatangelo, G. et al., 2020. *Hyaluronic acid: redefining its role. Cells*, Volume 9(7), p. 1743.
- Abdo, J., Sopko, N. & Milner, S. ..., 2020. The applied anatomy of human skin: a model for regeneration.. *Wound Medicine*.
- Abir-Awan, M. et al., 2019. Inhibitors of mammalian aquaporin water channels.. *International journal of molecular sciences*, Volume 20(7), p. 1589.
- Ablett, S. & Burdett, N., 1996. Short echo time MRI enables visualisation of the natural state of human stratum corneum water in vivo. *Magn. Reson. Imaging*, pp. 357-360.
- Adams, W. B. S., 2005. *Analysis of Facial Skin Thickness: Defining the Relative Thickness Index*. [Online]
Available at: <http://www.geocities.ws/foxydog1064/foxydogSk>
[Accessed 2020].
- Agache, P., Humbert, P. & Maibach, H., 2004. *Measuring the Skin*. Berlin: Springer.
- Al Hashimi, O. & Xiao, P., 2018. Epsilon Interactive Virtual User Manual (VUM). In *2018 International Conference on Computing, Electronics & Communications Engineering (iCCECE)*, pp. 138-143.
- Alarifi, J. et al., 2017. Facial skin classification using convolutional neural networks. In *International Conference Image Analysis and Recognition*, Springer, Cham, pp. 479-485.
- Albèr, C. et al., 2020. Effects of glycerol and urea on excised skin permeability and corneocyte hydration..
- Andersen ES, K. T., 2008. Evaluation of four non-invasive methods for examination and characterization of pressure ulcers. *Skin Res.Technol*, pp. 270-276.
- Anon., 2010. *Prestige Beauty Limited*. [Online]
Available at: http://www.prestigebeautyltd.com/dermalogica_face_mapping.htm
[Accessed 17 11 2020].
- Anon., 2013. *Robert K Mlosek*. [Online]
Available at: <https://pubmed.ncbi.nlm.nih.gov/23297834/>
[Accessed 2020].
- Anon., 2014. *Epsilon E100*. [Online]
Available at: <http://www.biox.biz/Products/Epsilon/E100ProductDescription.php>
[Accessed 08 June 2020].

Anon., 2014. *WoundSource*. [Online]

Available at: <https://www.woundsource.com/product/episcan-i-200>
[Accessed 2020].

Anon., n.d. *Biox System Ltd*. [Online]

Available at: <https://www.bioxsystems.com/products/epsilon-model-e100/product-description/>
[Accessed 2020].

Aragona, P., Simmons, P., Wang, H. & Wang, T. ..., 2019. Physicochemical Properties of Hyaluronic Acid–Based Lubricant Eye Drops.. *Translational vision science & technology*, Volume 8(6), pp. 2-2.

Bandara Dissanayake, K. M., 2019. New image analysis tool for facial pore characterization and assessment. *Wiley Online Library*.

Beeckman, D. & Campbell, J., 2015. Incontinence-associated dermatitis: moving prevention forward.

Bennett, S., Jones, C., Matheson, J.R., 2005. *Closed chamber and open chamber TEWL measurements: A comparison of Dermalab(R) and Aquaflex AF102 instruments*. In *Proceedings of the 2005 World Congress on Noninvasive Studies of the Skin*, s.l.: s.n.

Berardesca, E. P. F. S. M. a. M. H., 2006. Differences in stratum corneum pH gradient when comparing white Caucasian and black African-American skin.. *Br. J. Dermatol.* , pp. 855-857.

Berthaud, F. & Boncheva, M., 2011. Correlation between the properties of the lipid matrix and the degrees of integrity and cohesion in healthy human Stratum corneum. *Exp. Dermatol.*, pp. 255-262.

Bindra, R., Imhof, R., Mochan, A. & Eccleston, G. ..., 1994. Opto-thermal technique for in-vivo stratum corneum hydration measurement. *Le J. Phys*, pp. 465-468.

Biox Systems Ltd, 2014. *Skin Hydration Measurement Using Contact Imaging*, s.l.: s.n.

Bioxsystems, 2010. *FAQ*. [Online]

Available at: <https://www.biox.biz/FAQ/Epsilon/E-Answer06.php>
[Accessed 2020].

Black J, B. M. C. J. D. B. E. ..., 2007. *National Pressure Ulcer Advisory Panel's updated pressure ulcer staging system*, pp. 343-349.

Bollag, W., Aitkens, L., White, J. & Hyndman, K. ..., 2020. Aquaporin-3 in the epidermis: more than skin deep. *American Journal of Physiology-Cell Physiology*, Volume 318(6), pp. C1144-C1153..

Bonté, F., 2007. Skin hydration: a review on its molecular mechanisms. *Journal of Cosmetic Dermatology*, pp. 75-82.

Borzdynski, C., McGuiness, W. & Miller, C., 2016. Comparing visual and objective skin assessment with pressure injury risk.. *International wound journal*, Volume 13(4), pp. 512-518.

Bozorgtabar, B. et al., 2017. Investigating deep side layers for skin lesion segmentation. In *2017 IEEE 14th International Symposium on Biomedical Imaging (ISBI 2017)* , pp. 256-260).

Burk RS, L. V. G. M., 2013. *Measuring Skin Integrity Using High Frequency Ultrasound – A Validation Procedure*. s.l., s.n.

Cadavona, J., Rimtepathip, P. & Jacob, S., 2018. Moisturization.. *Journal of the Dermatology Nurses' Association* , Volume 10(3), pp. 158-160..

Cao, C., Xiao, Z., Wu, Y. & Ge, C., 2020. Diet and Skin Aging—From the Perspective of Food Nutrition.. *Nutrients*, Volume 12(3), p. 870.

Cerdà, J., Chauvigné, F. & Finn, R., 2017. The physiological role and regulation of aquaporins in teleost germ cells. In *Aquaporins*. Springer, Dordrecht., Volume 149-171.

Chambers, E. & Vukmanovic-Stejic, M., 2020. Skin barrier immunity and ageing.. *Immunology*, Volume 160(2), pp. 116-125.

Chantasart D, L. S., 2012. Structure enhancement relationship of chemical penetration enhancers in drug transport across the stratum corneum. *Pharmaceutics* . , pp. 71-92.

Chen, H., Lin, Y. & Chen, Y. 2., 2016 Identifying Chinese herbal medicine network for treating acne: implications from a nationwide database. *Journal of ethnopharmacology*, pp. 1-8.

Chen, L. et al., 2020. Classification and Treatment System for Facial Acne Vulgaris Based on Image Recognition. In *Elderly Health Services and Remote Health Monitoring*. Springer, Singapore., pp. 65-71.

Chilcott RP, D. C. E. A. A. C. B., 2002. Transepidermal water loss does not correlate with skin barrier function in vitro.. *J Invest Dermatol*, pp. 871-875.

Chilcott, R. & Price, S., 2008. *Principles and Practice of Skin Toxicology*. New Jersey: John Wiley & Sons.

Chirikhina, E. et al., 2020. In Vivo Assessment of Water Content, Trans-Epidermal Water Loss and Thickness in Human Facial Skin.. *Applied Sciences*, Volume 10(17), p. 6139.

Chu, M. a. K. N., 2011. Documentation of normal stratum corneum scaling in an average population: features of differences among age, ethnicity and body site. *Br. J. Dermatol.*, pp. 497-507.

Corte Technology, 2014. [Online]

Available at: <https://cortex.dk/scientific-ultrasound-dermascan-c/>
[Accessed 2020].

Cortex Technology, n.d. *Instruction Manual SkinLab*, s.l.: s.n.

Cowen, A. & Keltner, D., 2020. What the face displays: Mapping 28 emotions conveyed by naturalistic expression.. *American Psychologist*, Volume 75(3), p. 349.

Darvin, M. E., 2017. Keratin-water-NMF interaction as a three layer model in the human stratum corneum using in vivo confocal Raman microscopy. *Sci Rep* 7, 15900.

Dattola, A. et al., 2020. Role of Vitamins in Skin Health: A Systematic Review. *Current Nutrition Reports*, pp. 1-10.

De Paepe, K. et al., 2005. Validation of the VapoMeter, a closed unventilated chamber system to assess transepidermal water loss vs. the open chamber Tewameter.. *Skin Res. Technol.* 2005, 11, 61–69., pp. 61-69.

Deuticke, B., 2018. Bulk diffusion methods for measuring water permeability of biological membranes. In *Water Transport in Biological Membranes*. CRC Press., pp. 63-97.

Dines KA, S. P. B. J. H. C. C. K. C. J. e. a., 1984. High frequency ultrasonic imaging of skin: experimental results. *Ultrason Imaging.*, pp. 408-434.

Dissanayake, B. & Miyamoto, . K., 2019. New image analysis tool for facial pore characterization and assessment. *Skin Research and Technology*.

EEMCO Group., 2001. EEMCO guidance for the assessment of transepidermal water loss in cosmetic sciences. *Skin Pharmacol. Appl. Skin Physiol.*, pp. 117-128.

Egawa, M. a. T. H., 2008. Comparison of the depth profiles of water and water-binding substances in the stratum corneum determined in vivo by Raman spectroscopy. *Br. J. Dermatol.*, pp. 251-260.

Endly, D. & Miller, R., 2017. Oily skin: a review of treatment options. *The Journal of clinical and aesthetic dermatology*, Volume 10(8), p. 49.

Evans, R. et al., 2017. Human axillary skin condition is improved following incorporation of glycerol into the stratum corneum from an antiperspirant. *Archives of Dermatologi*.

Ezerskaia, A. et al., 2016. Quantitative and simultaneous non-invasive measurement of skin hydration and sebum levels.. *Biomedical optics express*, Volume 7(6), pp. 2311-2320.

Fenton, R., Murali, S. & Moeller, H., 2020. Advances in Aquaporin-2 trafficking mechanisms and their implications for treatment of water balance disorders.. *American Journal of Physiology-Cell Physiology*..

- Flament, F., Abric, A. & Amar, D., 2020. Gender-related differences in the facial aging of Chinese subjects and their relations with perceived ages.. *Skin Research and Technology*..
- Flynn, 1990. Physicochemical determinants of skin absorption. In: *Principles of Route to Route Extrapolation for Risk Assessment*.. New York: s.n., pp. 93-127.
- Fornage BD, M. M. D. M., 1993. Imaging of the skin with 20-MHz. *US. Radiology*, pp. 69-76.
- Gilaberte, Y., Prieto-Torres, L., Pastushenko, I. & Jarranz, A., 2016. Anatomy and Function of the Skin. In *Nanoscience in Dermatology. Academic Press.*, pp. 1-14.
- Giovanni, S., 1999. Variations in Facial Skin Thickness and Echogenicity with Site and Age. *Acta Derm Venereol*, pp. 366-369.
- Gniadecka M, Q. B., 1996. Assessment of dermal water by high-frequency ultrasound: comparative studies with nuclear magnetic resonance. *Br.J.Dermatol*, pp. 218-224.
- Golden, G. et al., 1986. Lipid thermotropic transitions in human stratum corneum.. *J. Investig. Dermatol.*, pp. 255-259.
- Golden, G. et al., 1987. Stratum corneum lipid phase transitions and water barrier properties. *Biochemistry*, pp. 2382-2388.
- Gross, e. a., 2016. *Analysis of Human Faces using a Measurement-Based Skin Reflectance Mode*. [Online]
Available at: <http://graphics.ucsd.edu/~henrik/papers/skin-analysis/skin-analysis.pdf>
[Accessed 2020].
- Gunathilake, R. S. N. S. B. e. a., 2009. pH-regulated mechanisms account for pigment-type differences in epidermal barrier function. *J. Invest. Dermatol.*, pp. 1719-1729.
- Gupta, V. & Sharma, V., 2019. Skin typing: Fitzpatrick grading and others. *Clinics in Dermatology*, Volume 37(5), pp. 430-436.
- Hahnel, E., Lichterfeld, A., Blume-Peytavi, U. & Kottner, J. ... , 2017. The epidemiology of skin conditions in the aged: a systematic review. *Journal of tissue viability*, Volume 26(1), pp. 20-28.
- Hameed, A., Akhtar, N., Khan, H. & Asrar, M., 2019. Skin sebum and skin elasticity: Major influencing factors for facial pores.. *Journal of Cosmetic Dermatology*, Volume 18(6), pp. 1968-1974.
- Hansen, J. & Yellin, W., 1972. NMR and Intrared Spectroscopic Studies of Stratum Corneum Hydration. In: *Water Structure at the Water-Polymer Interface*. Boston: Springer, pp. 19-28.
- Hara, M. K. K. W. M. e. a., 1993. Senile xerosis: functional, morphological, and biochemical studies. *Journal of Dermatology*, pp. 111-120.

- Has, C., 2018. Peeling skin disorders: a paradigm for skin desquamation.. *Journal of Investigative Dermatology*, Volume 138(8), pp. 1689-1691.
- Hashimoto-Kumasaka, K. T. K. a. T., 1993. Electrical measurement of the water content of the stratum corneum in vivo and in vitro under various conditions.. *Acta Derm. Venereol*, pp. 335-339.
- Healthline, 2010. *Facemapping*. [Online]
Available at: [Face mapping is one of them. It stems from an ancient Chinese belief that a person's skin is a reflection of their inner health.](#)
[Accessed 2020].
- Helvig EI, N. L., 2012. Use of high-frequency ultrasound to detect heel pressure injury in elders.. *J Wound.Ostomy.Continence.Nurs*, pp. 500-508.
- Hillebrand, G. L. M. a. M. K., 2001. The age-dependent changes in skin condition in African Americans, Asian Indians, Caucasians. East Asians and Latinos. *IFSCC Magazine.* , pp. 259-266.
- Horii I, N. Y. O. M. e. a., 1989. Stratum corneum hydration and amino acid content in xerotic skin. *British Journal of Dermatology*, pp. 587-592.
- Hubbard, K., 2019. Acne in aesthetics: a common skin condition and the practitioner's role in helping. *Journal of Aesthetic Nursing*, Volume 8(9), pp. 430-433.
- Huemer, W. & Ferran, Í., 2019. Beauty.. *New Essays in Aesthetics and the Philosophy of Art..*
- Huynh, A. & Priefer, R., 2020. Hyaluronic acid applications in ophthalmology, rheumatology, and dermatology. *Carbohydrate Research*, p. 489.
- Iizaka, S., 2017. Skin hydration and lifestyle-related factors in community-dwelling older people. *Archives of Gerontology and Geriatrics*, pp. 121-126.
- Ilyas, A., Kanwal, S. & Khalid, U. ..., 2020. Hormonal Inconsistency: A Sign of the Onset of Acneogenesis: Hormonal Imbalance Leads to Acne.. *PSM Biological Research*, Volume 5(4), pp. 166-177.
- Imhof, 2017. Stratum corneum hydration measurement using capacitance contact imaging.
- Imhof, R. et al., 1984. Optothermal transient emission radiometry. *J. Phys. E Sci. Instrum.*, pp. 521-525.
- Inomata, 2007. Skin roughness and Conspicuousness off fine wrinkles and skin pore.. *Cosmet Sci Soc*, pp. 103-107.
- Iuchi, K. et al., 2019. Estimation of blood concentrations in skin layers with different depths. Society for Imaging Science and Technol. *In Color and Imaging Conference*, pp. 290-294.

- Serup, J., 1992. A three-hour test for rapid comparison of effects of moisturizers and active constituents (urea). Measurement of hydration, scaling and skin surface lipidization by noninvasive techniques. *Acta Derm Venereol Suppl (Stockh)*, pp. 29-33.
- Jacobi, 1959. About the mechanism of moisture regulation in the horny layer of the skin.. *Proc Sci Sect Toilet Goods Assoc.*
- Jansen van Rensburg, S., Franken, A. & Du Plessis, J., 2019. Measurement of transepidermal water loss, stratum corneum hydration and skin surface pH in occupational settings: A review. *Skin Research and Technology*, Volume 25(5), pp. 595-605.
- Janssens, M. et al., 2014. Lipid to protein ratio plays an important role in the skin barrier function in patients with atopic eczema.. *British Journal of Dermatology*, pp. 1248-1255.
- JM., B., 2005. Moving toward consensus on deep tissue injury and pressure ulcer staging.. *Adv.Skin Wound Care.* , pp. 415-421.
- Kashibuchi, N. H. Y. O. K. a. T. H., 2002. Three-dimensional analyses of individual corneocytes with atomic force microscope: morphological changes related to age, location and to the pathologic skin conditions. *Skin Res. Technol*, pp. 203-211.
- Kelchen, M. et al., 2018. A pilot study to evaluate the effects of topically applied cosmetic creams on epidermal responses.. *Skin pharmacology and physiology*, Volume 31(5), pp. 269-282.
- Khan, Z. & Kellaway, I., 1989. Differential scanning calorimetry of dimethylsulphoxide-treated human stratum corneum.. *Int. J. Pharm.*, pp. 129-134.
- Kilpatrick-Liverman, L., Kazmi, P., Wolff, E. & Polefka, T., 2006. The use of near-infrared spectroscopy in skin care applications. *Skin Res. Technol.*, pp. 162-169.
- Kim, 2006. Comparison of Sebum secretion, skin type, pH in Humans with and without Acne. *Archives of Dermatology*, pp. 113-119.
- Kim, 2006. Comparison of Sebum secretion, skin type, pH in Humans with and without Acne. *Archives of Dermatology*, pp. 113-119.
- Koch, P. R. D. a. Z. Z. C. e. a. c.-l. e. I. S. B. (. P. a. F. K. e. p. 9. T. & F. N. Y. (., 2006. Cornified envelope and corneocyte-lipid envelope. In: *Skin Barrier*. New York: Taylor & Francis, p. 97–110.
- Koji Mizukoshi, K. T., 2013. Analysis of the skin surface and inner structure around pores on the face. *Skin Research and Technology*, pp. 23-29.
- Kong, L., 2007. Assessment of an Ultrasonic Dermal Scanner for Skin Thickness Measurements. *Med Eng Phys*.

Kunii, T. H. T. K. K. a. T. H., 2003. Stratum corneum lipid profile and maturation pattern of corneocytes in the outermost layer of fresh scars: the barrier dysfunction than do changes in intercellular lipids.. *British Journal of Dermatology*, pp. 351-360.

Kwon, H., 2019. Improvement of the skin condition according to the face mapping. *Journal of the Korean Applied Science and Technology*, Volume 36(4), pp. 1219-1223.

Labiotech, 2019. *This Biotech Uses Bacterial Proteins to Purify Water Faster*. [Online] Available at: <https://www.labiotech.eu/biotech-of-the-week/water-purification-aquaporin-osmosis/>

Lambers, H. P. S. B. A. P. H. a. F. P., 2006. Natural skin surface pH is on average below 5, which is beneficial for its resident flora. *Int. J. Cosmet. Sci.*, pp. 359-370.

Landis J, K. G. J. K. G., 1977. *The measurement of observer agreement for categorical data*. *Biometrics*. s.l.:159-174.

Lee, M. e. a., n.d. Comparison of stratum corneum thickness between two proposed methods of calculation using Raman spectroscopic depth profiling of skin water content. *Skin Res. Technol*, pp. 504-508.

Lee, M. et al., *Skin Res. Technol*. Comparison of stratum corneum thickness between two proposed methods of calculation using Raman spectroscopic depth profiling of skin water content.. *Skin Res. Technol*, pp. 504-508.

Lehman PA, F. T., 2014. Assessing topical bioavailability and bioequivalence: a comparison of the in vitro permeation test and the vasoconstrictor assay.. *Pharm Res.* , pp. 3529-3537.

Leung, H., 2002. Is skin ageing in the elderly caused by sun exposure or smoking?. *British Journal of Dermatology*, pp. 1187-1191.

Levine, A. & Markowitz, O., 2018. Introduction to reflectance confocal microscopy and its use in clinical practice. *JAAD Case Rep*, pp. 1014-1023.

Liaqat, S., Dashtipour, K., Arshad, K. & Ramzan, N., 2020. Non Invasive Skin Hydration Level Detection Using Machine Learning.. *Electronics*, Volume 9(7), p. 1086.

Limited, P. B., 2010. *dermalogica face mapping*. [Online] Available at: http://www.prestigebeauty ltd.com/dermalogica_face_mapping.htm [Accessed 17 11 2020].

Lixia Wang, X. W., 2019. Classification and influencing factors analysis of facial skin color in Chinese population. *Wiley Online*.

Logger JGM, M. C. O. J. P. M. V. E. P., 2019. Anatomical site variation of water content in human skin measured by the Epsilon: A pilot study.. *Skin Res Technol.*, pp. 333-338.

Logger, J., Olydam, J., Woliner-van der Weg, W. & van Erp, P., 2019. Noninvasive Skin Barrier Assessment: Multiparametric Approach and Pilot Study. *Cosmetics*.

LogicalSkincare, 2012. *Face Mapping*. [Online]

Available at:

<https://www.logicals skincare.co.uk/content/facemapping/#:~:text=Face%20mapping,Dermal%20Institute%20exclusively%20for%20Dermologica.&text=Rather%20than%20analysing%20the%20skin,potential%20problems%20and%20unique%20needs.>

[Accessed 2020].

Longport Inc., 2012. *Episcan i-200*. [Online]

Available at: <https://www.longportinc.com/episcan-i-200>

[Accessed 2020].

Longport., 2007. *EPISCAN I-200. Training Guide Quick Reference. 4.0.*, s.l.: Longport, Inc..

Lopez, S. L. F. I. M. F. H. G. G. ..., 2000. Transepidermal water loss, temperature and sebum levels on women's facial skin follow characteristic patterns. *Skin Res. Technol.*, Volume 6.

MacGrath, J. E. R. a. P., 2004. *Anatomy and organization of human skin*. In: *Rook's Textbook of Dermatology*. s.l.:Oxford.

Majaron, B. & Choi, B., 2003. *Temperature distribution in port wine stain following pulsed irradiation by a dual-wavelength Nd:YAG laser*. s.l.:s.n.

Mantis, 2014. High-frequency ultrasound bio microscopy of the normal canine haired skin. *Vet Dermatol*.

Marno, A. ..., 2020. War, Surgery and the Face: On the Perception of Photographs of Face Injured Soldiers of World War I in Present Art. In War and Art. *Ferdinand Schöningh.*, pp. 231-254.

Michalek, I., Loring, B. & John, S., 2017. A systematic review of worldwide epidemiology of psoriasis. *Journal of the European Academy of Dermatology and Venereology*, Volume 31(2), pp. 205-212.

Mitchener, T., Chan, R. & Simecek, J. ..., 2017. Oral–Maxillofacial Injury Surveillance of US Military Personnel in Iraq and Afghanistan 2001 to 2014. *Military medicine*, Volume 182(3-4), pp. e1767-e1773..

Mizukoshi, O., 2009. Age-related changes in 3D structure of cheek region. *J Soc Cosmet*, pp. 177-184.

Mojumdar, E., Pham, Q., Topgaard, D. & Sparr, E. ..., 2017. Skin hydration: interplay between molecular dynamics, structure and water uptake in the stratum corneum. *Scientific reports*. Volume 7(1), pp. 1-13.

- Mukherjee, S. et al., 2016. Sebum and hydration levels in specific regions of human face significantly predict the nature and diversity of facial skin microbiome..
- Nakazawa, H. et al., 2019. Simultaneous measurements of structure and water permeability in an isolated human skin stratum corneum sheet. *Polymers*, Volume 11(5), p. 829.
- Nguyen, J. & Duong, H., 2019. Anatomy, Head and Neck, Inferior Alveolar Arteries. In StatPearls [Internet].. *StatPearls Publishing*..
- Nkengne, A. et al., 2020. Visible characteristics and structural modifications relating to enlarged facial pores.. *Skin Research and Technology*.
- Nuutinen, J. et al., 2003. A closed unventilated chamber for the measurement of transepidermal water loss. *Skin Res. Technol.*, pp. 5-89.
- O'Goshi K, S. J., 2005. Inter-instrumental variation of skin capacitance measured with the Corneometer. *Skin Res Technol.*, pp. 107-109.
- Ohman, V. A., 1994. In vivo studies concerning pH gradient in Human Stratum Corneum and Upper Eidermis. *Acta Derm Venereol*, pp. 375-379.
- Oltulu, P. et al., 2018. Measurement of epidermis, dermis, and total skin thicknesses from six different body regions with a new ethical histometric technique. *Turkish Journal of Plastic Surgery*, Volume 26(2), p. 56.
- Paoli, B. & Procacci, M., 2019. Motivation and expectations of aesthetic patients.. *Minerva Psichiatrica*, Volume 60(4), pp. 180-90.
- Patrick, T., 1988. The water barrier function of the skin in relation to the water content of the SC, pH and skin lipids. *Acta Derm Venereol*, pp. 277-283.
- Pearson, K., 2018. Nutraceuticals and skin health: key benefits and protective properties. *Journal of Aesthetic Nursing*, pp. 35-40.
- Phillips, J., Reynolds, K. & Gordon, S., 2020. Dermal thickness and echogenicity using DermaScan C high frequency ultrasound: Methodology and reliability t-testing in people with and without primary lymphoedema. *Skin Research and Technology*, p. 26(6).
- Proksch, E., 2018. H in nature, humans and skin. *The Journal of Dermatology*, Volume 45(9), pp. 1044-1052.
- Proksch, E. et al., 2020. Dry skin management: practical approach in light of latest research on skin structure and function.. *Journal of Dermatological Treatment*, Volume 31(7), pp. 716-722.
- Qassem, M. & Kyriacou, P., 2014. Use of reflectance near-infrared spectroscopy to investigate the effects of daily moisturiser application on skin optical response and barrier function. *Biomed*.

Qassem, M. & Kyriacou, P., 2014. Use of reflectance near-infrared spectroscopy to investigate the effects of daily moisturiser application on skin optical response and barrier function. *J. Biomed. Opt.*.

Raj, N. et al., 2017. A fundamental investigation into aspects of the physiology and biochemistry of the stratum corneum in subjects with sensitive skin. *International journal of cosmetic science*, Volume 39(1), pp. 2-10.

Rawlings, A., 2003. Trends in stratum corneum research and the management of dry skin conditions.. *Int. J. Cosmet. Sci.* , pp. 63-95.

Reginelli, A. et al., 2020. A Preliminary Study for Quantitative Assessment with HFUS (High-Frequency Ultrasound) of Nodular Skin Melanoma Breslow Thickness in Adults Before Surgery: Interdisciplinary Team Experience.. *Current Radiopharmaceuticals*, Volume 13(1), pp. 48-55.

Reid, F., 2017. Losing Face: Trauma and Maxillofacial Injury in the First World War. In *Psychological Trauma and the Legacies of the First World War*. *Palgrave Macmillan, Cham.*, pp. 25-47.

Robertson, K. & Rees, J., 2010. Variation in epidermal morphology in human skin at different body sites as measured by reflectance confocal microscopy.. *Acta Derm. Venereol.*, pp. 368-373.

Rodriguez, R. et al., 2019. Single-channel permeability and glycerol affinity of human aquaglyceroporin AQP3.. *Biochimica et Biophysica Acta (BBA)-Biomembranes*, Volume 1861(4), pp. 768-775.

Rogiers, 2001. EEMCO guidance for the assessment of transepidermal water loss in cosmetic sciences.. *Skin Pharmacol. Appl.*, Issue 14, pp. 117-128.

Rohrbach, 2014. Preoperative Mapping of Nonmelanoma Skin Cancer Using Spatial Frequency Domain and Ultrasound Imaging. *Acad Radiol*, pp. 263-270.

Saadatmand, M. et al., 2017. Skin hydration analysis by experiment and computer simulations and its implications for diapered skin.. *Skin Research and Technology*, Volume 23(4), pp. 500-513.

Saeedi, M., Eslamifar, M. & Khezri, K., 2019. Kojic acid applications in cosmetic and pharmaceutical preparations. *Biomedicine & Pharmacotherapy*, pp. 582-593.

SA, I., 2009. *A Structure-Enhancement Relationship and Mechanistic Study of Chemical Enhancers on Human Epidermal Membrane Based on Maximum Enhancement Effect*, Ohio: University of Cincinnati.

Samadi, A. et al., 2020. Changes in skin barrier function following single and repeated applications of 4 types of moisturizers: A randomized controlled trial.. *Journal of the European Academ.*

Schmid-Wendtner MH, D.-M. D., 2008. Ultrasound technology in dermatology.. *Semin Cutan Med Surg.* , pp. 44-51.

Scikit, n.d. *Scikit-learn*. [Online]

Available at: <http://scikit-learn.org>

Sikkandar, H. & Thiyagarajan, R., 2019. Soft biometrics-based face image retrieval using improved grey wolf optimisation.. *IET Image Processing*, Volume 14(3), pp. 451-461.

Song, Y. et al., 2019. Mapping the face of young population in China: Influence of anatomical sites and gender on biophysical properties of facial skin.. *Skin Research and Technology*, Volume 25(3), pp. 325-332.

Spada, F., Barnes, T. & Greive, K., 2018. Skin hydration is significantly increased by a cream formulated to mimic the skin's own natural moisturizing systems. *Clinical, cosmetic and investigational dermatology*, Volume 11, p. 491.

Sriram, G. et al., 2018. Full-thickness human skin-on-chip with enhanced epidermal morphogenesis and barrier function. *Materials Today*, Volume 21(4), p. 326.

Stone, J., Patel, V. & Bailes, J., 2016. Sir Hugh Cairns and World War II British advances in head injury management, diffuse brain injury, and concussion: an Oxford tale. *Journal of neurosurgery*, Volume 125(5), pp. 1301-1314.

Sugiyama-Nakagiri.O, 2010. Involvement of IGF-1/IGFBP-3 signaling on the conspicuousness of facial pores. *Archives of Dermatology*, pp. 661-667.

Sugiyama-Nakagiri, O., 2010. Involvement of IGF-1/IGFBP-3 signaling on the conspicuousness of facial pores. *Archives of Dermatology*, pp. 661-667.

Tagami, H., 2008. Location-related differences in structure and function of the stratum corneum with special emphasis on those of the facial skin. *International Journal of Cosmetic Science*, pp. 413-434.

Tagami, H. K. K. a. O. K., 2003. Electrical properties of newborn skin. In: *Neonatal Skin Structure and Function*. s.l.:Hoath, S.B. and Maibach.

Tagami, H. O. M. I. K. K. Y. a. Y., 1980. Evaluation of skin surface hydration in vivo by electrical measurement. *Invest Dermatol.*, pp. 500-507.

Tagami & K., H. K. K. a. O., 2003. Electrical properties of newborn skin. In: *Neonatal Skin Structure and Function*. s.l.:Hoath, S.B. and Maibach..

Tamma, G. et al., 2018. Aquaporin membrane channels in oxidative stress, cell signaling, and aging: recent advances and research trends.. *Oxidative medicine and cellular longevi.*

Telofski, L. & M. A. & C. M. & S. G. ..., 2012. The Infant Skin Barrier: Can We Preserve, Protect, and Enhance the Barrier?. *Dermatology research and practice.. Dermatology research and practice.*

Thiagarajah, J.R. & Verkman, A., 2018. Water transport in the gastrointestinal tract .In *Physiology of the gastrointestinal tract. Academic Press.,* pp. 1249-1272.

Tikjøb G, K. V. S. J., 1984. Ultrasonic B-scanning of the human skin. An introduction of a new ultrasonic skin-scanner. *Acta Derm Venereol. ,* pp. 67-70.

Tognetti, L. et al., 2020. In *Technology in Practical Dermatology. Dermoscopy: fundamentals and technology advances.,* pp. 3-24.

Tsankov, N., Mateev, D. & Darlenski, R., 2018. Skin hydration, microrelief and greasiness of normal skin in Antarctica.. *Journal of the European Academy of Dermatology and Venereology,* Volume 32(3), pp. 482-485.

Tuckman, A., 2017. The potential psychological impact of skin condition. *Dermatology and therapy,* Volume 7(1), pp. 53-57.

van Logtestijn MD, D. E. S. G. T. R., 2015. Resistance to water diffusion in the stratum corneum is depth-dependent. *PLoS One..*

Voegeli, R., Gierschendorf, J., Summers, B. & Rawlings, A., 2019. from single point bio-instrumental evaluation to continuous visualization of skin hydration, barrier function, skin surface pH, and sebum in different ethnic skin. *Facial skin mapping.*

Voegeli, R. R. A. S. P. a. S. B., 2015. A novel continuous colour mapping approach for visualization of facial skin hydration and transepidermal water loss for four ethnic groups. *Int. J. Cosmet. Sci. ,* Volume 37, pp. 595-605.

Voegli, S., 2019. Facial skin mapping: from single point bio-instrumental evaluation to continuous visualization of skin hydration, barrier function, skin surface pH, and sebum in different ethnic skin types. *Wiley Online Library.*

Wa, C. & Maibach, H. M. t. h. f. B. p. S. R. T. 2. 1. 3., 2010. Mapping the human face: Biophysical properties. *Skin Res. Technol.,* pp. 38-54.

Wallace, L., Gwynne, L. & Jenkins, T., 2019. Challenges and opportunities of pH in chronic wounds. *Therapeutic Delivery,* Volume 10(11), pp. 719-735.

Walters, K. & Roberts, M., 2007. *Dermatologic, Cosmeceutic, and Cosmetic Development: Therapeutic and Novel Approaches.* s.l.: Boca Raton, FL, USA.

- Wang, C. et al., 2018. Ionic liquid—microemulsions assisting in the transdermal delivery of Dencichine: Preparation, in-vitro and in-vivo evaluations, and investigation of the permeation mechanism.. *Int. J. Pharm.*, pp. 121-130.
- Wang, L., Wan, X. & Xiao, G., 2019. Classification and influencing factors analysis of facial skin color in Chinese population. *Skin Research and Technology* , Volume 25(5), pp. 693-700.
- Warrier, A. K. A. H. R. B. J. a. W. R., 1996. A comparison of black and white skin using noninvasive methods.. *J. Soc. Cosmet. Chem.*, pp. 229-240.
- Watanabe, K., Saga, Springer & Cham., 2019. In Anatomical Variations in Clinical Dentistry. *Anatomy and Variations of the Lip*, pp. 177-184.
- Wegrzyn, M. et al., 2017. How individual face parts contribute to successful emotion recognition. PloS one. *Mapping the emotional face*, Volume 12(5), pp. 177-239.
- Wei L, X. W. W. L. e. a., 2007. Skin color measurement in Chinese female population: analysis of 407 cases from 4 major cities of China. *International Journal of Dermatology*, pp. 835-839.
- Wei Pan, X. Z. E. C. & P. X., 2014. *HYDRATION MEASUREMENT BY EPSILON FROM BIOX*. [Online] Available at: <https://www.skinobs.com/news/en/products/facials/hydration-measurement-by-epsilon-from-biox/> [Accessed 08 June 2020].
- Wei, L., Gan, Q. & Ji, T., 2018. Skin Disease recognition method based on image color and texture features.. *Computational and mathematical methods in medicine*.
- Wellner K, W. W., 1993. Quantitative evaluation of urea in stratum corneum of human skin. *Arch Dermatol Res.*, pp. 239-240.
- Westermann, T. et al., 2020. Measurement of skin hydration with a portable device (SkinUp® Beauty Device) and comparison with the Corneometer®. *Skin Research and Technology*..
- Whitney, Z., Jain, M. & Zito, P., 2020. Anatomy, Skin, Superficial Musculoaponeurotic System (SMAS) Fascia. *StatPearls [Internet]*.
- Wichrowski, K. S. G. K., 1996. Use of infrared spectroscopy for in vivo measurement of the stratum corneum moisturization after application of cosmetic preparations.. *International Journal of Cosmetic Science*, pp. 1-11.
- Wu, Y. et al., 2019. Reporting of ethical approval and informed consent in clinical research published in leading nursing journals: a retrospective observational study. *BMC Medical Ethics*, Volume 20(1), p. 94.
- Xiao, P. & Imhof, R., 1996. Optothermal skin-water concentration gradient measurement. *Proc. SPIE*, pp. 31-41.

- Xiao, P., Wong, W., Cottenden, A. & Imhof, R., 2012. In vivo stratum corneum over-hydration and water diffusion coefficient measurements using opto-thermal radiometry and TEWL Instruments.. *Int. J. Cosmet. Sci.*, pp. 328-331.
- Xiao, P. et al., 2020. The Development of a Skin Image Analysis Tool by Using Machine Learning Algorithms. *Cosmetics*, Volume 7(3), p. 67.
- Yang, L., 2019. Chinese Medicine for Major Depressive Disorder: Clinical Evidence, Patients' Experience and Expectations, and Doctors' Perceptions (Doctoral dissertation). *RMIT University*.
- Yano T, F. H. U. S. F. A., 1987. 40 MHz ultrasound diagnostic system for dermatologic examination. *IEEE Ultrasonics Symposium Proceeding*, pp. 875-878.
- Ya-Xian, Z. S. T. a. T. H., 1999. Number of cell layers of the stratum corneum in normal skin – relationship to the anatomical location on the body, age, sex and physical parameters.. *Archives of Dermatology*, pp. 555-559.
- Ye, C. et al., 2020. Skin sensitivity evaluation: What could impact the assessment results?.. *Journal of Cosmetic Dermatology*, Volume 19(5), pp. 1231-1238.
- Yonezawa, K. et al., 2018. Effects of moisturizing skincare on skin barrier function and the prevention of skin problems in 3-month-old infants: a randomized controlled trial. *The Journal of Dermatology*.
- Yousiopic, G., 1998. *Time Dependent Variations of the Skin Barrier Functions in Humans*, s.l.: s.n.
- Zannetti, A. et al., 2020. Role of Aquaporins in the Physiological Functions of Mesenchymal Stem Cells.. *Cells*, Volume 9(12), p. 2678.
- Zhai, H., Wilhelm, K. & Maibach, H., 2007. *Marzulli and Maibach's Dermatotoxicology*. Florida, USA: CRC Press.
- Zhang, L. A. A. S. P. S. V. S. M. L. R. Q. J. W. M. a. F. M., 2020. The Impact of Routine Skin Care on the Quality of Life. *Cosmetics*, Volume 7(3), p. 59.
- Zhang, X. et al., 2018. Capacitive Imaging for Skin Characterizations and Solvent Penetration Measurements.. *Cosmetics*.
- Zhao, C. et al., 2020. Variation of biophysical parameters of the skin with age, gender, and lifestyles. *Journal of Cosmetic Dermatology*.

Appendix: Ethical Approval

**London South Bank
University**

Direct line: 020-7815 6025
E-mail: mitchen5@lsbu.ac.uk
Ref: UREC 1412

Elena Chirikhina
33 Leysdown Road
London
SE9 3LY

Wednesday 25 June 2014

Dear Elena,

RE: Identify and document statistically significant difference in the skin's TEWL, hydration, pH and surface temperature as the function of a combination of the skin type, age and gender

Thank you for submitting this proposal and for your response to the reviewers' comments.

I am pleased to inform you that Full Chair's Approval has been given by Chair on behalf of the University Research Ethics Committee.

I wish you every success with your research.

Yours sincerely,



Nicola Mitchell

Secretary, LSBU Research Ethics Committee

cc:

Prof Shushma Patel, Chair, LSBU Research Ethics Committee